Aus der Klinik für Pädiatrie mit Schwerpunkt Hämatologie und Onkologie
der Medizinischen Fakultät Charité – Universitätsmedizin Berlin

DISSERTATION

A CRISPR activation screen identifies *ABCC1* as a potential therapeutic target in actinomycin D-resistant high-risk pediatric rhabdomyosarcoma

Identifikation von *ABCC1* als potenziellen Angriffspunkt in Actinomycin D-resistenten, pädiatrischen Hochrisiko-Rhabdomyosarkomen: ein CRISPR-Aktivationsscreen

zur Erlangung des akademischen Grades
Doctor medicinae (Dr. med.)

vorgelegt der Medizinischen Fakultät
Charité – Universitätsmedizin Berlin

von

Jennifer von Stebut

aus Hamburg

Datum der Promotion: 30.11.2023

Table of contents

1 List of tables and figures 4

2 List of abbreviations 5

3 Abstract 10

4 Introduction 11

4.1 Rhabdomyosarcoma 11

4.1.1 Genetics 11

4.1.2 Targeted therapies in RMS treatment 13

4.1.3 Histology 15

4.1.4 Clinical presentation 16

4.1.5 Treatment protocols 17

4.2 Actinomycin D 19

4.2.1 Mechanism of action 20

4.2.2 Side effects of chemotherapy 20

4.2.3 Resistance mechanisms 21

4.3 CRISPR technology in the study of drug resistance 22

5 Objectives 24

6 Material and Methods 25

6.1 Material 25

6.1.1 Technical equipment 25

6.1.2 Chemicals, reagents and buffers 31

6.1.3 Cell culture reagents and media 32

6.1.4 Bacteria work reagents and media 33

6.1.5 Cell lines 34

6.1.6 Kits 34

6.1.7 Plasmids and libraries 35

6.1.8 Competent cells 35

6.1.9 Primer sequences for barcoded NGS 35

6.1.10 sgRNA sequences for validation 37

6.1.11 Primers for qPCR 37

6.1.12 Western Blot 38

6.1.13 Software 39

6.2 Methods 40

6.2.1 Cell culture 40

6.2.2 Cell viability assays 41

6.2.3 Western Immunoblotting 42

6.2.4 DNA amplification 42

6.2.5 Bacterial transformation 43

6.2.6 Viral Transduction 43

6.2.7 CRISPR activation screen 45

6.2.8 Statistical analysis 47

7 Results 48

7.1 Rhabdomyosarcoma cell line models respond differently to actinomycin D 48

7.2 A pooled genome-wide CRISPR activation screen identifies *ABCC1* as a potential predictor for actinomycin D-resistance 51

7.3 Overexpression of *ABCC1* leads to increased resistance to actinomycin D 53

7.4 The ABCC1-inhibitor tetrandrine is synergistic with actinomycin D in ARMS cell lines 55

8 Discussion 57

9 Bibliography 63

10 Eidesstattliche Erklärung 79

10.1 Eidesstattliche Versicherung 79

11 Lebenslauf 80

12 Komplette Publikationsliste 82

13 Danksagung 83

14 Bescheinigung des akkreditierten Statistikers 84

1 List of tables and figures

Table 1: Examples of current targeted therapies in clinical trials for RMS. 14
Table 2: Risk stratification of RMS patients. 18
Table 3: Cell lines used in experiments with respective culture medium 40
Table 4: Clinical and molecular characteristics of the cell lines tested. 49

Figure 1: Genomic landscape of RMS. 12
Figure 2: Key pathways affected in both PAX fusion positive and negative RMS. 13
Figure 3: Histology of RMS. 15
Figure 4: Chemical structure of ActD and its interaction with double strand DNA. 20
Figure 5: Schematic depiction of SAM activation complex bound to DNA 22
Figure 6: RMS cell line models show a diverse response to ActD. 48
Figure 7: A genome-wide CRISPRa screen identifies multiple genes associated with resistance to ActD. 51
Figure 8: ABCC1 leads to higher resistance to ActD in Rh4 cells 53
Figure 9: Combination of ActD and tetrandrine has synergistic antitumoral effects in ARMS. 55

2 List of abbreviations

Abbreviation	Full description
°C	degrees centigrade
ABCB1	ATP Binding Cassette Subfamily B Member 1
ABCC1	ATP Binding Cassette Subfamily C Member 1
ABCC2	ATP Binding Cassette Subfamily C Member 2
ABCG2	ATP Binding Cassette Subfamily G Member 2
ActD	actinomycin D
ADP	adenosine diphosphate
ALK	Anaplastic lymphoma receptor tyrosine kinase
ARF	ADP ribosylation factor
ARMS	alveolar rhabdomyosarcoma
ATP	adenosine triphosphate
BCA	bicinchonic acid
BCR-ABL	Philadelphia chromosome
BRAF	B-Raf proto-oncogene, Serine/threonine kinase
BRD4	Bromodomain containing 4
CA	California
Cas9	CRISPR associated protein 9
cDNA	complementary deoxyribonucleid acid
CI	confidence interval
cm	centimeter
CO2	carbon dioxide
CRISPR	Clustered regularly interspaced short palindromic repeats
CRISPRa	CRISPR activation
CtBP2	c-terminal binding protein 2
CTLA-4	Cytotoxic T-lymphcyte-associated protein 4
CTNNB1	Catenin beta 1
DMEM	Dulbecco's modified eagle medium
DMSO	dimethyl sulfoxide
DNA	deoxyribonucleic acid
EDTA	ethylenediaminetetraacetic acid
EGFR	Epidermal growth factor receptor
EpSSG	European pediatric Soft Tissue Sarcoma Group
ERMS	embryonal rhabdomyosarcoma

et al.	et alia - and others
ETS1	Erythroblastosis proto-oncogene 1
EU	European Union
EXT	extremities
FBS	fetal bovine serum
FC	fold change
FGFR	Fibroblast growth factor receptor
FN	fusion negative
FOXO1	Forkhead box 01
FP	fusion positive
Fwd	forward
g	gram
gDNA	genomic DNA
GOF	gain of function
GRHL3	Grainyhead like transcription factor 3
h	hour
H&E	hematoxylin and eosin staining
HDAC	Histone deacetylase
HER2	Human epidermal growth factor receptor 2
HN-PM	parameningeal tumor
HN-non PM	non-parameningeal head and neck tumor
HPRT1	Hypoxanthine phosphoribosyltransferase 1
HRAS	Harvey rat sarcoma proto-oncogene
HSF1	Heat shock factor 1
i.v.	intravenous
IC50	Inhibitory concentration 50
IGF-1R	Insulin-like growth factor 1 receptor
IHC	immunohistochemistry
Ink4a	Inhibitor of CDK4 A
IRS	Intergroup Rhabdomyosarcoma Studies
IVA	ifosfamide, vincristine, actinomycin D
kg	kilogram
KRAS	Kirsten rat sarcoma proto-oncogene
L	Liter
LB	lysogeny broth
LOF	loss of function

log	logarithm
LOH	loss of heterozygosity
M	molar
MA	Massachusetts
mAb	mouse antibody
MAP	Mitogen-activated protein
MAPK	Mitogen-activated protein kinase
MDC	Max-Delbrück-Centrum für Molekulare Medizin
MDR	multidrug resistance
MEK	Mitogen-activated protein kinase kinase
Met	MET proto-oncogene, receptor tyrosine kinase
mg	milligram
min	minute
mL	milliliter
mm	millimeter
MOI	multiplicity of infection
MPH	MS2-P65-HSF1 activator helper complex
mRNA	messenger RNA
MRP	Multi-drug resistance-associated protein
MS2	Escherichia virus MS2
MYF3	Myogenic Differentiation 1
MYF4	Myogenin
MYOD1	Myogenic differentiation 1
MYOG	Myogenin
n	number of participants
NCOA2	Nuclear receptor coactivator 2
NF1	Neurofibromin 1
NFκB	Nuclear factor kappa-light chain-enhancer of activated B-cells
Ng	nanogram
NGS	Next Generation Sequencing
NIH	National Institutes of Health
nM	nanomolar
NRAS	Neuroblastoma rat sarcoma proto-oncogene
NT	non-targeted
OR	Oregon
ORB	orbita

p value	probability value
P/S	penicillin and streptomycin
P3F1	Paired box 3 - forkhead box 01 fusion
P65	Transcription factor p65
P7F1	Paired box 7 - forkhead box 01 fusion
PA	Philadelphia
PARP	Poly(ADP-ribose)-polymerases
PAX	Paired box
PBS	phosphate buffered saline
PCR	polymerase chain reaction
PD	progressive disease
PD-1	Programmed cell death protein 1
PD-L1	Programmed cell death 1 ligand 1
PDX	patient-derived xenograft
PEI	polyethylimine
pH	power of hydrogen
PIK3CA	Phosphatidylinositol-4,5-bisphosphonate 3-kinase catalytic subunit alpha
PTPN11	Protein tyrosine phosphatase non-receptor type 11
Q score	Phred quality score
qPCR	quantitative polymerase chain reaction
qRT-PCR	real-time quantitative polymerase chain reaction
RAD54L	RAD54 like
RAF	Rat fibrosarcoma
RAS	Rat sarcoma oncogene
Rev	reverse
RIPA	radioimmunoprecipitation assay
RMS	rhabdomyosarcoma
RNA	ribonucleic acid
RP53	Retinitis pigmentosa 53
RPA2	Replication protein A 32 kDa subunit
rpm	revolutions per minute
RPM	reads per million
RPMI	Roswell Park Memorial Institute 1640 Medium
RRA score	Robust ranking aggregation score
rRNA	ribosomal RNA

RTK	Receptor tyrosine kinase
SAM	Synergistic activation mediator
SD	stable disease
sgRNA	single guide ribonucleic acid
SMO	Smoothened
ssRMS	spindle cell/sclerosing RMS
TBS	tris-buffered saline
TP53	Tumor protein p53
Trp53	Cellular tumor antigen 53
UG non-BP	genitourinary non-bladder or prostate tumor
UG-BP	genitourinary bladder or prostate
UKCCCR	United Kingdom Coordinating Committee on Cancer Research
USA	United States of America
UV	ultraviolet
VAC	vincristine, actinomycin D, cyclophosphamide
VEGF	Vascular endothelial growth factor
VGLL2	Vestigial like family member 2
WA	Washington
WB	Western blot
WHO	World Health Organization
WWP2	WW domain containing E3 eubiquitin protein ligase 2
ZFAT	Zinc finger and AT-hook domain containing
µg	microgram
µL	microliter
µm	micrometer
µM	micromolar

3 Abstract

Rhabdomyosarcomas (RMS) are the most common childhood soft tissue tumors. Despite multimodal treatment regimen, around 20% of pediatric sarcoma patients still suffer from local relapses, indicating underlying resistance to common therapy. Translocation of *PAX3* and *FOXO1,* and the expression of the respective fusion protein, is known to predict adverse prognosis, but no significant improvement in patient outcome of these high-risk patients has been achieved in the last three decades. Here, we performed a genome-wide CRISPR activation screen in the fusion-positive cell line Rh4 to search for genes associated with resistance to actinomycin D (ActD), a drug commonly used in the treatment of RMS and other pediatric cancers such as nephroblastoma and Ewing's sarcoma. The top-ranking hit was the gene *ABCC1*, encoding for a drug efflux-pump. The expression of ATP-binding cassette (ABC) transporters like ABCC1 has long been suspected to play a role in multidrug resistance, however small molecule inhibitors targeting them are still not approved for clinical use. In this study, we were able to observe a synergistic relationship between ActD and the ABCC1 inhibitor tetrandrine, implying a possible benefit of the inhibition of ABCC1 in ActD-resistant RMS and highlighting the necessity of further preclinical and clinical investigations into the role of *ABCC1* in RMS in response to treatment.

Rhabdomyosarkome (RMS) sind die häufigsten pädiatrischen Weichteilsarkome. Trotz eines multimodalen Behandlungsansatzes leiden 20% aller pädiatrischen Sarkompatient*innen unter lokalen Rezidiven, was auf zugrundeliegende Resistenzmechanismen schließen lässt. Die Translokation von *PAX3* und *FOXO1* und die Expression des entsprechenden Fusionsproteins sind bekannte negative Prädiktoren für die Prognose von RMS. In den letzten 30 Jahren konnte jedoch keine Verbesserung des Therapieerfolges von Hochrisikopatienten erzielt werden. In dieser Studie nutzten wir einen genomweiten CRISPR-Aktivationsscreen in der fusionspositiven RMS-Zelllinie Rh4, um nach Genen zu suchen, die mit einer Resistenz gegenüber Actinomycin D (ActD) assoziiert sind. Dieses Chemotherapeutikum findet nicht nur bei RMS-Patient*innen, sondern auch in der Behandlung anderer pädiatrischer Tumoren wie dem Nephroblastom und dem Ewing-Sarkom Verwendung. Das Gen mit dem höchsten Rang war die Effluxpumpe *ABCC1*. Obwohl die Expression von ATP-binding cassette (ABC)-Transportern wie ABCC1 schon lange unter dem Verdacht steht, zu Multiresistenzen von Tumoren beizutragen, sind gezielte small molecule-Therapien noch nicht für den klinischen Gebrauch zugelassen. In dieser Studie konnten wir eine synergistische Beziehung zwischen ActD und dem ABCC1-Inhibitor Tetrandrine nachweisen, welches auf einen möglichen Vorteil einer Kombinationstherapie in ActD-resistenten RMS hinweist. Zudem unterstreicht unsere Studie die Notwendigkeit, die Rolle von *ABCC1* in RMS in präklinischen und klinischen Studien weiter zu erforschen.

4 Introduction

4.1 Rhabdomyosarcoma

Rhabdomyosarcomas (RMS) are a unique group of soft tissue neoplasms of mesenchymal origin (5). They are the most common soft tissue sarcoma in children and adolescents aged 20 years and younger. With an annual incidence of 4.5 cases per 1 million children, they account for roughly 4.5% of all pediatric cancers (6, 7). Less commonly found in adults, only 3% of diagnosed adult soft tissue sarcomas are RMS (8). Based on the historic characterization of RMS on histopathology alone, the WHO differentiates four RMS subtypes, namely embryonal (ERMS), alveolar (ARMS), pleomorphic and spindle cell/sclerosing RMS (ssRMS) (9). Advances in technology have allowed greater insight into the tumor pathogenesis enabling a more differentiated risk stratification of RMS in clinical practice and opening up the possibility of targeting molecular features to improve outcomes for patients.

4.1.1 Genetics

In comparison to adult tumors, RMS, like other pediatric tumors, show low rates of somatic mutations (10-12). RMS is associated with familiar cancer predisposition syndromes such as Li Fraumeni syndrome (germline mutation of *TP53*) (13), Costello syndrome (*HRAS* mutation) (14), Beckwith-Wiedemann syndrome (genomic imprinting disorder) (15) and Neurofibromatosis type 1 (mutation of *NF1*) (16). Nonetheless, RMS occurs mainly sporadically without any family history.

Large-scale genomic studies have identified two clearly distinct RMS groups, defined by the presence or absence of a chromosomal translocation that leads to a chimeric protein of *PAX3* or *PAX7* with *FOXO1* genes: Fusion-positive RMS (FP-RMS) and fusion-negative RMS (FN-RMS) (1). FN-RMS tumors are characterized by a heterogenous genetic makeup with an increased rate of point mutations, copy number variations as well as regions with loss of heterozygosity (Fig. 1). One of the most common features is a loss of heterozygosity at 11p15.5, a genetic region controlling for growth and development (17, 18). FN-RMS display a wide range of causative mutations in a few distinct signaling pathways. Interestingly, these pathways are also downstream targets of the PAX fusion protein (Fig. 2). The most common mutations involve the RAS and PIK3CA pathways (19-22). Mutation in genes associated to the RAS/MAPK pathways such as *PTPN11*, *BRAF*, *RAF*, *ALK* and *c-Met*, have been found to be mutated or overexpressed in RMS (23-25), highlighting the importance of this signaling pathway in FN-RMS (1, 26). Additionally, the tumor suppressor gene *TP53* was frequently found to be inactivated by somatic mutations (27). The functional roles of *RAS* and *TP53* were subsequently confirmed in genetically engineered

mouse models, suggesting they drive oncogenic events in some FN-RMS (28). Other commonly found mutations include *FGFR4*, a receptor tyrosine kinase highly expressed in RMS tissue (29), *NF1*, a known tumor suppressor and inhibitor of Ras (30), oncogene *PIK3CA*, proto-oncogene *CTNNB1* (31) and activating mutations of the Hedgehog signaling pathway (30)

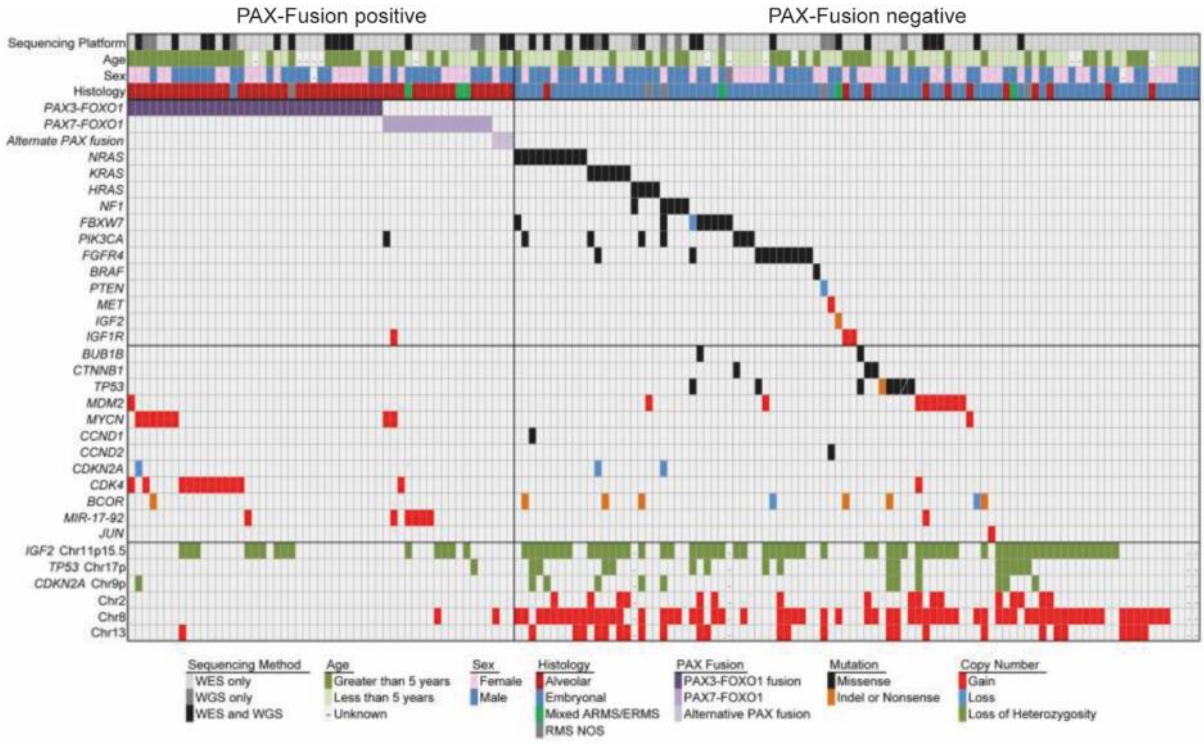

Figure 1: Genomic landscape of RMS.

Adapted from Shern et al. *Cancer Discov*. 2014 (1)

Tumors with a *PAX3* or *PAX7* translocation show only few somatic mutations apart from the translocation (Fig. 1). The chromosomal translocations *t*(2;13)(q35;q14) or *t*(1;13)(p36;q14) fuse the DNA-binding N-terminus of the *PAX3* or *PAX7* gene to the C-terminus of the *FOXO1* gene that contains both a DNA binding domain as well as a transactivation domain (1, 32-34). The resulting fusion encodes a chimeric oncoprotein that acts as a strong transcriptional activator (35, 36). Transcription factors act as control mechanisms that recruit and regulate the transcriptional apparatus (37). Oncogenic fusion genes involving transcription factors are not uncommon and often lead to increased downstream target activation (38). The PAX3-FOXO1 fusion protein is frequently overexpressed in ARMS (39) and has been shown to be a more potent transcriptional activator than wild-type *PAX3* (40). This results in high fusion protein levels in addition to the high activity of the transcription factor. Additionally, the PAX3-FOXO1 fusion protein has been shown to establish myogenic super enhancers in collaboration with myogenic transcription factors and the chromatin reader *BRD4* near genes such as *ALK*, *FGFR4* and *MYCN*, *MYOD1* and *MYOG* (41). Nevertheless, even though PAX-FOXO1 fusion proteins act as oncoproteins by

dysregulating a multitude of cellular pathways (42), genetic systems have shown that a PAX3-FOXO1 fusion alone is not sufficient for the development of RMS *in vivo*. Coexisting loss of function of *Trp53* or *Ink4a/ARF* were necessary for the generation of ARMS in mice models (43).

Even though RMS subtypes are categorized based on their histology, each subtype shows distinct genomic characteristics. Of all ARMS patients, 60% express a PAX3-FOXO1 fusion and 20% express a PAX7-FOXO1 fusion (34, 44), although other rare fusion variants have been reported in a small subset of patients as well (45, 46). Patients with a PAX3-FOXO1 fusion show significantly poorer outcome when compared to PAX7-FOXO1-positive patients (47). 20% of ARMS patients lack the expression of a fusion protein (48) and even though they show an alveolar histology, these tumors behave similarly to ERMS regarding clinical outcome and share similar somatic mutations, mutational burden and expression profiles (1, 49). This has led to an increased categorization of RMS based on the fusion status instead of the traditional histology-based separation of ERMS and ARMS and put a greater focus on the development of therapies directly aimed at the genomic alterations underlying RMS.

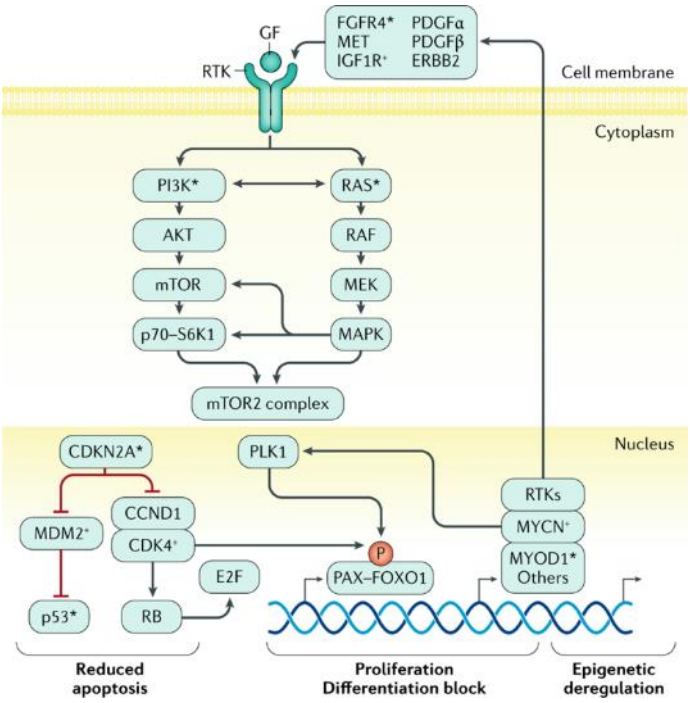

Figure 2: Key pathways affected in both PAX fusion positive and negative RMS.

From Skapek et al. *Nat Rev Dis Primer* 2019 (*2*)

4.1.2 Targeted therapies in RMS treatment

A multitude of clinical trials are currently focusing on specifically targeting RMS using new cytotoxic agents, new combinations of cytotoxic drugs, targeted therapies, immunotherapies or allogenic transplants (Table 1). Due to the rarity of RMS, these studies often focus on targets and drugs that have already been studied or approved in other cancers, such as bevacizumab, a monoclonal antibody targeting VEGF already approved for the treatment of metastatic colon and breast cancer, non-small-cell lung cancer, glioblastoma and other tumor types (50).

In FP-RMS, the PAX3-FOXO1 fusion presents the most direct target for therapy. Although transcription factors were once deemed as “undruggable” (51), multiple approaches to inhibition of transcription factors have shown promising results (52). The HDAC inhibitor entinostat was found to transcriptionally suppress the *PAX3-FOXO1* fusion gene and is currently being tested in

Phase I and Phase II trials (53). While treatments have been developed that successfully target oncogenic fusion proteins involved in signal transduction such as the *BCR-ABL* fusion in leukemia, drugs directly targeting the PAX3-FOXO1 fusion protein have yet to enter clinical trials (54). Nevertheless, downstream targets of PAX3-FOXO1, such as FGFR4 and ALK1 could potentially be used to treat FP-RMS. Indeed, the ALK inhibitor crizotinib is currently being tested in a Phase II trial in patients with advanced tumors caused by either *ALK* or *MET* alterations (55, 56). As mutations in the FGFR pathways have been found in various sarcoma subtypes, the FGFR inhibitor erdafitinib is being studied in patients with solid tumors, non-Hodgkin lymphoma or histiocytic disorders with FGFR mutations (57). Though FN-RMS do not have unifying mutations that could be targeted broadly, they frequently show alterations in the RAS/MAPK-pathway, which could be targeted through inhibition of MEK (58). The MEK1-inhibitor cobimetinib is currently in Phase I and II clinical trials (Table 1). Other drugs currently being tested in clinical trials in patients with rhabdomyosarcoma include the PI3K/TOR inhibitor temsirolimus (59), the PARP inhibitor olaparib (60) and PD-L1 inhibitors, though first results show no significant single-drug activity of nivolumab in common pediatric solid tumors (61). Despite these developments, the majority of patients with RMS are currently still being treated with surgical resection, radiotherapy and chemotherapy alone, highlighting the need to improve the current treatment regimen that is mostly based on the histopathological subtypes and clinical presentation while waiting for the approval of newer, more targeted drugs.

Table 1: Examples of current targeted therapies in clinical trials for RMS.

Shortened and adapted from Chen et al. *Front Oncol.* 2019 © Chen, Dorado Garcia, Scheer and Henssen (62)

Molecular Target	**Drug**	**Phase**	**Clinicaltrialsregister.eu identifier (European)**	**Clinicaltrials.gov identifier (USA)**
VEGF	Bevacizumab (mAb)	II	2013-003595-12	NCT01222715 NCT00643565
HDAC	Entinostat, Vorinostat	I/II	2008-008513-19; 2018-000127-14	NCT02780804 (Entinostat)
ALK	Crizotinib	II	2011-001988-52	
FGFR	Erdafitinib	II		NCT03210714; NCT03155620
PI3K/mTOR	Omipalisib, Temsirolimus	I/II	2007-000371-42	NCT00106353; NCT01222715
MEK1	Cobimetinib	I/II	2014-004685-25	
PARP	Olaparib	II		NCT03233204

PD-1/PD-L1	Nivolumab, Pembrolizumab, Atezolizumab	I/II	2014-004697-41; 2018-000127-14	NCT02304458

4.1.3 Histology

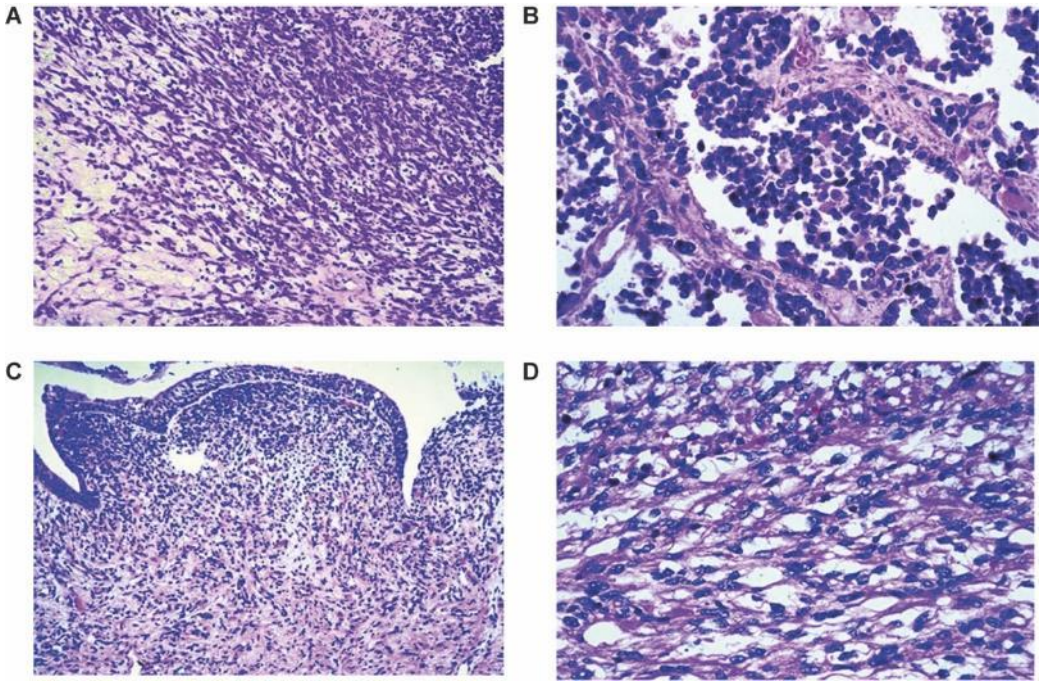

Figure 3: Histology of RMS.

(A) ERMS. Tumor shows dense condensation of rhabdomyoblasts in a loose myxoid stroma. (B) ARMS. Nests of round cells are separated by fibrous septa. (C) Botryoid RMS. Small-cell neoplasms with a condensation of tumor cells in subepithelial zone. (D) Spindle cell RMS. Spindle-shaped cells reminiscent of smooth muscle tumors. Reprinted from Parham D. *Mod Pathol* 2001 (3)

RMS are malignant tumors that resemble muscle progenitor cells (63), though they can arise from non-skeletal tissue as well (64). Due to this, the diagnosis of RMS depends on the identification of embryonic myogenesis, mostly defined by the presence of rhabdomyoblasts. The primitive mesenchymal cells show diverse degrees of differentiation and present histologically as variably shaped cells with dense eosinophilic cytoplasm, occasional round, eccentric nuclei and cytoplasmic cross-striations (5). Nevertheless, rhabdomyoblastic elements are not specific to RMS, but can also be found in other sarcomas, including malignant mesenchymoma, chondrosarcoma and liposarcoma (65). RMS tumor samples are usually obtained through small tissue needle biopsies or surgical resection and stained for myogenic markers such as desmin, muscle specific actin, myosin and myoglobin (66). Other immunohistochemical markers used to identify RMS are nuclear transcription factors that are aberrantly re-expressed in RMS, like MYOD1 and myogenin, which are both involved in the initiation of myogenesis (67-69). While myogenin is a highly sensitive and specific marker, other spindle cell soft tissue tumors can also

express the protein in rare cases (70). Though immunostaining is recommended for the diagnosis of RMS, it has no role in the differentiation of the RMS subtypes.

The classification of RMS is based on the distinct histopathological presentations of RMS and was first proposed by Horn and Enterline in 1958 (71). Smaller modifications to this classification over the years have led to the WHO-classification used today (9). ERMS show variable degrees of embryonic rhabdomyogenesis and present as small, round to elongated cells. These cells are packed into a mucus-like (myxoid) matrix with varying degrees of density (Fig. 3A). ARMS, on the other hand, vaguely resemble fetal alveoli when regarded through a microscope. The tumor cells are separated into smaller nests by intersecting fibrous septa (Fig. 3B). Though botryoid RMS got its name by the grape-like polypoid growth of the tumor, it is defined by a cambium layer - an epithelium with heightened subepithelial cellularity (Fig. 3C). Spindle-cell RMS is defined by the presence of at least 80% spindle cells with cigar-shaped nuclei (Fig. 3D). Pleomorphic RMS also show spindle cells, though they are arranged into large, intersecting bundles and carry hyperchromatic, irregularly-shaped nuclei with prominent nucleoli (72). As the histopathological markers mentioned above do not clearly differentiate RMS from other potentially myogenic neoplasms such as nephroblastoma, carcinosarcoma, Sertoli-Leydig cell tumor or malignant peripheral nerve sheath tumor, combining histopathological findings with the clinical presentation of the patient are critical to the management of the RMS patients.

4.1.4 Clinical presentation

The clinical presentations of RMS are heterogeneous and most often determined by the location of the primary tumor, the patient's age and the presence or absence of metastases (73). Showing distinct clinical, histologic and molecular characteristics, the various subtypes affect clinical outcome and the therapeutic approach (74).

ERMS is the most common subtype, making up 60% of all RMS cases. It is most often found in children under the age of five (63) and is usually located in the genitourinary tract or the head and neck region. It carries a favorable outcome (8).

ARMS is the most undifferentiated and aggressive subtype of RMS, comprising 20% of all diagnosed RMS cases (63). The aggressive nature and subsequent worse prognosis of ARMS was first observed in the late 1980s, where the first Intergroup Rhabdomyosarcoma Studies showed that ARMS were associated with higher clinical risk groups and a 75^{th} percentile estimate of survival duration of only 14 months (75). It occurs more frequently in adolescents and is usually found in the extremities, the genital region and the head and neck region, although other locations may be affected as well.

In contrast to other RMS subtypes, pleomorphic RMS most commonly affects adults between the ages of 60 and 80. Although it can be found in pediatric patients as well, less than 1% of pediatric

RMS are pleomorphic RMS (76). It shows complex karyotypes with no recurrent structural alterations (77) and primarily presents in the extremities, the chest and the abdomen. Not only do the clinical localization and the increased age of the patients contribute to a poor prognosis of pleomorphic RMS, but pleomorphic RMS have an overall poor survival compared to other adult sarcomas, with a majority of pleomorphic RMS cases metastasizing within the first 5 years of diagnosis (78, 79).

SsRMS has only recently been defined as a separate RMS subtype (9). Spindle cell RMS had previously been categorized as a prognostically favorable variant of ERMS and sclerosing RMS was first described as a hyaline sclerosing form of RMS with a pseudovascular growth pattern (80, 81). As both spindle cell RMS and sclerosing RMS show significant morphological overlap and have similar clinical localizations in the paratesticular and head and neck region, they are nowadays grouped together as ssRMS (82). They account for 5-10% of all RMS and can be divided into two further subgroups according to mutational status. SsRMS with NCOA2 gene rearrangements or NCOA2-VGLL2 fusions are mostly found congenitally or in infants and have a favorable prognosis (83). Due to the good prognosis, these patients are not treated with the same multimodal treatment regimen as patients with ARMS or even ERMS (84). Mutations in MYOD1 on the other hand, have a poor prognosis and occur in older children and adults (85). Due to the rarity of pleomorphic RMS and ssRMS, this manuscript will focus on ARMS and ERMS subtypes going forward.

4.1.5 Treatment protocols

RMS is a rare disease, which has made international cooperative trials crucial for the treatment and clinical study of the disease. RMS treatment is managed in regional groups such as the *Cooperative Weichteilsarkom Studiengruppe der Gesellschaft für pädiatrische Onkologie und Hämatologie* that focusses on the German speaking parts of the EU (86), the European pediatric Soft Tissue Sarcoma Study Group (EpSSG) that acts in the remaining European countries as well as Argentina, Brazil and Israel (87) and the Children's Oncology Group in North America (88). The risk stratification of RMS patients currently includes patient age, tumor size and site, lymph node involvement, possible metastases and the surgical group classification (Table 2) (89). Nevertheless, studies have shown that fusion status is the second most important risk factor next to metastatic status (90), which has led upcoming EpSSG trials to categotize RMS based on fusion status instead of histological classification (91).

Table 2: Risk stratification of RMS patients.

IRSG: Classification according to the Intergroup Rhabdomyosarcoma Study Group: Tumor completely resected (I), with microscopic margins (II), visual margins (III) or distant metastasis (IV). ORB: orbit; UG non-BP: genitourinary non-bladder or prostate tumor; HN-non PM: non-parameningeal head and neck tumor; HN-PM: parameningeal tumor; UG-BP: genitourinary bladder or prostate; EXT: extremities, adopted from Dasgupta et al. *Semin Pediatr Surg.* 2016 (7)

<table>
<tr><th>Metastasis</th><th>N-Status</th><th>Pathology</th><th>IRSG</th><th>Localization</th><th>Size/age</th><th>Subgroup</th><th>Risk-group</th></tr>
<tr><td rowspan="8">M0</td><td rowspan="6">N0</td><td rowspan="6">ERMS</td><td rowspan="2">I</td><td rowspan="2">Any</td><td>≤ 5 cm and < 10 years</td><td>A</td><td>Low</td></tr>
<tr><td>> 5 cm or ≥ 10 years</td><td>B</td><td rowspan="3">Standard</td></tr>
<tr><td rowspan="3">II, III</td><td>ORB, UG-non, BP, HN-non, PM</td><td>Any</td><td>C</td></tr>
<tr><td rowspan="2">EXT, UG-BP, HN-PM, others</td><td>≤ 5cm and < 10 years</td><td>D</td></tr>
<tr><td>> 5 cm or ≥ 10 years</td><td>E</td><td rowspan="3">High</td></tr>
<tr><td>N1</td><td>ERMS</td><td>II, III</td><td colspan="2">Any</td><td>F</td></tr>
<tr><td>N0</td><td>ARMS</td><td colspan="3">Any</td><td>G</td></tr>
<tr><td>N1</td><td>ARMS</td><td colspan="3">Any</td><td>H</td><td rowspan="2">Very high</td></tr>
<tr><td>M1</td><td colspan="6">Any</td><td>I</td></tr>
</table>

Ever since multi-agent chemotherapy started to be consistently used in the 1970s, the survival of pediatric RMS patients has improved dramatically from less than a third to a long-term survival rate of 70% (92, 93). The treatment of first-line RMS is currently based on a multimodal treatment protocol including a chemotherapy backbone, surgical resection and/or radiotherapy. The chemotherapy backbone used varies depending on the region: the North American regimen includes vincristine, actinomycin D (ActD) and cyclophosphamide (VAC regimen) (94) while in Europe cyclophosphamide is substituted by ifosfamide (IVA regimen) (95). As randomized trials have found no significant difference in patient outcome, the differing backbones continue to be used in their respective regions (96). Except for minor changes in duration of treatment, dosage

of drugs and the route of administration to maximize treatment efficiency while minimizing side effects, these chemotherapy backbones have remained the same since they were first established four decades ago (62, 97). RMS patients are treated based on their risk stratification. In the EpSSG treatment protocol, patients in the lowest risk group receive a local resection of the tumor and a combination of vincristine and ActD, while all following risk groups are treated with an IVA protocol in varying intensities with or without radiotherapy. Patients with stable disease (SD; tumor volume reduction <33%) or progressive disease (PD) proceed to the second line treatment. The treatment regimen then contains drugs not previously administered, such as topotecan, carboplatin or doxorubicin. If the tumor does not respond to the second line treatment, other chemotherapy regimen and local treatments are considered (72).

At the start of the 20th century, chemotherapy emerged as a new way to treat cancer. A plethora of compounds was screened on rodent models and patients, and polychemotherapy backbones were empirically determined without the knowledge of the underlying molecular determinants of chemosensitivity (98). While survival rates have greatly improved and currently range from 70-80% (78, 96), these improvements are mostly the result of decreased mortality of patients suffering from localized disease and patients with stage 4 disease still have a long-term event-free survival of less than 30% (99). The most common therapy failure nowadays is due to relapse of the primary tumor, with around 20% of pediatric sarcoma patients developing local relapses with or without combined systemic or lymph node relapse (95). Furthermore, there has not been significant progress in the outcome of RMS patients with advanced or metastatic disease, highlighting the need for further development of RMS treatment.

As all RMS patients receive vincristine and ActD independent of their risk group and location, optimizing these two therapy components could lead to better patient outcome without the need for extensive clinical testing of new drugs. While a multitude of studies focus on the understanding and reversal of vincristine resistance in adult cancers as well as neuroblastomas (100-102) mechanisms behind ActD-resistance are still poorly understood.

4.2 Actinomycin D

ActD is a cyclic polypeptide antibiotic first isolated from *Streptomyces antibioticus* in 1940 by Waksman and Woodruff (103) and is produced by many *Streptomyces* strains (104). Its anti-carcinogenic effect was first demonstrated 12 years later in 1952 (105) and soon after, clinical studies provided sufficient evidence for ActD to be commonly used in selected pediatric cancers (106). Today it is a standard chemotherapeutic drug for pediatric cancers such as RMS (95), nephroblastoma (107), Ewing sarcoma (108) and adult cancers including gestational trophoblastic neoplasia (109). Apart from its use in clinical practice as a chemotherapeutic drug, ActD is commonly used in research as an inhibitor of transcription (110).

4.2.1 Mechanism of action

Actinomycins are a family of chromopeptides composed of chromophores and two cyclic pentapeptide lactone rings (Fig. 4A) (104). Depending on the concentrations used, ActD can block both RNA expression and DNA replication. The aromatic ring intercalates into a pre-melted form of DNA called β-DNA, which can be found in transcription bubbles (4). The pentapeptide chains then lie in the minor groove of the DNA and form strong hydrogen bonds to guanine residues of the opposite DNA-chain, resulting in a severely distorted and slightly kinked, stable DNA-drug complex (Fig. 4B) (111, 112). Although ActD preferentially binds between a GpC nucleotide sequence, other binding sites and external binding to DNA have been reported as well (113-116). Through the intercalation, ActD immobilizes the transcriptional complex and impedes RNA synthesis by stabilizing topoisomerase I-DNA covalent complexes (117). Additionally, ActD stimulates cleavage induced by DNA topoisomerases I and II (118). Ribosomal RNA (rRNA) is most sensitive to ActD treatment, further inhibiting protein expression, although transcription resumes several hours after ActD had been removed from a cell culture medium in *in vitro* experiments (119-121). ActD induces the formation of γ-H2AX foci, indicating the presence of genotoxic stress, such as double strand breaks or stalled replication forks (122). Studies have shown that ActD not only inhibits transcription, but can inhibit the initiation of DNA replication, induce apoptosis via the p53-pathway and lead to cell death independent of p53 as well (123-125).

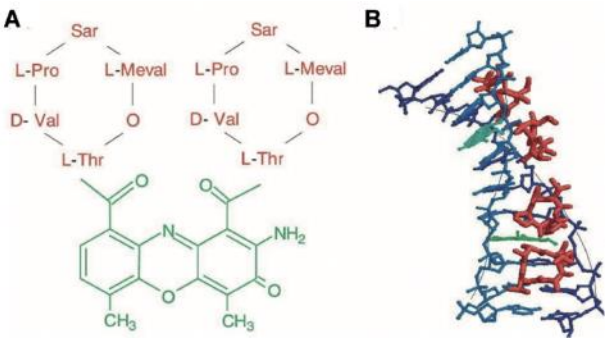

Figure 4: Chemical structure of ActD and its interaction with double strand DNA.

(A) Structure of ActD. The chromophore ring system is depicted in green, the pentapeptide lactone rings in red. (B) Model of 2 ActD molecules interacting with two DNA strands. Reprinted from Paramanathan et al., *Nucleic Acids Res*. 2012 (4)

4.2.2 Side effects of chemotherapy

Despite efforts to decrease the side effects of cancer treatments, pediatric patients still suffer from acute and long-term consequences of anti-cancer therapy. Acute side effects such as nausea and renal failure occur directly during or shortly after the administrations of chemotherapeutic agents and can be dose-limiting (126, 127). These side effects are not limited to pediatric patients but pose a great challenge in all oncologic patients. The long-term sequelae, however, have an especially great impact on pediatric patients, as they can persist for a long time after the primary cancer has been treated.

Cancer treatment leads to chronic medical problems that result in poor psychosocial health and health-related quality of life (128, 129). The development of secondary malignant neoplasms with

worse outcomes when compared to primary tumors is a well-known late effect of cancer treatment (130). Sarcoma patients are especially at risk, as they develop subsequent neoplasms in 6-10% of cases, one of the highest rates in pediatric oncology (131, 132). While the development of side effects is inherent to cancer treatment, the over-treatment of patients with non-suitable chemotherapy should be avoided at all costs. Tumors do not always respond to chemotherapy and relapses still pose a great challenge in RMS treatment today. Increased knowledge of resistance mechanisms to the specific drugs used in RMS could help in reducing inadequate therapies administered to patients by predetermining the tumors' drug sensitivity profile.

4.2.3 Resistance mechanisms

One of the main challenges of chemotherapy is the development of resistance to anti-cancer drugs. The treatments may induce multidrug resistance (MDR), associated with the expression of P-glycoproteins, drug efflux pumps modifying the cells' sensitivity to a variety of drugs through decreased cellular accumulation (133). Hill et al. confirmed ActD as a substrate for numerous drug efflux pumps in RMS. In mouse models, overexpression of ABCB1, ABCC1, ABCC2 and ABCG2 leads to lower intracellular accumulation of ActD and higher plasma concentrations of ActD (134, 135). Additionally, Prados et al. confirmed the induction of a MDR phenotype in ERMS mediated by the P-glycoprotein MDR1, also known as ABCB1, by *in vivo* treatment with polychemotherapy (136). Although it has been shown that polymorphisms in the *ABCB1* gene affect P-glycoprotein-mediated transport of ActD *in vitro* (137), no correlation between *ABCB1* genotypes and key pharmacokinetic parameters such as the systemic clearance of ActD could be observed in pediatric patients (138). These findings highlight the need for further insights into the development of chemoresistance in RMS and the use of novel methods to bridge the gap between *in vitro* modelling and the treatment of patients in daily clinical routine.

Resistance to chemotherapy can be defined as the ability of cancer cells to survive despite antineoplastic treatment and can be categorized into two main subgroups: primary and secondary chemoresistance. Primary chemoresistance describes the inherent resistance of tumors to certain drugs. This is mostly linked to intratumor heterogeneity. A tumor does not consist of identical cells and there is a possibility that subpopulations of tumor cells show inherent resistance to the chemotherapeutic drug used. During treatment, the resistant cells survive and are able to multiply, causing either primary drug failure or relapses. Secondary resistances are the resistance mechanisms that develop after the cancer cell has been exposed to the respective drug (139, 140). Differentiating between these two mechanisms of chemoresistance poses great challenges. As most experimental set-ups study bulk populations of cancer cells, it cannot be determined if certain tumor cells are inherently resistant to the treatment used or if they developed the resistance only after contact with the drug. To separate the two mechanisms, one would have to

resort to single cell technologies. Chen et al., for example, used single cell technologies to identify diverse tumor subpopulations and their influence on differential primary response to chemotherapy (141).

4.3 CRISPR technology in the study of drug resistance

While studying mechanisms of chemoresistance in rare cancers, one must often rely on a limited number of cell lines that do not always portray the same spectrum of drug responses as patient tumors. To increase the ability to study these mechanisms, one can either enrich for resistant cell populations by treating tumor cells with an increasing concentration of the drug in question, or specifically induce genetic perturbations with the intent of inducing chemoresistance. The genetic changes can be classified into two main categories: loss of function or gain of function. Research centering on loss of function has mostly been based on RNA interference, a method enabling a genome-scale screen for specific phenotypes (142, 143). Genome-scale screenings of gain of function perturbations have been limited due to the cost and complexity of complementary DNA (cDNA) library overexpression systems that are often difficult to clone (144).

The use of RNA-guided endonuclease Cas9 of the bacterial CRISPR antiviral system has enabled a simpler way to modify specific genomic loci and has made the transduction of large libraries possible in size-restricted vector systems (130). The Cas9 is directed to specific locations in the genome by single guide RNAs (sgRNAs) that are complementary to the target DNA sequence. Here, the endonuclease cleaves the DNA, resulting in a loss of function of the respective gene (145). It is also possible to use a catalytically inactive Cas9 (dCas9) to modulate gene expression of a target gene without DNA cleavage. Nevertheless, gene activation achieved though sgRNAs alone is limited, leading to the need of activation systems to increase gene expression (146). In 2012, Konermann *et al*. first established a genome-scale CRISPR-Cas9 complex-based screen with the addition of three activation domains, resulting in stable gene overexpression with minimal off-target activity. In natural systems, locally concentrated transcription factors lead to the induction of transcription and the coordinated response of the transcription machinery (147). To mimic this response, they introduced a hairpin aptamer that leads to selective binding of dimerized MS2 bacteriophage coat proteins, which recruits the transcription factor VP64. Additionally, they used P65, a NFκB transactivating subunit that shares

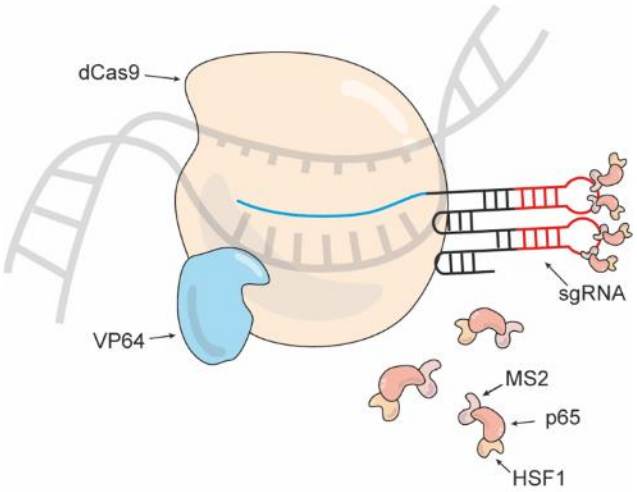

Figure 5: Schematic depiction of SAM activation complex bound to DNA

common co-factors with VP64 but recruits a distinct subset of transcription factors and chromatin remodeling complexes. The activation domain of HSF1 was added as the third activation domain (Fig. 5). This combination of sgRNA, dCas9-VP64 and MS2-p65-HSF1 is summarized under the name synergistic activation mediator (SAM) and leads to highly improved gene overexpression in comparison to earlier activation complexes (144, 148). Konermann *et al*. used this SAM-mediated gene activation to create a pooled, genome-scale transcriptional activation screening with robust transcription at a low multiplicity of infection (MOI), confirming known resistance mechanisms to BRAF inhibitors in melanoma and suggesting new mechanisms of resistance through an unbiased screening. Forward genetic screenings are a powerful tool for the unbiased discovery and functional characterization of specific genetic elements associated with a phenotype of interest that can be used to study a wide array of resistance mechanisms in tumors (149).

5 Objectives

Despite great advances, the outcome of children with high-risk RMS remains very low. While the multi-faceted treatment regimen often leads to primary remission, many patients suffer from relapses, indicating the development of resistance to the drugs used. The current treatment protocol counteracts this with the introduction of additional cytotoxic drugs, though this inevitably brings a higher risk of life-threatening acute toxicities and increased late effects. Additionally, there is a consensus that current treatments have reached their maximum capabilities. ActD is a chemotherapeutic used on RMS patients of all risk groups, though the mechanisms underlying resistance to ActD are not yet fully understood. A greater understanding of these mechanisms could lead to a more specific treatment of patients, as resistant tumors could be identified beforehand and the treatment protocol altered accordingly. Additionally, these resistance mechanisms could potentially be specifically circumvented, rendering the tumor sensitive to the first line drug. In view of the above, this study has focused on the following questions:

1. Are any known markers associated with a resistance to ActD in RMS cell lines?

2. The activation of which genes leads to an increased resistance to ActD in a high-risk RMS cell line?

3. Can the activated genes be circumvented to sensitize RMS cell lines to ActD?

6 Material and Methods

6.1 Material

6.1.1 Technical equipment

6.1.1.1 Scales

Name	Manufacturer
Precision scale 572	Kern & Sohn GmbH, Balingen, DE
Research R200D analytical balance	Sartorius AG, Göttingen, DE

6.1.1.2 Water baths

Name	Manufacturer
Water bath WTB15	Memmert GmbH + Co. KG, Schwabach, DE
Water bath WBT12	Carl Roth GmbH + Co. KG, Karlsruhe, DE

6.1.1.3 Cell culture

Name	Catalog Nr.	Manufacturer
BINDER™ Series CB CO_2 Incubator, 210L, Stainless Steel	15602206	Thermo Fisher Scientific, Waltham, MA, US
Thermo Scientific™ Safe 2020 Class II Biological Safety Cabinets	51026638	Thermo Fisher Scientific, Waltham, MA, US
AC 02 aspiration system	981423101	Andreas Hettich GmbH & Co. KG, Tuttlingen, DE
TC20™ automated cell counter	1450102	Bio-Rad Laboratories, Inc., Hercules, CA, US
Cell Counting Slides for TC10™/TC20™ Cell Counter, Dual chamber	1450011	Bio-Rad Laboratories, Inc., Hercules, CA, US
FALCON® 100 mm TC-treated Cell Culture Dish	353003	Corning Inc., Corning, NY, US
FALCON® 50 mm TC-treated Cell Culture Dish with 20 mm Grid	353025	Corning Inc., Corning, NY, US
FALCON® 175cm^2 Rectangular Straight Neck Cell Culture Flask with Vented Cap	353112	Corning Inc., Corning, NY, US

FALCON™ 15 mL Conical Centrifuge Tubes	10773501	Thermo Fisher Scientific, Waltham, MA, US
FALCON™ 50 mL Conical Centrifuge Tubes	10788561	Thermo Fisher Scientific, Waltham, MA, US
Injekt® Luer Solo 20 mL	4606205V	B. Braun Melsungen AG, Melsungen, DE
Syringe-driven filters 0,22 µm	FCA206030	Guangzhou Jet Bio-Filtration Co., Ltd., Guangzhou, CN
Syringe-driven filters 0,45 µm	FCA406030	Guangzhou Jet Bio-Filtration Co., Ltd., Guangzhou, CN
Argos Technologies Pipetting Reservoir, 25mL Capacity	B3125-100NS	Cole-Parmer Instrument Company, LLC., Vernon Hills, IL, US
Argos Technologies Pipetting Reservoir, 50 mL Capacity	B3150-50	Cole-Parmer Instrument Company, LLC., Vernon Hills, IL, US
Argos Technologies Pipette Basins, 12 Channel x 3 mL	GZ-04395-33	Cole-Parmer Instrument Company, LLC., Vernon Hills, IL, US
Micro tube 0.5 mL SafeSeal	72.704.400	Sarstedt AG & Co. KG, Nümbrecht, DE
Micro tube 1.5 mL SafeSeal	72.706.400	Sarstedt AG & Co. KG, Nümbrecht, DE
Micro tube 2.0 mL SafeSeal	72.695.400	Sarstedt AG & Co. KG, Nümbrecht, DE
Multiply®-µStrip Pro 8-strip	72.991.002	Sarstedt AG & Co. KG, Nümbrecht, DE
Brady™ BMP™21 LAB Label Printer	15208957	Thermo Fisher Scientific, Waltham, MA, US
Gene Pulser/MicroPulser Electroporation Cuvettes, 0.2 cm gap	1652086	Bio-Rad Laboratories, Inc., Hercules, CA, US
MicroPulser™ Electroporator	1652100	Bio-Rad Laboratories, Inc., Hercules, CA, US

6.1.1.4 Bacteria work

Name	Catalog Nr.	Manufacturer
Campingaz™ Labogaz 206 Bunsen Burner	10710232	Thermo Fisher Scientific, Waltham, MA, US
Heratherm™ incubator environmental chamber	50129111	Thermo Fisher Scientific, Waltham, MA, US
Ultrospec™ 1100 *pro*	80-2112-00	Amersham plc, Little Chalfont, UK
Semi-micro cuvettes	67.742	Sarstedt AG & Co. KG, Nümbrecht, DE
ColiRollers™ plating beads	71013	MilliporeSigma, Burlington, MA, US
Petri dish, 94/16 mm, with vents	633180	Greiner Bio-One, Kremsmünster, AT
FALCON™ Round-Bottom Polystyrene Test Tubes	10568531	Thermo Fisher Scientific, Waltham, MA, US
Parafilm® “M” Laboratory film	P7793	Merck Group, Darmstadt, DE
Amicon Ultra-15 Centrifugal Filter Unit with Ultracel-100 membrane	UFC910008	MilliporeSigma, Burlington, MA, US

6.1.1.5 Microscope

Name	Manufacturer
Revolve	Echo, San Diego, CA, US

6.1.1.6 Centrifuges

Name	Catalog Nr.	Manufacturer
Centrifuge 5810 R	5811000015	Eppendorf AG, Hamburg, DE
Centrifuge 5424 R	5404000210	Eppendorf AG, Hamburg, DE
mySPIN 6 Mini Centrifuge	75004061	Thermo Fisher Scientific, Waltham, MA, US
Centrifuge 5427 R	5409000535	Eppendorf AG, Hamburg, DE
E-Centrifuge	1090003	Wealtech Corporation, Sparks, NV, US

6.1.1.7 Shakers

Name	Catalog Nr.	Manufacturer
Reax top	541-10000-00	Heidolph Instruments, Schwabach, DE
Reax 2000 Vortexer	HEIREAX2000	Heidolph Instruments, Schwabach, DE
RS-TR05	XK30.1	Phoenix Instrument GmbH, Garbsen, DE
Vortex-Genie 2	SI-0236	Scientific Industries, Inc., Nohemia, NY, US
MS3 basic	0003617000	IKA-Werke, Staufen im Breisgau, DE
Stirrer RCT basic	0003810000	IKA-Werke, Staufen im Breisgau, DE
Thermomixer compact	T1317	Eppendorf AG, Hamburg, DE

6.1.1.8 Plate reader and plates

Name	Catalog Nr.	Manufacturer
Costar® Assay plate 96 well, white	CLS3922-100EA	Corning Inc., Corning, NY, US
TC plate 6 well standard f	83.3920	Sarstedt AG & Co. KG, Nümbrecht, DE
TC plate 12 well standard f	83.3921	Sarstedt AG & Co. KG, Nümbrecht, DE
TC plate 48 well standard f	83.3923	Sarstedt AG & Co. KG, Nümbrecht, DE
TC plate 96 well standard f	83.3924	Sarstedt AG & Co. KG, Nümbrecht, DE
Microtest Plate 96 Well, F	82.1581	Sarstedt AG & Co. KG, Nümbrecht, DE
SYNERGY™ LX Multi-Mode Microplate Reader		BioTek Instruments, Inc., Winooski, VT, US

6.1.1.9 PCR

Name	Catalog Nr.	Manufacturer
Mastercycler® nexus GX2	6336000015	Eppendorf AG, Hamburg, DE

CFX97 Touch Real-Time PCR Detection System	1855195	Bio-Rad Laboratories, Inc., Hercules, CA, US
Microwave 800W		SEVERIN
PCR workstation	732-2542	VWR International, Radnor, PA, US
FrameStar® 96 Well Skirted PCR Plate	4ti-LB0960	4titude, Wotton, UK

6.1.1.10 Western Blot

Name	Catalog Nr.	Manufacturer
PowerEase™ 300W Power Supply	PS0301	Thermo Fisher Scientific, Waltham, MA, US
2-Gel Tetra and Blotting Module	1660827EDU	Bio-Rad Laboratories, Inc., Hercules, CA, US
Invitrogen™ XCell *SureLock*™ Mini-Cell	EI0001	Thermo Fisher Scientific, Waltham, MA, US
PVDF Western Blotting Membranes	03010040001	Roche Holding AG, Basel, CH
ChemiDoc™ XRS+ system	1708265	Bio-Rad Laboratories, Inc., Hercules, CA, US

6.1.1.11 Fridges and freezers

Name	Catalog Nr.	Manufacturer
Glass line		Liebherr, Bulle, CH
Premium no – frost		Liebherr, Bulle, CH
ProfiLine		Liebherr, Bulle, CH
BioCision® CoolCell® FTS30	BCS-170	Brooks Life Sciences, Chelmsford, MS, US
Nalgene® Mr. Frosty™ Cryo Freezing Container	5100-0001	Thermo Fisher Scientific, Waltham, MA, US
CryoPure Tube 1.6 mL white	72.380	Sarstedt AG & Co. KG, Nümbrecht, DE
Comfort		Liebherr, Bulle, CH
CryoPlus™ Lagerungssystem	7406	Thermo Fisher Scientific, Waltham, MA, US
CRYOSPEED® MED	7727-37-9	Linde plc, Dublin, IE

MDF-U700VX		Sanyo Electric Co., Ltd., Osaka, JP

6.1.1.12 Pipettes and pipette tips

Name	Catalog Nr.	Manufacturer
PIPETBOY pro	156 401	Integra lifesciences, Plainsboro Township, NJ, US
Easypet® 3	4430000018	Eppendorf AG, Hamburg, DE
S1 Pipet Filler	9521	Thermo Fisher Scientific, Waltham, MA, US
Accu-jet® pro	26300	Brand GmbH & Co. KG, Wertheim, DE
Eppendorf Research® plus 0,1 – 2,5 µL	3123000012	Eppendorf AG, Hamburg, DE
Eppendorf Research® plus 0,5 - 10 µL	3123000020	Eppendorf AG, Hamburg, DE
Eppendorf Research® plus 2 - 20 µL	3123000098	Eppendorf AG, Hamburg, DE
Eppendorf Research® plus 10 - 100 µL	3123000047	Eppendorf AG, Hamburg, DE
Eppendorf Research® plus 20 - 200 µL	3123000101	Eppendorf AG, Hamburg, DE
Eppendorf Research® plus 100 - 1000 µL	3123000063	Eppendorf AG, Hamburg, DE
Eppendorf Research® plus 12-channel 10 – 100 µL	3125000044	Eppendorf AG, Hamburg, DE
Multipipette® E3	4987000371	Eppendorf AG, Hamburg, DE
SurPhob SafeSeal Spitzen 10 µL	VT0200	Biozym Scientific GmbH, Hessisch Oldendorf, DE
SurPhob SafeSeal Spitzen 100 µL	VT0230	Biozym Scientific GmbH, Hessisch Oldendorf, DE
SurPhob SafeSeal Spitzen 200 µL	VT0240	Biozym Scientific GmbH, Hessisch Oldendorf, DE
SurPhob SafeSeal Spitzen 1250 µL	VT0270	Biozym Scientific GmbH, Hessisch Oldendorf, DE
Falcon® Serological pipet 5 mL	357543	Corning Inc., Corning, NY, US
Falcon® Serological pipet 10 mL	357551	Corning Inc., Corning, NY, US
Falcon® Serological pipet 25 mL	357525	Corning Inc., Corning, NY, US
Argos Technologies® Plastic Pasteur Pipettes	GZ-04395-12	Cole-Parmer Instrument Company, LLC., Vernon Hills, IL, US

Pasteur pipettes, without cotton plug	4522.1	Carl Roth GmbH + Co. KG, Karlsruhe, DE
Combitips® advanced 2,5 mL	0030089421	Eppendorf AG, Hamburg, DE
Combitips® advanced 0,5 mL	0030089448	Eppendorf AG, Hamburg, DE
SurPhob Spitzen Reload 10 µL	VT0103	Biozym Scientific GmbH, Hessisch Oldendorf, DE
SurPhob Spitzen Reload 200 µL	VT0143	Biozym Scientific GmbH, Hessisch Oldendorf, DE
SurPhob Spitzen Reload 1250 µL	VT0173	Biozym Scientific GmbH, Hessisch Oldendorf, DE

6.1.1.13 Others

Name	**Manufacturer**
Docu-pH+ Meter	Sartorius AG, Göttingen, DE
MSC-Advantage™ Class II Biological Safety Cabinets	Thermo Fisher Scientific, Waltham, MA, US
Systec V-120	Systec GmbH, Linden, DE
NanoDrop™ Spectrophotometer ND-1000	PEQLAB Biotechnologie GmbH, Erlangen, DE
4150 TapeStation	Agilent technologies, Santa Clara, CA, US
Illumina NextSeq500 Sequencing System	Illumina, Inc., San Diego, CA, US
Mid Output Flow Cell (130M)	Illumina, Inc., San Diego, CA, US
Sonoplus GM70	Bandelin electronic GmbH & Co. KG

6.1.2 Chemicals, reagents and buffers

6.1.2.1 Chemicals

Name	**Catalog Nr.**	**Manufacturer**
Trans-IT® LT1 reagent	MIR2300	Mirus Bio LLC, Madison, WI, US
Skim milk powder for blotting	42590.2	Serva Electrophoresis, Heidelberg, DE
Nuclease-Free Water	AM9937	Ambion GmbH, Berlin, DE
$MgCl_2$ 50 mM	F-510Mg	Thermo Fisher Scientific, Waltham, MA, US

$MgSO_4$	230391	Merck Group, Darmstadt, DE
Gel Loading Dye Purple (6X)	B70724S	New England Biolabs, Ipswich, MA, US
Precision Plus Protein Dual Color Standards	161-0374	Bio-Rad Laboratories, Inc., CA, USA
10mM Ultrapure dNTPs Mix	E0503-02	EURx Sp., Gdansk, PL

6.1.2.2 Enzymes and Buffers

Name	Catalog Nr.	Manufacturer
T7 DNA Ligase	MO318L	New England Biolabs, Ipswich, MA, US
T4 Polynucleotide Kinase	MO201S	New England Biolabs, Ipswich, MA, US
T4 DNA Ligase	MO202S	New England Biolabs, Ipswich, MA, US
PNK buffer (10X)	Bo201S	New England Biolabs, Ipswich, MA, US
Rapid Ligation Kit	K1422	Thermo Fisher Scientific, Waltham, MA, US
T4 DNA Ligase buffer (10X)	B0202A	Thermo Fisher Scientific, Waltham, MA, US
Purified BSA (100X)	B9001S	New England Biolabs, Ipswich, MA, US
FastDigest Esp3I	FD0454	Thermo Fisher Scientific, Waltham, MA, US
NEBNext® High Fidelity PCR Master Mix 2X	M0541S	New England Biolabs, Ipswich, MA, US

6.1.3 Cell culture reagents and media

Name	Catalog Nr.	Manufacturer
Gibco™ Dulbecco's Modified Eagle Medium (DMEM)	12491015	Thermo Fisher Scientific, Waltham, MA, US
Gibco™ Roswell Park Memorial Institute (RPMI) 1640 Medium	12633012	Thermo Fisher Scientific, Waltham, MA, US

Gibco™ PBS (phosphate buffered saline) pH7.4 (10X)	70011044	Thermo Fisher Scientific, Waltham, MA, US
Gibco™ Premium Plus FBS	A4766	Thermo Fisher Scientific, Waltham, MA, US
Gibco™ Penicillin-Streptomycin	15140122	Thermo Fisher Scientific, Waltham, MA, US
Gibco™ Trypsin-EDTA (0.05%)	25300054	Thermo Fisher Scientific, Waltham, MA, US
Gibco™ OptiMEM™	31985062	Thermo Fisher Scientific, Waltham, MA, US
Hygromycin B 50mg/mL	10687010	Invitrogen AG, Carlsbad, CA, US
Incidin™ oxywipe S	3082240	Ecolab Deutschland GmbH, Monheim am Rhein, DE
Dimethylsulfoxid	A994.1	Carl Roth GmbH + Co. KG, Karlsruhe, DE

6.1.4 Bacteria work reagents and media

Name	**Catalog Nr.**	**Manufacturer**
LB-Media (Luria/Miller)	X968.2	Carl Roth GmbH + Co. KG, Karlsruhe, DE
Yeast extract	2363.3	Carl Roth GmbH + Co. KG, Karlsruhe, DE
Agar powder	20767.232	VWR International, Radnor, PA, US
Poly(ethylene glycol)	P4338-500G	Sigma-Aldrich, St. Louis, MO, US
TRIS Pufferan® ≥99,9%, p.a.	4855.2	Carl Roth GmbH + Co. KG, Karlsruhe, DE
Glycin, ≥99% Blotting Grade	0079.3	Carl Roth GmbH + Co. KG, Karlsruhe, DE
Tryptone from casein pancreatic	48647.02	Serva Electrophoresis, Heidelberg, DE

6.1.5 Cell lines

Name	Histology	Gender	Age (years)	RRID
Rh4	ARMS	Female	7	CVCL_5916
Rh30	ARMS	Male	17	CVCL_0041
Rh41	ARMS	Female	7	CVCL_2176
Kym1	ERMS	Male	9 months	CVCL_3007
T174	ERMS	Male	44	CVCL_U955
RD	ERMS	Female	7	CVCL_1649
TE381.T	ERMS	Female	7	CVCL_1751
Rh18	ARMS	Female	2	CVCL_1659
hTERT-RPE1	Telomerase immortalized retinal pigment epithelium	Female	1	CVCL_4388
BJ	Foreskin fibroblast	Male	<1 month	CVCL_3653
HEK293T	Transformed human embryonic kidney cells	Female	Fetus	CVCL_0063

6.1.6 Kits

Name	Catalog Nr.	Manufacturer
QIAprep® Spin Miniprep Kit	27104	Qiagen, Hilden, DE
NucleoBond® Xtra Midi	740410.50	Macherey-Nagel GmbH & Co. KG, Düren, DE
NucleoBond ® Xtra Maxi	740414.50	Macherey-Nagel GmbH & Co. KG, Düren, DE
Quick-DNA™ Midiprep Plus Kit	D4075	Zymo Research Europe GmbH, Freiburg, DE
SG qPCR Master Mix	E0401-02	Roboklon GmbH, Berlin, DE
Transcriptor First Strand cDNA Synthesis Kit	04896866001	Roche Holding AG, Basel, CH
Pierce ECL Western Blotting Substrate	32106	Thermo Fisher Scientific, Waltham, MA, US
SuperSignal West Femto Maximum Sensitivity Substrate	34095	Thermo Fisher Scientific, Waltham, MA, US
CellTiter-Glo® Luminescent Cell Viability Assay	G7571	Promega, Madison, WI, US

RNeasy® Mini Kit	74104	Qiagen, Hilden, DE
NucleoSpin® TriPrep	740966.50	Macherey-Nagel GmbH & Co. KG, Düren, DE
Pierce BCA Protein Assay Kit	23225	Thermo Fisher Scientific, Waltham, MA, US

6.1.7 Plasmids and libraries

Name	**Addgene cat. no.**	**Acquired from**
pMD2.G	12259	Didier Trono (check PgBD5 paper)
psPAX2	12260	Didier Trono
lentiSAMv2 backbone	75112	Addgene, Watertown, MA, USA
lentiMPHv2	89308	Addgene, Watertown, MA, USA
Human SAM library, lentiSAMv2, 2-plasmid system	1000000078	Addgene, Watertown, MA, USA
NextSeq PhiX Control Kit	FC-110-3002	Illumina, Inc., San Diego, CA, USA

6.1.8 Competent cells

Name	**Acquired from**
XL10-Gold® Ultracompetent Cells	Agilent Technologies, Inc., Santa Clara, CA, USA
Stbl3™ Chemically Competent E. coli	Thermo Fisher Scientific, Waltham, MA, USA

6.1.9 Primer sequences for barcoded NGS

Primer	**Sequence (Barcode = bold)**	**Sample**
NGS-Lib-Fwd-1	AATGATACGGCGACCACCGAGATCTA CACTCTTTCCCTACACGACGCTCTTCC GATCTTAAGTAGAGGCTTTATATATCT TGTGGAAAGGACGAAACACC	

NGS-Lib-Fwd-2	AATGATACGGCGACCACCGAGATCTA CACTCTTTCCCTACACGACGCTCTTCC GATCTATCATGCTTAGCTTTATATATC TTGTGGAAAGGACGAAACACC	
NGS-Lib-Fwd-3	AATGATACGGCGACCACCGAGATCTA CACTCTTTCCCTACACGACGCTCTTCC GATCTGATGCACATCTGCTTTATATAT CTTGTGGAAAGGACGAAACACC	
NGS-Lib-Fwd-4	AATGATACGGCGACCACCGAGATCTA CACTCTTTCCCTACACGACGCTCTTCC GATCTCGATTGCTCGACGCTTTATATA TCTTGTGGAAAGGACGAAACACC	
NGS-Lib-Fwd-5	AATGATACGGCGACCACCGAGATCTA CACTCTTTCCCTACACGACGCTCTTCC GATCTTCGATAGCAATTCGCTTTATAT ATCTTGTGGAAAGGACGAAACACC	
NGS-Lib-Fwd-6	AATGATACGGCGACCACCGAGATCTA CACTCTTTCCCTACACGACGCTCTTCC GATCTATCGATAGTTGCTTGCTTTATA TATCTTGTGGAAAGGACGAAACACC	
NGS-Lib-Fwd-7	AATGATACGGCGACCACCGAGATCTA CACTCTTTCCCTACACGACGCTCTTCC GATCTGATCGATCCAGTTAGGCTTTAT ATATCTTGTGGAAAGGACGAAACACC	
NGS-Lib-Fwd-8	AATGATACGGCGACCACCGAGATCTA CACTCTTTCCCTACACGACGCTCTTCC GATCTCGATCGATTTGAGCCTGCTTTA TATATCTTGTGGAAAGGACGAAACAC C	
NGS-Lib-Fwd-9	AATGATACGGCGACCACCGAGATCTA CACTCTTTCCCTACACGACGCTCTTCC GATCTACGATCGATACACGATCGCTTT ATATATCTTGTGGAAAGGACGAAACA CC	
NGS-Lib-Fwd-10	AATGATACGGCGACCACCGAGATCTA CACTCTTTCCCTACACGACGCTCTTCC	

	GATCTTACGATCGATGGTCCAGAGCTT TATATATCTTGTGGAAAGGACGAAAC ACC	
NGS-Lib-SAM-Rev-1	CAAGCAGAAGACGGCATACGAGAT**TC** **GCCTTG**GTGACTGGAGTTCAGACGTG TGCTCTTCCGATCTGCCAAGTTGATAA CGGACTAGCCTT	0h
NGS-Lib-SAM-Rev-2	CAAGCAGAAGACGGCATACGAGAT**AT** **AGCGTC**GTGACTGGAGTTCAGACGTG TGCTCTTCCGATCTGCCAAGTTGATAA CGGACTAGCCTT	DMSO
NGS-Lib-SAM-Rev-4	CAAGCAGAAGACGGCATACGAGAT**AT** **TCTAGG**GTGACTGGAGTTCAGACGTG TGCTCTTCCGATCTGCCAAGTTGATAA CGGACTAGCCTT	ActD

6.1.10 sgRNA sequences for validation

Gene	Primer	Direction	Sequence
ABCC1	1	Forward	CACCgCAGCCGGACCAGCCACCTCT
		Reverse	AAACAGAGGTGGCTGGTCCGGCTGc
	2	Forward	CACCgCCTTGGAGGATCTGGGGTGG
		Reverse	AAACCCACCCCAGATCCTCCAAGGc
	3	Forward	CACCgTAGGCCCACCCGCTCGCGGA
		Reverse	AAACTCCGCGAGCGGGTGGGCCTAc
NT	1	Forward	CACCGCTGAAAAAGGAAGGAGTTGA
		Reverse	AAACTCAACTCCTTCCTTTTTCAGC
	2	Forward	CACCGAAGATGAAAGGAAAGGCGTT
		Reverse	AAACAACGCCTTTCCTTTCATCTTC
U6-Fwd			CGTGACGTAGAAAGTAATAATTTCTTGGG

All sgRNA oligos were ordered from Eurofins Scientific, Luxemburg, LUX

6.1.11 Primers for qPCR

Gene	Direction	Sequence
ABCC1	Forward	CTTCTTCTTCAAGGCCATCCACG
	Reverse	CTGGGGCCTTCGTGTCATTCAC

6.1.12 Western Blot

6.1.12.1 Primary antibodies

Target	Catalog Nr.	Species	Dilution	Blocking	Manufacturer
a-Tubulin	3873S	Mouse	1:1000	5% milk in TBS-T	Cell Signaling Technology, Inc., Danvers, MA, US
FKHR (Foxo1)	Sc-374427	Mouse	1:100	5% milk in TBS-T	Santa Cruz Biotechnology, Inc., Dallas, TX, US
P53	2527S	Rabbit	1:1000	5% milk in TBS-T	Cell Signaling Technology, Inc., Danvers, MA, US
pRPA32 (S4/S8)	A300-245A	Rabbit	1:2000	5% BSA in TBS-T	Bethyl Laboratories, Montgomery, TX, US
RPA32/RPA2 p(T21)	Ab109394	Rabbit	1:50000	5% BSA in TBS-T	Abcam, Cambridge, UK

6.1.12.2 Secondary antibodies

Target	Catalog Nr.	Species	Dilution	Blocking	Manufacturer
Mouse	115-035-003	Goat	1:5000	10% milk in TBS-T	Jackson ImmunoResearch Laboratories, Inc., West Grove, PA, US
Rabbit	111-035-144	Goat	1:5000	10% milk in TBS-T	Jackson ImmunoResearch Laboratories, Inc., West Grove, PA, US

6.1.12.3 Western Blot materials

Name	Catalog Nr.	Manufacturer
Novex WedgeWell 10% Tris-Glycine Gel	XP00105BOX	Invitrogen AG, Carlsbad, CA, US
NuPAGE 3-8% Tris-Acetate Gel	EA03755BOX	Invitrogen AG, Carlsbad, CA, US
PhosSTOP EASYpack	04906837001	Roche Holding AG, Basel, CH
cOmplete™ mini EDTA-free Protease Inhibitor Cocktail	11836170001	Roche Holding AG, Basel, CH
4X Laemmli Sample Buffer	1610747	Bio-Rad Laboratories, Inc., Hercules, CA, US

2-Mercaptoethanol	1610710	Bio-Rad Laboratories, Inc., Hercules, CA, US
Immun-Blot® PVDF Membrane	1620177	Bio-Rad Laboratories, Inc., Hercules, CA, US
SuperSignal™ West Femto Maximum Sensitivity Substrate	34094	Thermo Fisher Scientific, Waltham, MA, US

6.1.13 Software

Name	**Manufacturer**
Adobe Photoshop®	Adobe Inc., San José, CA, US
Adobe Illustrator®	Adobe Inc., San José, CA, US
RStudio	RStudio Inc., Boston, MA, US
ImageJ	Wayne Rasband, NIH
ColonyArea, ImageJ plug-in	
Bio-Rad CFX Manager	Bio-Rad Laboratories, Inc., Hercules, CA, US
FlowJo V10	FlowJo LLC, Ashland, OR, USA
Microsoft Office	Microsoft Corporation, Redmond, WA, US
EndNote X9	Clarivate Analytics, Philadelphia, PA, US
bcl2fastq v2.20.0.422	Illumina, Inc., San Diego, CA, US
count_spacers.py	
mageck-0.5.9.4.tar.gz	
GraphPad Prism 8	GraphPad Software, CA, US
SnapGene® Viewer	GSL Biotech LLC, San Diego, CA, US
Labguru	BioData Ltd., Cambridge, MA, US
Gen5 3.0	BioTek Instruments, Inc., Winooski, VT, US

6.2 Methods

6.2.1 Cell culture

All cell culture work was performed under a laminar flow hood. The hood was sterilized by a 30 min exposure to UV light and sprayed with 70% ethanol to ensure a sterile work environment.

6.2.1.1 Passaging cell lines

Tumor cell lines were cultivated in either DMEM or RPMI medium supplemented with 10% fetal calf serum (FCS) and 1% penicillin/streptomycin (see Table 3) in 10 cm^2 cell culture dishes at 37°C in 5% CO_2. Growing medium was kept at 37°C in a water bath prior to use. All cell lines were regularly monitored for mycoplasma infection. If cell confluency exceeded 90%, cells were split in a 1:10 ratio. Only Rh18 was passaged in a 1:5 ratio due to its slower doubling time. Cells were washed with 5 mL of PBS to remove any remaining culture medium and then incubated for 10 minutes with trypsin. Cells were counted by mixing them in a 1:1 ratio with 0.02% trypan blue on an automated BioRad TC20 cell counter.

Table 3: Cell lines used in experiments with respective culture medium

Cell line name	Culture medium
Rh4	DMEM
Rh30	DMEM
Rh41	DMEM
Kym1	RPMI
T174	DMEM
RD	DMEM
TE381.T	DMEM
Rh18	RPMI
hTERT-RPE1	DMEM
BJ	RPMI
HEK293T	DMEM

6.2.1.2 Long-term storage of cell lines and thawing from cryopreservation

To freeze the cells for long-term storage, we used a specific freezing medium which maintains the highest cell viability possible. Here, we used 500 µL of a 9:1 mix of heat-inactivated FBS and dimethyl sulfoxide (DMSO) per cryovial containing 1-3 x 10^6 cells. The cryovials were quickly

transferred to a -80°C freezer in a Mr.Frosty™ freezing container filled with isopropanol to ensure a steady freezing rate of -1°C/min. After a 24 h freezing period, cryovials were transferred to a -140°C liquid nitrogen tank for storage.

Due to the potential accumulation of mutations in culture, all cell lines were discarded if they exceeded a passage number of 30. New, low-passage cells were then thawed from stocks. Due to the toxicity of high concentrations of DMSO in the freezing medium, cells were thawed in a water bath and spun down for 5 min at 1200 rpm directly after thawing. Freezing medium was aspirated and cell pellets resuspended in 1 mL of fresh cell culture medium, before being transferred to a 10 cm^2 cell culture dish.

6.2.1.3 Pelleting cells

Approximately one million cells were collected for each cell pellet. Cells were sedimented for 5 min at 1200 rpm and the supernatant was aspirated. Cells were then washed with 1 mL of PBS and spun down again for 5 min at 1200 rpm. PBS was aspirated and pellets stored at -80°C for further experiments.

6.2.2 Cell viability assays

6.2.2.1 Luminescence-based cell viability

To determine cell viability, cells were seeded into flat-bottom white 96 well plates with a density of 1000 cells per well in triplicates. Cells were incubated for 24 h to allow attachment to the wells before being treated with decreasing concentrations of ActD, tetrandrine or a combination of both. Cell viability was measured after 72 h using the CellTiterGlo® Luminescent Cell Viability Assay, which emits luminescence based on the ATP content of the sample (proportional to cell viability) (150). After 10 min of incubation, protected from light and under constant shaking, we measured the luminescence on a Synergy LX multiplate reader. All values were normalized to the according DMSO-treated control, which was assumed to be the highest viability.

6.2.2.2 Crystal violet staining

We seeded 2500 cells per well of a 24-well cell culture plate and let the cells adhere for 24 h. We then treated the cells with either 1, 2 or 4 nM of ActD for 10 days. After treatment, we aspirated the growing medium, washed the cells with 500 µL of PBS and fixed the cells with 1% formaldehyde in PBS for 20 min. We then stained the cells with a 0.1% crystal violet in 70% ethanol solution. Cells were stained for 20 min, washed with PBS and dried overnight. The stained cells were then scanned and cell density determined optically and using the ColonyArea plug-in for ImageJ.

6.2.3 Western Immunoblotting

Cells pellets were lysed using RIPA buffer (15 mM HEPES, 150 mM NaCl, 10 mM EGTA, 2% Triton X-100) supplemented with phosphatase and protease inhibitor as per manufacturer's instructions. After 20 min incubation time, samples were sonicated for 10 seconds at a 70% cycle intensity. Protein concentration was determined using a BCA assay. Sample concentration was adjusted for all samples (accounting for 10 µg per loading), and 4X Laemmli buffer with 2-mercaptoethanol (100 µL of 2-mercaptoethanol per 900 µL 4X Laemmli buffer) was added to the protein lysate. Samples were denatured at 95°C for 10 min prior to loading onto a 10% Tris-Glycin precast gel. Gels were run at 90 V for 10 min and then at 120 V until the buffer front reached the bottom of the gel. A polyvinylidene fluoride (PVDF) membrane was activated in 100% methanol. Then, protein was transferred onto the membrane at 90 V for 90 min at 4°C. The protein-containing membrane was blocked for 1 h in 5% milk in TBS + 0,1% Tween-20 (TBS-T), and then incubated with diluted primary antibody in 5% milk in TBS-T overnight at 4°C at the dilution specified in 6.1.12.1. After washing 3 times for 5 min with TBS-T, the membranes were incubated with the corresponding horseradish peroxidase (HRP)-conjugated secondary antibody diluted in 10% milk in TBS-T for 1 h at room temperature at the dilution specified in 6.1.12.2. Membranes were washed in the same conditions as before, developed and imaged on a ChemiDoc XRS System with exposure time dependent on the target protein. To quantify changes in protein expression, we measured the intensity of each band and its corresponding lane intensity. After subtracting background signal, we calculated the ratio of the band and the loading control of that lane.

6.2.4 DNA amplification

6.2.4.1 Standard PCR

We used polymerase chain reactions (PCRs) to amplify DNA using a variety of polymerases based on the targeted genes. The reaction components included polymerase with its respective reaction buffer, template DNA and dNTPs needed to synthesize new DNA sequences. Additionally, a forward and reverse primer was added to each reaction. These primers were designed using Primer-BLAST, which uses Primer3, BLAST and a global alignment algorithm to design primers and avoid primer pairs, which could lead to non-specific amplifications (151). The melting temperature of the primers was set between 65°C and 75°C, with a maximum difference of 5°C. After assembly, all PCR reactions were transferred to a preheated thermocycler. Thermocycling conditions varied depending on the polymerase used.

6.2.4.2 Quantitative PCR

RNA was extracted from cell pellets (see 6.2.1.3) using the RNeasy Mini Kit. RNA was reverse transcribed using the Transcriptor First Strand cDNA Synthesis Kit. qPCR was performed using SG qPCR Master Mix, 1 µg of cDNA per 20 µL reaction and the primers listed under 4.1.10. This qPCR kit uses SYBR Green, a dye binding DNA, to measure DNA content of the respective gene during qPCR (152). Hypoxanthine phosphoribosyltransferase 1 (HPRT1), a housekeeping gene, was used as an endogenous control (153). Using the $\Delta\Delta C_T$ method (154), gene expression was calculated as a fold change of the NT-sgRNA controls, normalized to HPRT1 expression.

6.2.5 Bacterial transformation

To produce competent cells for bacterial transformation, we set up bacterial cultures in 50 mL bacterial growth medium (LB medium with 100 µg/mL ampicillin, 10 mM $MgCl_2$ and a 1:1000 dilution of chloramphenicol) overnight before expanding the cultures in 300 mL of bacterial growth medium in the morning and incubating for 3-4 hours at 37°C. When an optical density of the sample measured at a wavelength of 600 nM (OD_{600}) reached 0.4 - 0.6, bacteria was aliquoted to 50 mL vessels and incubated on ice for 15 min. After spinning down the samples at 4°C (15 min, 2500 rpm), each cell pellet was dissolved in 1.5 mL transformation buffer (1 g polyethylenglycol 3000, 100 µL 1 M $MgCl_2$, 100 µL 1 M $MgSO_4$, 0.5 mL DMSO, 10 mL LB media) and incubated on ice for 30 min. Plasmids to be inserted into competent cells were previously cloned using a Golden Gate assembly reaction (155). After the addition of the ligations, cells were incubated on ice for 30 min. We used the heat shock method for transformation, creating pores in the plasma membranes of competent cells by heating up the cells at 42°C for 20 s. Afterwards, 800 µL SOC medium was added to each ligation before an incubation time of 1 h at 37°C whilst shaking (550 rpm). Bacteria was spun down at 5000 rpm for 2 min and the pelleted cells were plated on LB plates with 100 µg/mL ampicillin using glass beads.

6.2.6 Viral Transduction

6.2.6.1 Plasmid amplification

To amplify our plasmids, we cultured the plasmid-containing Stbl3 bacteria on a LB agar plate with 100 µg/mL ampicillin at 37°C overnight. We then picked an isolated colony and expanded it in LB media with 100 µg/mL ampicillin at 37°C overnight. Plasmids were purified using the NucleoBond® Xtra Maxi kit and confirmed on an agarose gel (for correct size) and Sanger sequencing (for correct sequence).

To amplify the pooled sgRNA library, due to the higher scale needed, we electroporated XL10-Gold Ultracompetent bacteria. Using pulsed electric currents, electroporation creates transient pores in the cell membranes, allowing for passage genetic material into the target cells.

Electrocompetent bacteria, cuvettes and media were kept on ice for the whole experiment. Using a MicroPulser™ Electroporator, we electroporated 40 µL of bacteria in 9 replicates, containing 1 µL of plasmid library each, using the preset program Ec2 (V = 2.5 kV) according to the manufacturer's instructions. After electroporation, we immediately added 1 mL of SOC medium to each cuvette and incubated the cell suspension for 1 h at 37°C. Bacteria was then plated on a total of 40 agar plates with 100 µg/mL ampicillin, spreading the resuspended bacteria with glass beads. After an overnight culture at 37°C, all colonies were collected and combined using ice-cold PBS and a cell scraper. Bacteria was spun down (5 min at 14 000 rpm) and plasmids extracted using the NucleoBond® Xtra Maxi kit.

6.2.6.2 Lentivirus production

To produce lentivirus containing the plasmid of interest, we used HEK293T cells and TransIt-LT1 reagent. HEK293T cells were grown in antibiotic-free media 24 h before transfection to reach a 60% confluency. HEK293T cells were then transfected with the plasmid of interest and the two packaging plasmids pMD2.G and psPAX2 at a 2:1:1 ratio, mixed with serum-free medium and TransIT-LT1 according to the manufacturer's instructions. After 24 h, we changed the growing media to collection media containing DMEM with 30% added FCS. The next day, virus was collected and stored at 4°C, while new collection media was added to the cells to obtain a second batch of lentivirus the following day. Both batches were combined and virus was filtered using a 0.45 µm filter, aliquoted into 1 mL cryovials and stored at -80°C. To produce sgRNA library-containing virus, one million HEK293T cells were seeded into T175 plates (17 plates in total) in antibiotic-free media and incubated for 24 h. Cells were transfected with the sgRNA library, pMD2.G and psPAX2 packaging vectors (2:1:1 ratio) and polyethylimine (PEI) transfecting reagent pre-incubated for 15 min. Similarly, two batches of virus were prepared, concentrated using Amicon Ultra-15 tubes, aliquoted and stored at -80°C.

6.2.6.3 Assessing viral titer

To assess the titer of virus produced in 6.2.6.2, we seeded HEK293T cells in a 12-well plate at 1,5 million cells per well. After allowing the cells to grow for 24 h, we aspirated the media and treated the cells with the following dilutions of virus with media and polybrene for each lentivirus to be tested:

Viral supernatant [mL]	Growing media [mL]	Polybrene [µL]
1	0.5	1.5
0.01	1.49	1.5
0.1	1.4	1.5

We incubated the treated cells overnight and replaced the media with DMEM containing blasticidin as the selection antibiotic before incubating the cells for 48 h. After incubation, we removed the media to count the number of floating cells before trypsinizing the adherent cells to assess the number of vital cells by trypan blue staining (see 6.2.1.1).

6.2.6.4 Mammalian cell transduction

For each transduction, we prepared a 6-well plate for the respective lentiviral vector containing our gene of interest, lentiviral vector with the non-targeting sequence and a control well with no virus. We seeded 5 million of target cells in 2 mL of the appropriate media containing 10% FCS and 1% penicillin/streptomycin. After an overnight incubation, OptiMEM was added to the virus to bring the volume up to 1 mL, additionally 2 µL of the polybrene stock was added to ensure a final polybrene concentration of 8 µg/mL. Growing media was aspirated from the cells and gently replaced with 1 mL of virus containing polybrene. Cells were then incubated for 48 h at 37°C. After the incubation time, the media was replaced with 2 mL of appropriate media (see Table 3) containing 10% FCS and 1% penicillin/streptomycin and the respective selection antibiotic. Over the following week, cell growth was carefully observed, passaging cells as necessary. Once the control without viral infection was devoid of cells, successfully transduced cells were grown with selection antibiotic for three to four further days to ensure that only transduced cells remained.

6.2.7 CRISPR activation screen

The genome-wide CRISPRa screen was performed as previously described by Joung *et al*. (148). We first amplified the lentiSAMv2 backbone and the lentMPHv2 plasmid, containing the MS2-P65-MSF1 activator helper complex, as described at 6.2.6.1. After purification and confirmation of these plasmids, we amplified the pooled sgRNA library. Rh4 cells were transduced with the lentiMPHv2 plasmid using polybrene and selected for with hygromycin. Seven T300 flasks with 15 x 10^6 each of Rh4 cells with stably integrated lentiMPH were then transduced with 1800 µL virus (MOI: 0,3) and 6 µL polybrene. The selection antibiotic blasticidin was added a day after transduction.

After selection, cells were split into five T300 plates with 7.5 x 10^6 cells each per condition and treated the following day with 2 nM of ActD and DMSO respectively. Cells were passaged when needed while under selection with 200 µg/mL hygromycin. Cells were counted and harvested for gDNA extraction after 10 days. Genomic DNA was harvested using the Zymo Research Quick-gDNA™ MidiPrep kit according to the manufacturer's instructions and amplified by PCR using the NEBNext High Fidelity PCR Master Mix, the pooled sgRNA library template, a unique NGS-Lib-Fwd primer and the NGS-Lib-SAM-Rev primer to barcode the samples according to step 33 of the protocol described by Joung *et al*. (148). We used 10 different NGS-Lib-Fwd primers and 1

NGS-Lib-SAM-Rev barcode primer (see 6.1.9) for each of the screening conditions. All samples for each condition were pooled and purified using the QIAquick PCR Purification Kit. The pooled samples were quantified and quality-controlled using TapeStation with a 1:20 dilution.

6.2.7.1 Illumina Sequencing, read alignment, counting and normalization

The pooled libraries were sent to the Scientific Genomics Platform of the Max-Delbrück-Centrum für Molekulare Medizin (MDC) and deep-sequenced on an Illumina NextSeq500 using one Mid Output flow cell with a read length of 1 x 81 bp + 8 bp Index. The 20% PhiX Control v3 library was loaded as an in-run control for sequencing quality.

After sequencing, we received a raw read count of 106 million reads. We demultiplexed using bcl2fastq v2.20.0.422. There was no lane splitting and we allowed for a maximum of one mismatched base pair per read. After demultiplexing, 94-97% of the reads were perfectly matched and 3-6% contained one mismatch in the barcode. A total of 18,164,108 reads (17%) could not be assigned. The quality of the sequencing platform was determined using the Phred quality score (Q score), a score indicating the probability of a base being called incorrectly (156). The accuracy of the runs ranged between 88-95% at a base call accuracy of ≥ 99,9% (≥ Q30). Count files were created using count_spacers.py. To normalize the reads, we calculated the reads per million (RPM) in comparison to the total number of reads of the sample. The reads of the guide were divided by the total number of reads of the sample and multiplied by 1 million. To calculate the fold change (FC) of the guides, we used the following formula:

$$FC = log_2(\frac{RPM_{sample} + 1}{RPM_{DMSO} + 1})$$

Additionally, we utilized the Model-based Analysis of Genome-wide CRISPR/Cas9 Knockout (MAGeCK) method as described by Li *et al*. to prioritize the sgRNAs and genes (157). For this, raw read counts were median normalized and variance of read counts was modeled using mean variance modeling. Using the learned mean variance model, the statistical significance of each sgRNA was determined. Subsequently, genes were ranked according to positive or negative selection using a robust rank aggregation (RRA) algorithm (Robust Rank Aggregation v 0.5.6.) (158). Based on these two ranking systems, the most interesting overrepresented genes were picked for validation according to known gene functions.

6.2.7.2 Validation of CRISPRa-screen hits

To validate the hits of the CRISPRa screen, we cloned annealed top- and bottom-strand primers for each of the candidate genes as well as 2 non targeted sgRNAs (NT) individually into the library backbone plasmid (sequences see 6.1.10). After expanding the plasmids as described in 6.2.6,

we produced lentivirus of the respective sgRNAs. We then transduced Rh4 cells stably expressing the MPH activating plasmid with virus and selected with blasticidin. SgRNA-mediated gene upregulation was determined by qPCR (primers see 6.1.11).

6.2.8 Statistical analysis

In cell line experiments, cell culture wells were used as biological replicates (159). Due to the number of cell lines and replications, a normalized distribution of the results could not be determined. Therefore, all statistical analyses were carried out using the Mann-Whitney *U* test. Correlations were calculated using both Spearman and Pearson correlations.

7 Results

7.1 Rhabdomyosarcoma cell line models respond differently to actinomycin D

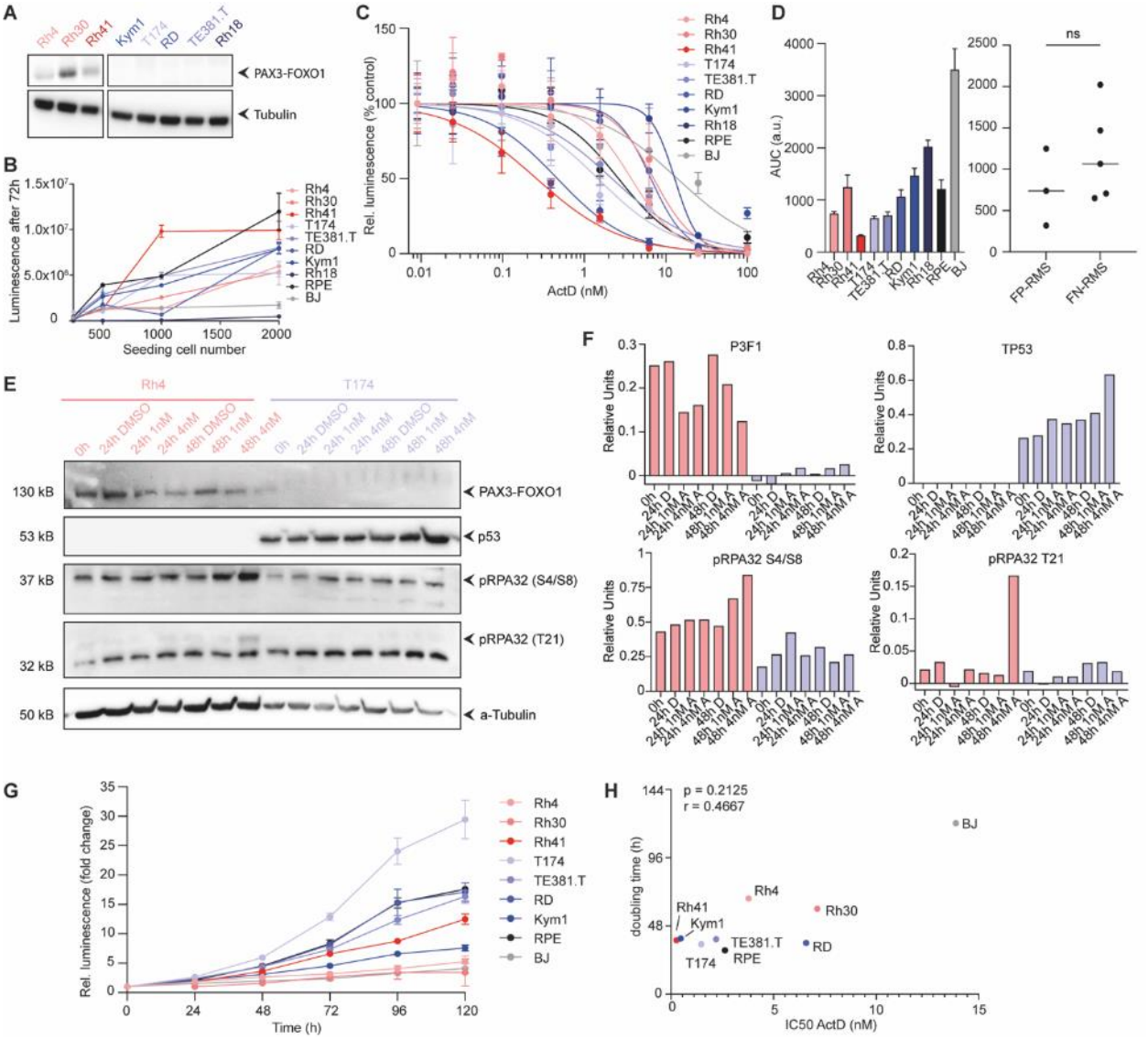

Figure 6: RMS cell line models show a diverse response to ActD.

(A) Western immunoblotting of PAX3-FOXO1 in a set of RMS cell lines. (B) Cell viability assay of RMS and non-transformed cell lines after 72 h incubation time. (C) Cell viability assay of FP-RMS and FN-RMS cell lines and the non-transformed cell lines RPE and BJ after 72 h incubation with ActD (n = 3). (D) AUC of dose-response curves of RMS and non-transformed cell lines treated with ActD (C) and comparison of the mean AUC of dose-response curves of fusion positive RMS and fusion negative RMS cell lines (Mann-Whitney *U* test; p = 0.5714). (E) Western immunoblotting of PAX3-FOXO1, RPA phosphorylation, and TP53 in Rh4 (FP-RMS) and T174 (FN-RMS), treated at different times with ActD or DMSO, tubulin used as loading control. (F) Quantification of the Western immunoblotting (E) in Rh4 and T174. Relative band intensity was calculated in relation to the corresponding tubulin loading control. D: DMSO, A: actinomycin D. Red: Rh4, Blue: T174. (G) Cell growth assay of RMS and non-transformed cell lines (n = 3). (H) Correlation of growth rate (defined as doubling time in h) and sensitivity to ActD (measured as IC50) (Spearman rank coefficient r = 0.4667, p = 0.2125 ns).

To study the effects of ActD in RMS, we used a set of 9 RMS cells for which the fusion status was determined using Western immunoblotting (Fig. 6A). Rh4, Rh30 and Rh41 present the protein fusion, as shown by the presence of PAX3-FOXO1 on the protein level. Kym1, T174, RD, TE381.T and Rh18 do not show an expression of the fusion protein, classifying them as FN-RMS. These findings are in line with previous studies which classify Rh4, Rh30 and Rh41 as ARMS and Kym1, T174, RD, TE381.T and Rh18 as ERMS (160) (Table 4). To maintain consistency, we first seeded RMS and untransformed cell lines in varying cell densities and measured the cell viability after 72 h. As multiple cell lines, namely Rh41, T174 and BJ, stagnated in growth when a seeding density of 1000 cells per well was surpassed (Fig. 6B), we chose a seeding of 1000 cells per well for all future experiments in 96 well plates. We determined the sensitivity of RMS cell lines to ActD by exposing them to varying concentrations of ActD and comparing them to two immortalized control cell lines (RPE and BJ) (Fig. 6C). RMS cell lines showed diverse sensitivity to ActD, with inhibitory concentrations 50 (IC_{50}) ranging from 0.26 nM (Rh41) to 12.9 nM (Rh18). Even though previous studies have shown a significantly poorer outcome of patients with the PAX3-FOXO1 fusion in comparison to FN patients (47), no statistically significant difference between FP-RMS and FN-RMS cell lines were observed in response to ActD, which responded better than untransformed cells (Mann-Whitney *U* test, p = 0.5714) (Fig. 6C).

Table 4: Clinical and molecular characteristics of the cell lines tested.

Summary of Fig. 6A, E and previous studies by Taylor *et al.* (27) and Felix *et al.* (161)

Cell line	**Rh4**	**Rh30**	**Rh41**	**T174**	**RD**	**TE381.T**	**Kym1**	**Rh18**
Histology	ARMS	ARMS	ARMS	ERMS	ERMS	ERMS	ERMS	ERMS
Fusion-status	+	+	+	-	-	-	-	-
Wt-TP53	-	-	-	+	-	+	-	+

ActD can bind to DNA and interfere with RNA and DNA synthesis (111, 112, 117). Because of that, ActD increases replication stress by inducing single strand breaks in the DNA, leading to DNA damage (122). We hypothesized that RMS cells exposed to ActD would also experience an increase in DNA damage. RPA32 is a commonly used marker for DNA damage (162). Serine 4 and 8 sites are phosphorylated by DNA-PKs after replication stress and the phosphorylation of Threonine 21 is a crucial step within the DNA damage response (163). RPA32 is known to bind and stabilize single-strand DNA intermediates that form upon DNA stress. RPA32 quickly binds to DNA at sites of replication fork stalling to protect the DNA and promote its repair (162). To study the effects of ActD in DNA damage generation, we treated two RMS cell lines (Rh4 and T174) with two concentrations of ActD (1 and 4 nM) and determined the protein levels of PAX3-FOXO1, TP53 and phosphorylated RPA32 (S8/S4, T21) at different times (0, 24 and 48 h) (Fig.

6E, 6F). Treatment with ActD led to slightly higher levels of phosphorylated RPA32 (32 kDa subunit, RPA32) in both Rh4 and T174, especially at S4/S8 (Fig. 6F). This is consistent with the accepted hypothesis that treatment with ActD leads to stalled replication forks and increased genotoxic stress (122). Additionally, T174 showed an increased expression of the tumor suppressor TP53 after both 24 and 48 h incubation with ActD (Fig. 6F). TP53 is stabilized following genotoxic stress and is involved in the regulation of cell cycle arrest, cell senescence and apoptosis (164).

Because ActD inhibits transcription as well as DNA replication, we hypothesized that cells with higher proliferation rates would be more sensitive to treatment with ActD. To study this, we analyzed the growth rate of all RMS and non-transformed cells (Fig. 6G) and compared it to their corresponding IC_{50} value. We did not observe a significant correlation between growth rate (doubling time in hours) and sensitivity of our cell lines to ActD (IC_{50} in nM) using Spearman correlation (Spearman rank coefficient r = 0.4667, p = 0.2125) (Fig. 6H). Disregarding the outlier BJ, Pearson's correlation was not statistically significant either (Pearson coefficient r = 0.4505, p = 0.2626, 95 % CI = -0.3724 – 0.8768). Taken together, this data suggests that although ActD increases DNA damage in RMS cells, the growth rate of cell line models was not sufficient in explaining differences in ActD sensitivity, implicating other underlying resistance mechanisms.

7.2 A pooled genome-wide CRISPR activation screen identifies *ABCC1* as a potential predictor for actinomycin D-resistance

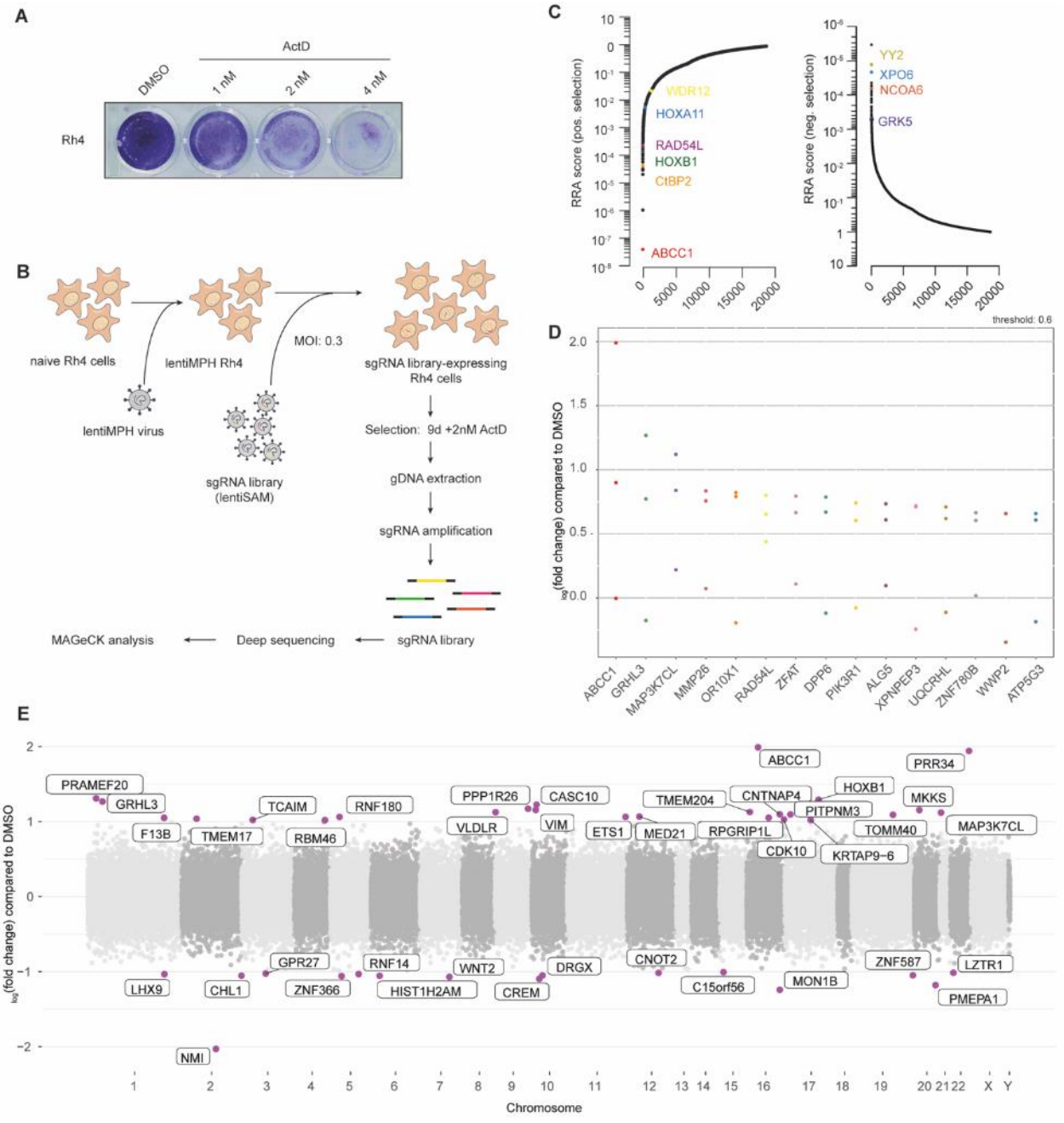

Figure 7: A genome-wide CRISPRa screen identifies multiple genes associated with resistance to ActD.

(A) Cristal violet staining of Rh4 cells incubated for 9 days with ActD. (B) Schematic representation of the workflow for the genome-wide CRISPRa screen. (C) Waterfall plot of genes ranked by their RRA score calculated using MAGeCK. Ranking dependent on either enrichment (left) or depletion (right) of the genes in the sample treated with ActD when compared to the untreated control (DMSO). (D) Log-normalized fold changes of the sgRNAs of the 15 most overrepresented genes after ActD selection in comparison to untreated (DMSO) cell populations. (E) Log-normalized fold changes of all genes (mean of single sgRNAs) after ActD selection in comparison to untreated (DMSO) cell populations, distributed by chromosome position.

Current therapeutic regimens fail partly due to the emergence of resistant cancer cells that do not respond to the treatment (165). In order to identify resistance mechanisms that can limit the antitumor activity of ActD, we performed an unbiased genome-wide CRISPR activation (CRISPRa) screen (144), targeting the promoter region of all genes and increasing their expression. Because FP-RMS have lower survival rates and frequently develop chemoresistance (48), we chose the FP-RMS cell line Rh4, whose response to ActD was representative for all FP-RMS cell lines (Fig. 6C). We determined the optimal concentration of ActD as 2 nM, as it had strong antitumor activity but allowed a small fraction of cells to survive (Fig. 7A).

To prepare the screen, we first stably integrated the MPH-transcription activating complex into Rh4 cells and transduced these with a library of 72,000 sgRNAs targeting the promoter region of all known genes (148). Because this system uses a deactivated Cas9 protein, it recruits the MPH complex, increasing the transcription of the corresponding gene, instead of cutting the DNA at the respective location. By transducing cells at a low multiplicity (MOI: 0.3), it was ensured that each cell received only one sgRNA at most, therefore only overexpressing one gene at a time. We applied the previously determined selection pressure of 2 nM ActD for 9 days before harvesting genomic DNA with the integrated sgRNA. We then barcoded and amplified the sgRNAs specifically and sent them for deep sequencing on an Illumina NextSeq500 at the Science Genomics Platform of the MDC (Fig. 7B).

The resulting reads were analyzed using the Model-based Analysis of Genome-wide CRISPR/Cas9 Knockout (MAGeCK) method to identify candidate genes over- or underrepresented after ActD treatment. This method adjusts for library sizes and read count distributions using median normalization. The significance of the difference in read counts between the treatment and control groups was determined and the sgRNAs ranked based on the calculated p-values (157). Using a modified robust ranking aggregation (RRA) score (158), we ranked the sgRNAs to identify positively or negatively selected genes (Fig. 7C). Secondly, we calculated fold changes of the sgRNAs in comparison to cells treated with DMSO only. As genes overrepresented after ActD selection could be linked to resistance and underrepresented genes could play a role in drug sensitivity, we focused on the positively selected genes. Gene enrichment was equally distributed across the genome (Fig. 7E), confirming that no bias was introduced during the experiment. Among the most differentially expressed genes were *ABCC1*, a drug efflux pump previously associated with multi-drug resistance (134), the transcription factor *GRHL3* (166), and *RAD54L*, a gene known to be involved in homologous recombination and DNA repair (167) (Fig. 7D, 7E). Remarkably, ABCC1, as well as other drug efflux pumps of the ABC family, has previously been linked to resistance to ActD and other chemotherapeutic drugs in cancer, including RMS (134, 168). Taken together, our screen identified multiple genes that could induce resistance to ActD in RMS, including the drug efflux pump ABCC1.

7.3 Overexpression of *ABCC1* leads to increased resistance to actinomycin D

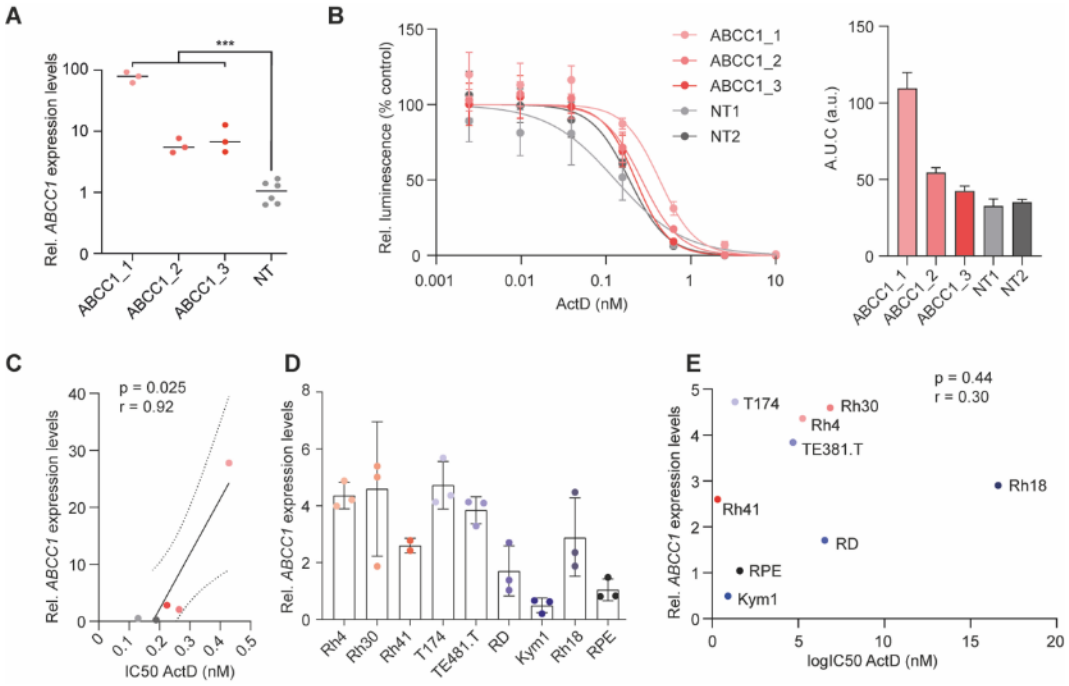

Figure 8: ABCC1 leads to higher resistance to ActD in Rh4 cells.

(A) qPCR analysis of cells transduced with the three ABCC1 sgRNAs in comparison to non-targeted guides (Mann-Whitney *U* test; p = 0.0004 ***). (B) Cell viability assay of the transduced Rh4 cells after 72 h of incubation with ActD. Quantification of the Area Under the Curve (AUC) on the right. (C) Correlation of relative *ABCC1* expression levels and the resistance of cells to ActD of the transduced Rh4 cells (measured as the IC50) (Pearson coefficient r = 0.9243, p = 0.0247, 95% CI = 0.2279 – 0.9951). (D) Relative *ABCC1* expression levels in RMS cell lines as determined by qPCR. (E) Correlation of relative *ABCC1* expression levels and resistance to ActD of RMS cell lines (measured as IC50) (Spearman rank coefficient r = 0.3000, p = 0.4366 ns).

Because *ABCC1* was the top enriched gene in our screening (Fig. 7C) and there is evidence that this drug efflux pump is linked to chemoresistance (134, 136), we decided to study the effect of ABCC1 in RMS more specifically. To validate the role of *ABCC1* in the resistance to ActD, we individually transduced Rh4 cells with three sgRNAs targeting the promoter region of *ABCC1*. To rule out off-target effects of the lentiviral system, we additionally transduced Rh4 cells with two non-targeting (NT) sgRNAs and used them as controls for all further experiments. In order to determine the expression levels of *ABCC1*, we designed PCR primers specifically targeting this gene. After RNA extraction, we synthesized cDNA and performed a quantitative PCR (qPCR). SgRNAs targeting *ABCC1* were sufficient to increase *ABCC1* mRNA levels 4.6 to 92.2 times higher than the non-targeting counterparts (Fig. 8A), confirming a statistically significant overexpression of *ABCC1* in Rh4 cells expressing the MPH activation complex (Mann-Whitney *U* test, p = 0.0004). Next, we treated the transduced Rh4 cells overexpressing *ABCC1* with ActD and measured cell viability after an incubation time of 72 hours. Cells overexpressing *ABCC1*

showed a slightly increased IC_{50} (Fig. 8B). Furthermore, we were able to determine a statistically significant correlation between *ABCC1* expression and the resistance to ActD (measured as IC_{50}) in the transduced cell lines (Pearson coefficient r = 0.9243, p = 0.0247, 95% confidence interval = 0.2279 – 0.9951) (Fig. 8C). These results suggest that increased *ABCC1* expression leads to higher resistance to ActD, consistent with our CRISPRa results.

To analyze if *ABCC1* expression levels could explain the variability in ActD response in our RMS cell line cohort, we determined *ABCC1* mRNA levels in all our RMS cell lines and RPE-hTERT. RMS cell lines showed higher levels of *ABCC1* in general when compared to the immortalized fibroblast cell line (Fig. 8D). However, we couldn't determine if this is a tumor-specific effect. When compared, there was no statistically significant correlation between *ABCC1* expression levels and resistance to ActD (IC_{50}) (Spearman correlation coefficient r = 0.3000, p = 0.4366) (Fig. 8E), indicating that other factors may have a greater influence in ActD resistance than differing *ABCC1* expression levels. Overall, we show that although ABCC1 overexpression leads to higher resistance to ActD, it is not sufficient to explain the different response of RMS cell line models to ActD.

7.4 The ABCC1-inhibitor tetrandrine is synergistic with actinomycin D in ARMS cell lines

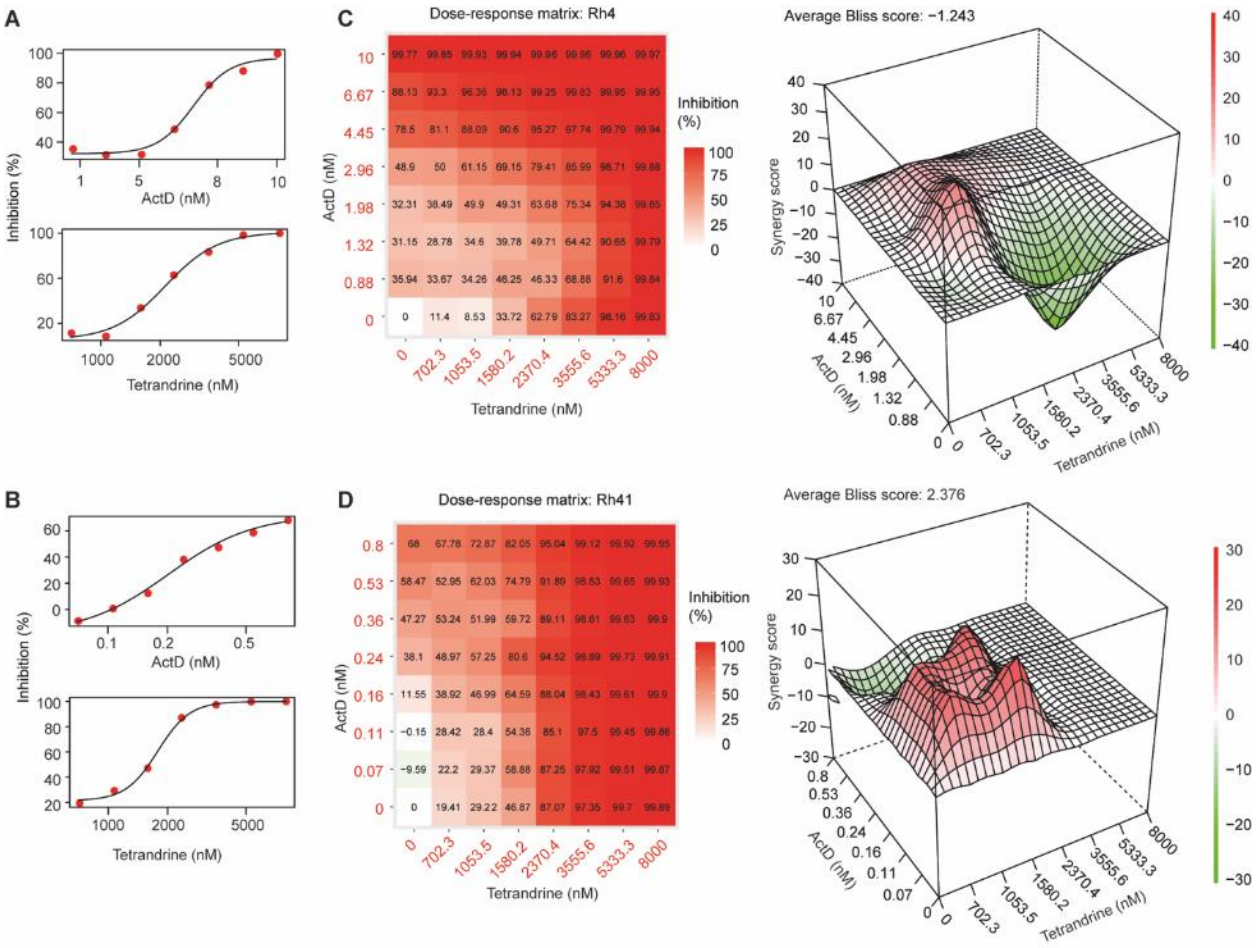

Figure 9: Combination of ActD and tetrandrine has synergistic antitumoral effects in ARMS.

(A) Single agent efficacy of ActD and tetrandrine in Rh4 cells. (B) Single agent efficacy of ActD and tetrandrine in Rh41 cells. (C) Combination treatment of tetrandrine and ActD in Rh4. The central matrix indicates the inhibitory capacity of both drugs combined. The right panel shows the combination scores calculated using the Bliss independence algorithm (average Bliss score = -1.243). (D) Combination treatment of tetrandrine and ActD in Rh41. The central matrix indicates the inhibitory capacity of both drugs combined. The right panel shows the combination scores calculated using the Bliss independence algorithm (average Bliss score = 2.376).

ABCC1 is known to induce multidrug resistance in many tumors (169). As such, there is a clinical interest in developing inhibitors targeting ABCC1, as that could potentially re-sensitize tumors to therapy. Tetrandrine, a bisbenzyl isoquinolone alkaloid isolated from a *Stephania tetrandra*, is a calcium channel clocker that can modulate drug efflux pumps, including ABCC1 (170-172). It has previously shown anti-proliferative properties and has already undergone clinical trials in non-small cell lung cancer as a combination treatment with gemcitabine and cisplatin (173, 174). In those studies, it showed an improved short-term efficacy and a lower rate of adverse side effects than chemotherapy alone. In esophageal squamous carcinoma, treatment with tetrandrine led to an inhibition of multi-drug resistance-associated protein 1 (MRP1), also known as ABCC1, *in vitro*

(171). In multi-drug resistant breast cancer, tetrandrine showed synergistic activity with paclitaxel as well (175).

Because we observed that ABCC1 overexpression leads to higher ActD resistance, we hypothesized that adding tetrandrine could resensitize tumors to ActD. To test our hypothesis, we first determined the effect of single agent treatment on the FP-RMS cell lines Rh4 and Rh41 (Fig. 9A, B). Based on the results of single drug testing, we treated Rh4 and Rh41 cells with increasing concentrations of both ActD and tetrandrine combined and measured cell viability after an incubation time of 72 h. Of note, tetrandrine treatment alone had poor antitumor activity in Rh4 and Rh41 RMS cells (Fig. 9A-B). Nevertheless, the combination treatment with ActD was strongly synergistic (Bliss independence algorithm) (Fig. 9C-D). This implies that by combining both drugs we achieved higher inhibition of cell viability than what would have been achieved if the two drugs had been administered subsequently (176, 177). Taken together, our data shows that tetrandrine has the potential to reverse ABCC1-mediated resistance to ActD in RMS and could be a new therapeutic approach for patients suffering from refractory RMS.

8 Discussion

Multimodal treatment regimen containing ActD have dramatically improved the outcome of RMS patients. Despite long-term survival rates of 70%, around 20% of sarcoma patients still suffer from local relapses, indicating underlying resistance to modern therapy. In this study, we were able to confirm the role of ABCC1, a drug efflux pump, in the resistance of RMS to ActD *in vitro*. Additionally, we show that inhibition of ABCC1 leads to increased sensitivity of RMS cell lines to ActD. If proven effective in further studies, these findings could extend the response of RMS patients that develop ActD-resistance by including an inhibitor of ABCC1 in combination with ActD.

To better understand ActD-resistance, we first reported the baseline sensitivity of RMS cell lines to ActD. ActD is a very potent cytotoxic molecule, including for RMS. However, non-transformed controls were inhibited at similar drug concentrations (Fig. 6C, D). Because of its structure, ActD is able to intercalate into the DNA strand and prevent DNA replication in fast-replicating cells, including, but not limited to, cancer cells (111, 117). In our study, non-transformed cells had similar growth rates as RMS cells (Fig. 6G), therefore limiting our ability to compare the response to ActD of RMS with fully differentiated cells, which typically do not undergo mitosis, or do it at a much slower rate. Of note, one of the ERMS cell lines, Rh18, had the highest IC_{50} of our cohort, including non-cancer cell lines, but its growth rate was also significantly slower.

Next, we needed to confirm that the concentrations we used *in vitro* are comparable to the concentrations used clinically. In their 2014 study, Hill *et al.* measured plasma concentrations of ActD in children with RMS 24 h after receiving a short i.v. infusion of ActD at 0.4 to 1.6 mg/m^2, with a maximal concentration of 2 mg for bigger children. They reported a great variability in concentrations, with the median plasma concentration being at 1.8 µg/L (0.7 to 4.8 µg/L; n = 73; corresponding to 0.5 to 3.8 nM) (138). In our study, the measured IC_{50} values for RMS cell lines ranged from 0.26 to 12.9 nM (Fig. 6C). This data indicates that some cell lines would be resistant to ActD at concentrations used in the clinic. Nonetheless, our data suggests that the bioactive concentrations of ActD as an antitumor drug overlap with the concentrations causing common chemotherapy side effects, such as bone marrow suppression, hair loss or gastrointestinal diseases, caused by the reduction in dividing cells (178-180). Therefore, any effort to reduce the dosage of ActD while maintaining its antitumor properties can result in less side effects and sequelae.

Despite FP-RMS having a poor prognosis and frequently becoming chemoresistant (47, 48), we did not observe significant differences between FP-RMS and FN-RMS regarding ActD sensitivity (Fig. 6A, C). Many of the cell lines used in the study were established decades ago from patients that received several rounds of chemotherapy and records are not available. As such, it is

possible that these cell lines were exposed to some chemotherapeutics, including ActD, and developed resistance subsequently. Furthermore, monolayer cell culture does not reflect the real biology of a tumor, where other factors such as irrigation, immunogenicity and bioavailability of the drug play an important role in drug sensitivity. Retrospective analyses of patient records are a more reliable tool to determine outcome and emergence of resistance. While we do not intend to identify the origin of ActD resistance in these cellular models, we are confident that some of them can be considered resistant, as (i) they have a similar response as non-cancer cells and (ii) their IC_{50} is higher than the concentration achievable in plasma.

In addition to blocking DNA transcription and replication, ActD can induce DNA damage at higher doses. In response to DNA damage, cells elicit a complex signaling pathway that senses the DNA lesion and marks it for repair. RPA is a heterotrimeric, single-stranded DNA (ssDNA)-binding protein complex with 3 subunits (70, 32 and 14 kDa) (181). Replication stress and other forms of DNA damage lead to increased levels of ssDNA, resulting in increased levels of bound RPA (182). RPA then recruits and activates ATR, which in turn phosphorylates the 32 kDa RPA subunit (RPA32) together with DNA-dependent protein kinases (DNA-PK) at conserved phosphorylation sites during the G1/S transition (183, 184). Serine 4 and serine 8 (S4/S8) are phosphorylated by DNA-PK and help to maintain genome stability after replication stress through the regulation of replication fork restart, homologous recombination at double-strand breaks, mitotic catastrophe and cell survival (163). The phosphorylation of T21 is also a crucial step within the DNA damage response and is regulated by multiple DNA damage response protein kinases, including ATR and DNA-PK (185). In this study, we analyzed the induction of DNA damage by ActD by measuring phosphorylation of RPA32 at S4/S8 and T21 after treatment of the RMS cell lines Rh4 and T174 with ActD. These two cells represent both types of RMS. For Rh4, we only observed an increase in RPA32 phosphorylation after 48 h of treatment. On the other hand, in T174, the effect was already observable after 24 h and maintained after 48 h (Fig. 6F). Our previous experiments showed that Rh4 has an IC_{50} of ActD at 3.783 nM and T174 at 1.472 nM (Fig. 6C). Consistently, T174 also showed earlier signs of DNA damage, suggesting that ActD-induced DNA damage and the ability of cells to respond to it affect the overall sensitivity to ActD.

Previous studies have shown that ActD leads to TP53-dependent apoptosis at low doses. At higher concentrations, ActD results in TP53-independent apoptosis due to the inhibition of RNA transcription as well (186). Genotoxic stress leads to the stabilization of TP53 and an increase of the expression of the respective gene. This leads to the transcription of genes associated with cell cycle arrest, apoptosis, cell senescence and cell metabolism (164). TP53 is one of the most well-known tumor suppressor genes and regulates the CDK inhibitor p21 and the enzyme CDC25C, initiating cell cycle arrest (187). Additionally, TP53 regulates the expression of proteins such as BAX, PUMA, NOXA and APAF-1, which play a big role in the induction of apoptosis (188). For these reasons, we examined the levels of TP53 in the cell lines Rh4 and T174 after treatment

with both 1 nM and 4 nM ActD (Fig. 6E, F). In the cell line Rh4, the antibody used could not detect any TP53. As Rh4 is known to harbor a TP53 mutation (Table 4), we hypothesize that these cells do not express a functional TP53 protein. In T174, after 24 h of treatment with ActD there is an increase in TP53. The induction was even higher at a later timepoint with the highest concentration of ActD tested (4 nM). Though these results indicate an activation of TP53 in T174 cells after ActD treatment, they do not prove the induction of apoptosis. To validate an induction of apoptosis through ActD, further studies examining proteins and enzymes involved in the later phases of the apoptotic pathways, such as active (cleaved) caspase 3 would need to follow (189). ActD has long been known to inhibit transcription and preferentially inhibit highly transcribed genes such as genes encoding for rRNA, as the high number of polymerases are sterically affected by bound ActD, stacking up and interfering with the initiation of transcription (121). We therefore hypothesized that sensitivity to ActD is linked to higher proliferation rates. Here, we show that cell lines with a lower doubling time have a statistically significant lower IC_{50} of ActD when using Pearson's correlation (Pearson coefficient r = 0.8566, p = 0.0032) (Fig. 6H). Nevertheless, Pearson's correlation is strongly influenced by outliers (190). We therefore calculated Pearson's linear correlation again after excluding the immortalized fibroblast cell line BJ (Fig. 6H), which then showed no statistically significant correlation (Pearson coefficient r = 0.4505, p = 0.2626). Likewise, Spearman's correlation, a monotonic correlation based on rank more robust against outliers, could not show a statistically significant correlation of proliferation rates and ActD sensitivity (Spearman rank correlation r = 0.4667, p = 0.2125). We therefore concluded that other mechanisms may have a stronger influence on drug sensitivity than proliferation rates. Interestingly, we observed a reduction in PAX3-FOXO1 protein levels after treatment with ActD. While more experiments need to be performed, given the pivotal role of PAX3-FOXO1 in FP-RMS tumorigenesis, modulation of its expression could potentially provide a temporal advantage for cells to tolerate ActD at the expense of their growth capacity.

In this study, we aimed to identify resistance mechanisms against ActD in RMS. Using a CRISPRa screen, we identified *ABCC1*, a gene encoding for a drug efflux pump, as the top candidate for resistance to ActD *in vitro* (Fig. 7C, D, E). There has long been a known correlation between the expression of multidrug resistance proteins, which lead to decreased intracellular accumulation of cytotoxic drugs and the outcome of chemotherapy. Nevertheless, the exact role of drug transporters in the outcome of RMS is controversial (191). While Kuttesch *et al.* concluded that p-glycoproteins are not associated with any clinical features or response to chemotherapy (192), a more recent study done by Citti *et al.* in 2012 shows that ABCC1 was significantly more frequent in group III and IV tumors and that ABCC1 levels were increased in tumor samples after chemotherapy (193). Additionally, Seitz *et al*. observed a significant upregulation of ABCC1 after treatment with ActD and vincristine in ARMS xenotransplants (194). Consistent with these findings, *ABCC1* was the most highly overrepresented gene after ActD treatment in our screen,

while other drug efflux pumps were not overrepresented to such a high degree. These findings lead us to further investigate the role of *ABCC1* in ActD-resistance.

To confirm the findings of our CRISPR/dCas9 activation screen, we cloned the sgRNAs targeting *ABCC1* into Rh4 cells individually. The level of *ABCC1* expression changes was comparable to other CRISPR/dCas9 activation screens like the one conducted by Konermann *et al.*, where mRNA fold activation ranged from around 6-fold up to 1,500-fold depending on the target gene (144). Furthermore, we were able to show that the induction of *ABCC1* was sufficient to increase resistance to ActD significantly in Rh4 cells (Fig. 8C). To further investigate the role of *ABCC1* in ActD resistance, we measured *ABCC1* expression levels in all our available cell lines and compared this to the cell lines' respective IC_{50} of ActD (Fig. 8D, E). Though *ABCC1* expression levels did not significantly correlate with IC_{50}s of ActD in our limited cell line cohort, we were nonetheless able to show a tendency towards increased resistance with increased *ABCC1* levels (Fig. 8E). In this study, we were able to observe the role of *ABCC1* in ActD resistance in one cell line, namely Rh4. To confirm that ABCC1 can lead to resistance to ActD in more diverse molecular backgrounds, future analyses of the role of *ABCC1* in a variety of RMS cell lines, including FN-RMS cell lines, would be needed. Additionally, measurement of intracellular ActD concentration in RMS cells dependent *ABCC1* expression using liquid chromatography-mass spectrometry could increase the robustness of this study, as conducted in the 2013 study by Hill *et al.* (134).

Because ABCC1 led to resistance against ActD in our study, inhibiting ABCC1 could represent a therapeutic option to circumvent ActD resistance. Tetrandrine, an ABCC1 inhibitor, has already undergone clinical trials in non-small cell lung cancer as a combination treatment with gemcitabine and cisplatin (173, 174). In our study, we observed a synergistic relationship between tetrandrine and ActD at clinically relevant doses (Fig. 9A, B), indicating that tetrandrine could, at least partially, reverse chemoresistance to ActD. At high concentrations, the synergistic effect was milder. This could, in part, be explained due to the fact that combination studies are limited by the effect of the drugs. When a drug alone is sufficient to inhibit growth in the majority of the cell population, the addition of a second drug does not seem justified. Of note, we did not include any FN-RMS cells, but we have no reasons to suspect that they would behave differently, suggesting that the combination would benefit not only low-risk, but also high-risk RMS patients.

As tetrandrine has not been shown to be specific for *ABCC1*, future studies could focus on investigating other ABC inhibitors, such as the leukotriene receptor antagonist MK571. In addition to its use as a bronchodialator, MK571 has been shown to inhibit both ABCC1, ABCC2 and ABCC4 (195-197). In their 2015 study, Tivnan *et al*. showed an increased sensitivity of glioblastoma cell lines to the cytotoxic drugs vincristine, temozolomide and etoposide after ABCC1 inhibition by MK571 (195). Additionally, Saleeb *et al*. demonstrated a significant benefit of a combined treatment with MK571 and the VEGF inhibitor sunitinib in papillary renal cell

carcinoma cell lines (197). Though MK571 is not specific to ABCC1, a comparison with tetrandrine could provide further proof of the role of ABCC1 in ActD-resistant RMS.

The use of immortalized human cancer cell lines has long been the standard to study cancer in an *in vitro* setting. Although cell lines show distinct differences to their primary tumor and the clinical relevance of data acquired from them has been increasingly questioned, they remain an integral part in studying drug efficacy (198, 199). The clinical significance of cell line experiments can be limited, as they only capture the biology of the single tumor they were taken from. The increasing rise of large-scale cell line panels allows for broader research into cancer biology. Studies such as the Cancer Cell Line Encyclopedia, published in 2012 and updated in 2019, not only share gene expression data, but also copy number variation data, RNA splicing data, DNA methylation data, Next Generation Sequencing of more than a thousand cell lines. The datasets are paired with pharmacologic profiles of a multitude of drugs and can therefore be used as predictors of drug sensitivity (200-204). Integrating our results with these publically available databases could provide insights into the applicability of our screen in other tumors and the role of ABCC1 in other pediatric tumor types. It is worth mentioning that RMS is a rare entity, and is typically underrepresented in these types of databases, further limiting our ability to identify RMS-specific vulnerabilities.

Despite growing knowledge of cancer biology, there is still a disconnection between basic research, clinical research and the treatment of patients (205). More emphasis is being put into translational research that tries to bridge the gap between basic and clinical research. In recent years, patient-derived xenografts (PDX) have been increasingly used to study tumorigenesis in an *in vivo* setting. Human tumor tissue is implanted into immunodeficient mice, establishing stable models that can be passaged safely from mouse to mouse while maintaining the original features of the patients' tumors (206, 207). These models are frequently used in preclinical outcome prediction, drug efficacy evaluation, the testing of personalized therapies and the identification of biomarkers and present a big step towards more clinically relevant tumor models (208, 209). Clinical studies of rare diseases are often limited by small patient cohorts. In these cases, PDX models serve as more realistic models compared to conventional *in vitro* modelling using cancer cell lines, allowing for easier translation into clinical practice. In PDX models of medulloblastoma, Rusert *et al.* conducted genome sequencing, gene expression profiling and a high-throughput drug screening. They were able to identify new potential therapies such as ActD for group 3 medulloblastoma, even though the drug is only rarely used in medulloblastoma treatment (210). This study shows the possibility of using PDX-models to move away from a "one-size-fits-all" approach in the treatment of pediatric malignancies towards a more patient-specific chemotherapy. Using PDX-models, we might be able to validate the role of ABCC1 in ActD resistance in an *in vivo* setting and lead the way for a more personalized therapy regimen, even using standard chemotherapeutics.

Even though multiple studies have focused on the role of ABC transporters in malignant tumors, preclinical findings have not often translated into the clinical setting. Hill *et al*. showed that a knock-out of *Abcb1a/1b* resulted in higher plasma concentrations of ActD in mice. Nevertheless, they were unable to prove a significant impact of *ABCB1* genotypes in patient responses to chemotherapy (134, 138). In their 2014 study, Mohelnikova-Duchonova *et al*. were able to show a significantly deregulated expression of ABC transporters in pancreatic ductal adenocarcinoma in comparison to nonmalignant tissue, even though *ABCC1* expression was previously determined nearly ubiquitous in human tissues, questioning their use as a target for anti-cancer therapy (169, 211). Additionally, multiple studies were able to identify *ABCC1* polymorphisms, some of them significantly associated with drug resistance and patient outcome (212-216). These findings highlight the need for future studies into the clinical significance of *ABCC1* polymorphisms as a possible biomarker for ActD sensitivity in RMS patients.

Taken together, we conclude that ABCC1 overexpression induces ActD resistance in RMS cell line models, and while more data is required, ABCC1 could become a biomarker of chemoresistance in RMS. The addition of the ABCC1 inhibitor tetrandrine, as well as other potential efflux pump inhibitors, could help extend the effectiveness of current standard of care therapies in RMS patients, greatly increasing their prognosis.

9 Bibliography

1. Shern JF, Chen L, Chmielecki J, Wei JS, Patidar R, Rosenberg M, Ambrogio L, Auclair D, Wang J, Song YK, Tolman C, Hurd L, Liao H, Zhang S, Bogen D, Brohl AS, Sindiri S, Catchpoole D, Badgett T, Getz G, Mora J, Anderson JR, Skapek SX, Barr FG, Meyerson M, Hawkins DS, Khan J. Comprehensive genomic analysis of rhabdomyosarcoma reveals a landscape of alterations affecting a common genetic axis in fusion-positive and fusion-negative tumors. Cancer Discov. 2014;4(2):216-31.

2. Skapek SX, Ferrari A, Gupta AA, Lupo PJ, Butler E, Shipley J, Barr FG, Hawkins DS. Rhabdomyosarcoma. Nat Rev Dis Primers. 2019;5(1):1.

3. Parham DM. Pathologic classification of rhabdomyosarcomas and correlations with molecular studies. Mod Pathol. 2001;14(5):506-14.

4. Paramanathan T, Vladescu I, McCauley MJ, Rouzina I, Williams MC. Force spectroscopy reveals the DNA structural dynamics that govern the slow binding of Actinomycin D. Nucleic Acids Res. 2012;40(11):4925-32.

5. Parham DM, Ellison DA. Rhabdomyosarcomas in adults and children: an update. Arch Pathol Lab Med. 2006;130(10):1454-65.

6. Ognjanovic S, Linabery AM, Charbonneau B, Ross JA. Trends in childhood rhabdomyosarcoma incidence and survival in the United States, 1975-2005. Cancer. 2009;115(18):4218-26.

7. Dasgupta R, Fuchs J, Rodeberg D. Rhabdomyosarcoma. Semin Pediatr Surg. 2016;25(5):276-83.

8. Kashi VP, Hatley ME, Galindo RL. Probing for a deeper understanding of rhabdomyosarcoma: insights from complementary model systems. Nat Rev Cancer. 2015;15(7):426-39.

9. Fletcher CDM BJ, Hogendoorn P, Mertens F. WHO Classification of Tumours of Soft Tissue and Bone. 2013.

10. Pugh TJ, Morozova O, Attiyeh EF, Asgharzadeh S, Wei JS, Auclair D, Carter SL, Cibulskis K, Hanna M, Kiezun A, Kim J, Lawrence MS, Lichenstein L, McKenna A, Pedamallu CS, Ramos AH, Shefler E, Sivachenko A, Sougnez C, Stewart C, Ally A, Birol I, Chiu R, Corbett RD, Hirst M, Jackman SD, Kamoh B, Khodabakshi AH, Krzywinski M, Lo A, Moore RA, Mungall KL, Qian J, Tam A, Thiessen N, Zhao Y, Cole KA, Diamond M, Diskin SJ, Mosse YP, Wood AC, Ji L, Sposto R, Badgett T, London WB, Moyer Y, Gastier-Foster JM, Smith MA, Guidry Auvil JM, Gerhard DS, Hogarty MD, Jones SJ, Lander ES, Gabriel SB, Getz G, Seeger RC, Khan J, Marra MA, Meyerson M, Maris JM. The genetic landscape of high-risk neuroblastoma. Nat Genet. 2013;45(3):279-84.

11. Zhang J, Benavente CA, McEvoy J, Flores-Otero J, Ding L, Chen X, Ulyanov A, Wu G, Wilson M, Wang J, Brennan R, Rusch M, Manning AL, Ma J, Easton J, Shurtleff S, Mullighan C, Pounds S, Mukatira S, Gupta P, Neale G, Zhao D, Lu C, Fulton RS, Fulton LL, Hong X, Dooling DJ, Ochoa K, Naeve C, Dyson NJ, Mardis ER, Bahrami A, Ellison D, Wilson RK, Downing JR, Dyer MA. A novel retinoblastoma therapy from genomic and epigenetic analyses. Nature. 2012;481(7381):329-34.

12. Pugh TJ, Weeraratne SD, Archer TC, Pomeranz Krummel DA, Auclair D, Bochicchio J, Carneiro MO, Carter SL, Cibulskis K, Erlich RL, Greulich H, Lawrence MS, Lennon NJ, McKenna A, Meldrim J, Ramos AH, Ross MG, Russ C, Shefler E, Sivachenko A, Sogoloff B, Stojanov P, Tamayo P, Mesirov JP, Amani V, Teider N, Sengupta S, Francois JP, Northcott PA, Taylor MD, Yu F, Crabtree GR, Kautzman AG, Gabriel SB, Getz G, Jager N, Jones DT, Lichter P, Pfister SM, Roberts TM, Meyerson M, Pomeroy SL, Cho YJ. Medulloblastoma exome sequencing uncovers subtype-specific somatic mutations. Nature. 2012;488(7409):106-10.

13. Li FP, Fraumeni JF, Jr. Rhabdomyosarcoma in children: epidemiologic study and identification of a familial cancer syndrome. J Natl Cancer Inst. 1969;43(6):1365-73.

14. Gripp KW. Tumor predisposition in Costello syndrome. Am J Med Genet C Semin Med Genet. 2005;137C(1):72-7.

15. Brioude F, Kalish JM, Mussa A, Foster AC, Bliek J, Ferrero GB, Boonen SE, Cole T, Baker R, Bertoletti M, Cocchi G, Coze C, De Pellegrin M, Hussain K, Ibrahim A, Kilby MD, Krajewska-Walasek M, Kratz CP, Ladusans EJ, Lapunzina P, Le Bouc Y, Maas SM, Macdonald F, Ounap K, Peruzzi L, Rossignol S, Russo S, Shipster C, Skorka A, Tatton-Brown K, Tenorio J, Tortora C, Gronskov K, Netchine I, Hennekam RC, Prawitt D, Tumer Z, Eggermann T, Mackay DJG, Riccio A, Maher ER. Expert consensus document: Clinical and molecular diagnosis, screening and management of Beckwith-Wiedemann syndrome: an international consensus statement. Nat Rev Endocrinol. 2018;14(4):229-49.

16. Varan A, Sen H, Aydin B, Yalcin B, Kutluk T, Akyuz C. Neurofibromatosis type 1 and malignancy in childhood. Clin Genet. 2016;89(3):341-5.

17. Scrable H, Cavenee W, Ghavimi F, Lovell M, Morgan K, Sapienza C. A model for embryonal rhabdomyosarcoma tumorigenesis that involves genome imprinting. Proc Natl Acad Sci U S A. 1989;86(19):7480-4.

18. Smith AC, Choufani S, Ferreira JC, Weksberg R. Growth regulation, imprinted genes, and chromosome 11p15.5. Pediatr Res. 2007;61(5 Pt 2):43R-7R.

19. Stratton MR, Fisher C, Gusterson BA, Cooper CS. Detection of point mutations in N-ras and K-ras genes of human embryonal rhabdomyosarcomas using oligonucleotide probes and the polymerase chain reaction. Cancer Res. 1989;49(22):6324-7.

20. Wilke W, Maillet M, Robinson R. H-ras-1 point mutations in soft tissue sarcomas. Mod Pathol. 1993;6(2):129-32.

21. Chen Y, Takita J, Hiwatari M, Igarashi T, Hanada R, Kikuchi A, Hongo T, Taki T, Ogasawara M, Shimada A, Hayashi Y. Mutations of the PTPN11 and RAS genes in rhabdomyosarcoma and pediatric hematological malignancies. Genes Chromosomes Cancer. 2006;45(6):583-91.

22. Ramadan F, Fahs A, Ghayad SE, Saab R. Signaling pathways in Rhabdomyosarcoma invasion and metastasis. Cancer Metastasis Rev. 2020;39(1):287-301.

23. Crose LE, Linardic CM. Receptor tyrosine kinases as therapeutic targets in rhabdomyosarcoma. Sarcoma. 2011;2011:756982.

24. Hou J, Dong J, Sun L, Geng L, Wang J, Zheng J, Li Y, Bridge J, Hinrichs SH, Ding SJ. Inhibition of phosphorylated c-Met in rhabdomyosarcoma cell lines by a small molecule inhibitor SU11274. J Transl Med. 2011;9:64.

25. Taulli R, Scuoppo C, Bersani F, Accornero P, Forni PE, Miretti S, Grinza A, Allegra P, Schmitt-Ney M, Crepaldi T, Ponzetto C. Validation of met as a therapeutic target in alveolar and embryonal rhabdomyosarcoma. Cancer Res. 2006;66(9):4742-9.

26. Ney GM, McKay L, Koschmann C, Mody R, Li Q. The Emerging Role of Ras Pathway Signaling in Pediatric Cancer. Cancer Res. 2020;80(23):5155-63.

27. Taylor AC, Shu L, Danks MK, Poquette CA, Shetty S, Thayer MJ, Houghton PJ, Harris LC. P53 mutation and MDM2 amplification frequency in pediatric rhabdomyosarcoma tumors and cell lines. Med Pediatr Oncol. 2000;35(2):96-103.

28. Shern JF, Yohe ME, Khan J. Pediatric Rhabdomyosarcoma. Crit Rev Oncog. 2015;20(3-4):227-43.

29. Taylor JGt, Cheuk AT, Tsang PS, Chung JY, Song YK, Desai K, Yu Y, Chen QR, Shah K, Youngblood V, Fang J, Kim SY, Yeung C, Helman LJ, Mendoza A, Ngo V, Staudt LM, Wei JS, Khanna C, Catchpoole D, Qualman SJ, Hewitt SM, Merlino G, Chanock SJ, Khan J. Identification of FGFR4-activating mutations in human rhabdomyosarcomas that promote metastasis in xenotransplanted models. J Clin Invest. 2009;119(11):3395-407.

30. Paulson V, Chandler G, Rakheja D, Galindo RL, Wilson K, Amatruda JF, Cameron S. High-resolution array CGH identifies common mechanisms that drive embryonal rhabdomyosarcoma pathogenesis. Genes Chromosomes Cancer. 2011;50(6):397-408.

31. Shukla N, Ameur N, Yilmaz I, Nafa K, Lau CY, Marchetti A, Borsu L, Barr FG, Ladanyi M. Oncogene mutation profiling of pediatric solid tumors reveals significant subsets of embryonal rhabdomyosarcoma and neuroblastoma with mutated genes in growth signaling pathways. Clin Cancer Res. 2012;18(3):748-57.

32. Goulding MD, Chalepakis G, Deutsch U, Erselius JR, Gruss P. Pax-3, a novel murine DNA binding protein expressed during early neurogenesis. EMBO J. 1991;10(5):1135-47.

33. Barr FG, Galili N, Holick J, Biegel JA, Rovera G, Emanuel BS. Rearrangement of the PAX3 paired box gene in the paediatric solid tumour alveolar rhabdomyosarcoma. Nat Genet. 1993;3(2):113-7.

34. Davis RJ, D'Cruz CM, Lovell MA, Biegel JA, Barr FG. Fusion of PAX7 to FKHR by the variant t(1;13)(p36;q14) translocation in alveolar rhabdomyosarcoma. Cancer Res. 1994;54(11):2869-72.

35. Galili N, Davis RJ, Fredericks WJ, Mukhopadhyay S, Rauscher FJ, 3rd, Emanuel BS, Rovera G, Barr FG. Fusion of a fork head domain gene to PAX3 in the solid tumour alveolar rhabdomyosarcoma. Nat Genet. 1993;5(3):230-5.

36. Bennicelli JL, Edwards RH, Barr FG. Mechanism for transcriptional gain of function resulting from chromosomal translocation in alveolar rhabdomyosarcoma. Proc Natl Acad Sci U S A. 1996;93(11):5455-9.

37. Lee TI, Young RA. Transcriptional regulation and its misregulation in disease. Cell. 2013;152(6):1237-51.

38. Rabbitts TH. Chromosomal translocations in human cancer. Nature. 1994;372(6502):143-9.

39. Davis RJ, Barr FG. Fusion genes resulting from alternative chromosomal translocations are overexpressed by gene-specific mechanisms in alveolar rhabdomyosarcoma. Proc Natl Acad Sci U S A. 1997;94(15):8047-51.

40. Fredericks WJ, Galili N, Mukhopadhyay S, Rovera G, Bennicelli J, Barr FG, Rauscher FJ, 3rd. The PAX3-FKHR fusion protein created by the t(2;13) translocation in alveolar rhabdomyosarcomas is a more potent transcriptional activator than PAX3. Mol Cell Biol. 1995;15(3):1522-35.

41. Gryder BE, Yohe ME, Chou HC, Zhang X, Marques J, Wachtel M, Schaefer B, Sen N, Song Y, Gualtieri A, Pomella S, Rota R, Cleveland A, Wen X, Sindiri S, Wei JS, Barr FG, Das S, Andresson T, Guha R, Lal-Nag M, Ferrer M, Shern JF, Zhao K, Thomas CJ, Khan J. PAX3-FOXO1 Establishes Myogenic Super Enhancers and Confers BET Bromodomain Vulnerability. Cancer Discov. 2017;7(8):884-99.

42. Xia SJ, Holder DD, Pawel BR, Zhang C, Barr FG. High expression of the PAX3-FKHR oncoprotein is required to promote tumorigenesis of human myoblasts. Am J Pathol. 2009;175(6):2600-8.

43. Keller C, Arenkiel BR, Coffin CM, El-Bardeesy N, DePinho RA, Capecchi MR. Alveolar rhabdomyosarcomas in conditional Pax3:Fkhr mice: cooperativity of Ink4a/ARF and Trp53 loss of function. Genes Dev. 2004;18(21):2614-26.

44. Johnson SF, Cruz C, Greifenberg AK, Dust S, Stover DG, Chi D, Primack B, Cao S, Bernhardy AJ, Coulson R, Lazaro JB, Kochupurakkal B, Sun H, Unitt C, Moreau LA, Sarosiek KA, Scaltriti M, Juric D, Baselga J, Richardson AL, Rodig SJ, D'Andrea AD, Balmana J, Johnson N, Geyer M, Serra V, Lim E, Shapiro GI. CDK12 Inhibition Reverses De Novo and Acquired PARP Inhibitor Resistance in BRCA Wild-Type and Mutated Models of Triple-Negative Breast Cancer. Cell Rep. 2016;17(9):2367-81.

45. Sumegi J, Streblow R, Frayer RW, Dal Cin P, Rosenberg A, Meloni-Ehrig A, Bridge JA. Recurrent t(2;2) and t(2;8) translocations in rhabdomyosarcoma without the canonical PAX-FOXO1 fuse PAX3 to members of the nuclear receptor transcriptional coactivator family. Genes Chromosomes Cancer. 2010;49(3):224-36.

46. Liu J, Guzman MA, Pezanowski D, Patel D, Hauptman J, Keisling M, Hou SJ, Papenhausen PR, Pascasio JM, Punnett HH, Halligan GE, de Chadarevian JP. FOXO1-FGFR1 fusion and amplification in a solid variant of alveolar rhabdomyosarcoma. Mod Pathol. 2011;24(10):1327-35.

47. Missiaglia E, Williamson D, Chisholm J, Wirapati P, Pierron G, Petel F, Concordet JP, Thway K, Oberlin O, Pritchard-Jones K, Delattre O, Delorenzi M, Shipley J. PAX3/FOXO1 fusion gene status is the key prognostic molecular marker in rhabdomyosarcoma and significantly improves current risk stratification. J Clin Oncol. 2012;30(14):1670-7.

48. Sorensen PH, Lynch JC, Qualman SJ, Tirabosco R, Lim JF, Maurer HM, Bridge JA, Crist WM, Triche TJ, Barr FG. PAX3-FKHR and PAX7-FKHR gene fusions are prognostic indicators in alveolar rhabdomyosarcoma: a report from the children's oncology group. J Clin Oncol. 2002;20(11):2672-9.

49. Williamson D, Missiaglia E, de Reynies A, Pierron G, Thuille B, Palenzuela G, Thway K, Orbach D, Lae M, Freneaux P, Pritchard-Jones K, Oberlin O, Shipley J, Delattre O. Fusion gene-negative alveolar rhabdomyosarcoma is clinically and molecularly indistinguishable from embryonal rhabdomyosarcoma. J Clin Oncol. 2010;28(13):2151-8.

50. Garcia J, Hurwitz HI, Sandler AB, Miles D, Coleman RL, Deurloo R, Chinot OL. Bevacizumab (Avastin(R)) in cancer treatment: A review of 15 years of clinical experience and future outlook. Cancer Treat Rev. 2020;86:102017.

51. Dang CV, Reddy EP, Shokat KM, Soucek L. Drugging the 'undruggable' cancer targets. Nat Rev Cancer. 2017;17(8):502-8.

52. Bushweller JH. Targeting transcription factors in cancer - from undruggable to reality. Nat Rev Cancer. 2019;19(11):611-24.

53. Bharathy N, Berlow NE, Wang E, Abraham J, Settelmeyer TP, Hooper JE, Svalina MN, Bajwa Z, Goros MW, Hernandez BS, Wolff JE, Pal R, Davies AM, Ashok A, Bushby D, Mancini M, Noakes C, Goodwin NC, Ordentlich P, Keck J, Hawkins DS, Rudzinski ER, Mansoor A, Perkins TJ, Vakoc CR, Michalek JE, Keller C. Preclinical rationale for entinostat in embryonal rhabdomyosarcoma. Skelet Muscle. 2019;9(1):12.

54. Nguyen TH, Barr FG. Therapeutic Approaches Targeting PAX3-FOXO1 and Its Regulatory and Transcriptional Pathways in Rhabdomyosarcoma. Molecules. 2018;23(11).

55. Wierdl M, Tsurkan L, Chi L, Hatfield MJ, Tollemar V, Bradley C, Chen X, Qu C, Potter PM. Targeting ALK in pediatric RMS does not induce antitumor activity in vivo. Cancer Chemother Pharmacol. 2018;82(2):251-63.

56. Megiorni F, McDowell HP, Camero S, Mannarino O, Ceccarelli S, Paiano M, Losty PD, Pizer B, Shukla R, Pizzuti A, Clerico A, Dominici C. Crizotinib-induced antitumour activity in human alveolar rhabdomyosarcoma cells is not solely dependent on ALK and MET inhibition. J Exp Clin Cancer Res. 2015;34:112.

57. Napolitano A, Ostler AE, Jones RL, Huang PH. Fibroblast Growth Factor Receptor (FGFR) Signaling in GIST and Soft Tissue Sarcomas. Cells. 2021;10(6).

58. Yohe ME, Gryder BE, Shern JF, Song YK, Chou HC, Sindiri S, Mendoza A, Patidar R, Zhang X, Guha R, Butcher D, Isanogle KA, Robinson CM, Luo X, Chen JQ, Walton A, Awasthi P, Edmondson EF, Difilippantonio S, Wei JS, Zhao K, Ferrer M, Thomas CJ, Khan J. MEK inhibition induces MYOG and remodels super-enhancers in RAS-driven rhabdomyosarcoma. Sci Transl Med. 2018;10(448).

59. Geoerger B, Kieran MW, Grupp S, Perek D, Clancy J, Krygowski M, Ananthakrishnan R, Boni JP, Berkenblit A, Spunt SL. Phase II trial of temsirolimus in children with high-grade glioma, neuroblastoma and rhabdomyosarcoma. Eur J Cancer. 2012;48(2):253-62.

60. Hattinger CM, Patrizio MP, Magagnoli F, Luppi S, Serra M. An update on emerging drugs in osteosarcoma: towards tailored therapies? Expert Opin Emerg Drugs. 2019;24(3):153-71.

61. Davis KL, Fox E, Merchant MS, Reid JM, Kudgus RA, Liu X, Minard CG, Voss S, Berg SL, Weigel BJ, Mackall CL. Nivolumab in children and young adults with relapsed or refractory solid tumours or lymphoma (ADVL1412): a multicentre, open-label, single-arm, phase 1-2 trial. Lancet Oncol. 2020;21(4):541-50.

62. Chen C, Dorado Garcia H, Scheer M, Henssen AG. Current and Future Treatment Strategies for Rhabdomyosarcoma. Front Oncol. 2019;9:1458.

63. Leiner J, Le Loarer F. The current landscape of rhabdomyosarcomas: an update. Virchows Arch. 2020;476(1):97-108.

64. Drummond CJ, Hatley ME. A Case of mistaken identity: Rhabdomyosarcoma development from endothelial progenitor cells. Mol Cell Oncol. 2018;5(4):e1448246.

65. Woodruff JM, Perino G. Non-germ-cell or teratomatous malignant tumors showing additional rhabdomyoblastic differentiation, with emphasis on the malignant Triton tumor. Semin Diagn Pathol. 1994;11(1):69-81.

66. Parham DM, Barr FG. Classification of rhabdomyosarcoma and its molecular basis. Adv Anat Pathol. 2013;20(6):387-97.

67. Folpe AL. MyoD1 and myogenin expression in human neoplasia: a review and update. Adv Anat Pathol. 2002;9(3):198-203.

68. Rekhi B, Gupta C, Chinnaswamy G, Qureshi S, Vora T, Khanna N, Laskar S. Clinicopathologic features of 300 rhabdomyosarcomas with emphasis upon differential expression of skeletal muscle specific markers in the various subtypes: A single institutional experience. Ann Diagn Pathol. 2018;36:50-60.

69. Sebire NJ, Malone M. Myogenin and MyoD1 expression in paediatric rhabdomyosarcomas. J Clin Pathol. 2003;56(6):412-6.

70. Cessna MH, Zhou H, Perkins SL, Tripp SR, Layfield L, Daines C, Coffin CM. Are myogenin and myoD1 expression specific for rhabdomyosarcoma? A study of 150 cases, with emphasis on spindle cell mimics. Am J Surg Pathol. 2001;25(9):1150-7.

71. Horn RC, Jr., Enterline HT. Rhabdomyosarcoma: a clinicopathological study and classification of 39 cases. Cancer. 1958;11(1):181-99.

72. E*p*SSG. RMS 2005 a protocol for non metastatic rhabdomyosarcoma. 2008.

73. Dagher R, Helman L. Rhabdomyosarcoma: an overview. Oncologist. 1999;4(1):34-44.

74. Smith LM, Anderson JR, Qualman SJ, Crist WM, Paidas CN, Teot LA, Pappo AS, Link MP, Grier HE, Wiener ES, Breneman JC, Raney RB, Maurer HM, Donaldson SS. Which patients with microscopic disease and rhabdomyosarcoma experience relapse after therapy? A report from the soft tissue sarcoma committee of the children's oncology group. J Clin Oncol. 2001;19(20):4058-64.

75. Newton WA, Jr., Gehan EA, Webber BL, Marsden HB, van Unnik AJ, Hamoudi AB, Tsokos MG, Shimada H, Harms D, Schmidt D, et al. Classification of rhabdomyosarcomas and related sarcomas. Pathologic aspects and proposal for a new classification--an Intergroup Rhabdomyosarcoma Study. Cancer. 1995;76(6):1073-85.

76. Furlong MA, Mentzel T, Fanburg-Smith JC. Pleomorphic rhabdomyosarcoma in adults: a clinicopathologic study of 38 cases with emphasis on morphologic variants and recent skeletal muscle-specific markers. Mod Pathol. 2001;14(6):595-603.

77. Noujaim J, Thway K, Jones RL, Miah A, Khabra K, Langer R, Kasper B, Judson I, Benson C, Kollar A. Adult Pleomorphic Rhabdomyosarcoma: A Multicentre Retrospective Study. Anticancer Res. 2015;35(11):6213-7.

78. Malempati S, Hawkins DS. Rhabdomyosarcoma: review of the Children's Oncology Group (COG) Soft-Tissue Sarcoma Committee experience and rationale for current COG studies. Pediatr Blood Cancer. 2012;59(1):5-10.

79. Ruiz-Mesa C, Goldberg JM, Coronado Munoz AJ, Dumont SN, Trent JC. Rhabdomyosarcoma in adults: new perspectives on therapy. Curr Treat Options Oncol. 2015;16(6):27.

80. Cavazzana AO, Schmidt D, Ninfo V, Harms D, Tollot M, Carli M, Treuner J, Betto R, Salviati G. Spindle cell rhabdomyosarcoma. A prognostically favorable variant of rhabdomyosarcoma. Am J Surg Pathol. 1992;16(3):229-35.

81. Mentzel T, Katenkamp D. Sclerosing, pseudovascular rhabdomyosarcoma in adults. Clinicopathological and immunohistochemical analysis of three cases. Virchows Arch. 2000;436(4):305-11.

82. Yasui N, Yoshida A, Kawamoto H, Yonemori K, Hosono A, Kawai A. Clinicopathologic analysis of spindle cell/sclerosing rhabdomyosarcoma. Pediatr Blood Cancer. 2015;62(6):1011-6.

83. Mosquera JM, Sboner A, Zhang L, Kitabayashi N, Chen CL, Sung YS, Wexler LH, LaQuaglia MP, Edelman M, Sreekantaiah C, Rubin MA, Antonescu CR. Recurrent NCOA2 gene rearrangements in congenital/infantile spindle cell rhabdomyosarcoma. Genes Chromosomes Cancer. 2013;52(6):538-50.

84. Whittle SB, Hicks MJ, Roy A, Vasudevan SA, Reddy K, Venkatramani R. Congenital spindle cell rhabdomyosarcoma. Pediatr Blood Cancer. 2019;66(11):e27935.

85. Agaram NP, Chen CL, Zhang L, LaQuaglia MP, Wexler L, Antonescu CR. Recurrent MYOD1 mutations in pediatric and adult sclerosing and spindle cell rhabdomyosarcomas: evidence for a common pathogenesis. Genes Chromosomes Cancer. 2014;53(9):779-87.

86. Dantonello TM, Int-Veen C, Schuck A, Seitz G, Leuschner I, Nathrath M, Schlegel PG, Kontny U, Behnisch W, Veit-Friedrich I, Kube S, Hallmen E, Kazanowska B, Ladenstein R, Paulussen M, Ljungman G, Bielack SS, Klingebiel T, Koscielniak E, Cooperative Weichteilsarkom S. Survival following disease recurrence of primary localized alveolar rhabdomyosarcoma. Pediatr Blood Cancer. 2013;60(8):1267-73.

87. Ferrari A, Trama A, De Paoli A, Bergeron C, Merks JHM, Jenney M, Orbach D, Chisholm JC, Gallego S, Glosli H, De Salvo GL, Botta L, Gatta G, Bisogno G, Group RAW. Access to clinical trials for adolescents with soft tissue sarcomas: Enrollment in European pediatric Soft tissue sarcoma Study Group (EpSSG) protocols. Pediatr Blood Cancer. 2017;64(6).

88. Hawkins DS, Spunt SL, Skapek SX, Committee COGSTS. Children's Oncology Group's 2013 blueprint for research: Soft tissue sarcomas. Pediatr Blood Cancer. 2013;60(6):1001-8.

89. Oberlin O, Rey A, Lyden E, Bisogno G, Stevens MC, Meyer WH, Carli M, Anderson JR. Prognostic factors in metastatic rhabdomyosarcomas: results of a pooled analysis from United States and European cooperative groups. J Clin Oncol. 2008;26(14):2384-9.

90. Hibbitts E, Chi YY, Hawkins DS, Barr FG, Bradley JA, Dasgupta R, Meyer WH, Rodeberg DA, Rudzinski ER, Spunt SL, Skapek SX, Wolden SL, Arndt CAS. Refinement of risk stratification for childhood rhabdomyosarcoma using FOXO1 fusion status in addition to established clinical outcome predictors: A report from the Children's Oncology Group. Cancer Med. 2019;8(14):6437-48.

91. Gallego S, Zanetti I, Orbach D, Ranchere D, Shipley J, Zin A, Bergeron C, de Salvo GL, Chisholm J, Ferrari A, Jenney M, Mandeville HC, Rogers T, Merks JHM, Mudry P, Glosli H, Milano GM, Ferman S, Bisogno G, European Paediatric Soft Tissue Sarcoma Study G. Fusion

status in patients with lymph node-positive (N1) alveolar rhabdomyosarcoma is a powerful predictor of prognosis: Experience of the European Paediatric Soft Tissue Sarcoma Study Group (EpSSG). Cancer. 2018;124(15):3201-9.

92. Pappo AS, Shapiro DN, Crist WM, Maurer HM. Biology and therapy of pediatric rhabdomyosarcoma. J Clin Oncol. 1995;13(8):2123-39.

93. Kaatsch P, Grabow D, Spix C. German Childhoof Cancer Registry - Annual Report 2017 (1980-2016). Institue of Medical Biostatistics, Epidemiology and Informatics (IMBEI) at the University Medical Center of the Johannes Gutenberg University Mainz; 2018.

94. Maurer HM, Beltangady M, Gehan EA, Crist W, Hammond D, Hays DM, Heyn R, Lawrence W, Newton W, Ortega J, et al. The Intergroup Rhabdomyosarcoma Study-I. A final report. Cancer. 1988;61(2):209-20.

95. Koscielniak E, Harms D, Henze G, Jurgens H, Gadner H, Herbst M, Klingebiel T, Schmidt BF, Morgan M, Knietig R, Treuner J. Results of treatment for soft tissue sarcoma in childhood and adolescence: a final report of the German Cooperative Soft Tissue Sarcoma Study CWS-86. J Clin Oncol. 1999;17(12):3706-19.

96. Crist WM, Anderson JR, Meza JL, Fryer C, Raney RB, Ruymann FB, Breneman J, Qualman SJ, Wiener E, Wharam M, Lobe T, Webber B, Maurer HM, Donaldson SS. Intergroup rhabdomyosarcoma study-IV: results for patients with nonmetastatic disease. J Clin Oncol. 2001;19(12):3091-102.

97. Ruymann FB. The development of VAC chemotherapy in rhabdomyosarcoma: what does one do for an encore? Curr Oncol Rep. 2003;5(6):505-9.

98. DeVita VT, Jr., Chu E. A history of cancer chemotherapy. Cancer Res. 2008;68(21):8643-53.

99. Breneman JC, Lyden E, Pappo AS, Link MP, Anderson JR, Parham DM, Qualman SJ, Wharam MD, Donaldson SS, Maurer HM, Meyer WH, Baker KS, Paidas CN, Crist WM. Prognostic factors and clinical outcomes in children and adolescents with metastatic rhabdomyosarcoma--a report from the Intergroup Rhabdomyosarcoma Study IV. J Clin Oncol. 2003;21(1):78-84.

100. Jiang L, Wang P, Sun YJ, Wu YJ. Ivermectin reverses the drug resistance in cancer cells through EGFR/ERK/Akt/NF-kappaB pathway. J Exp Clin Cancer Res. 2019;38(1):265.

101. Zhang Y, Yang SH, Guo XL. New insights into Vinca alkaloids resistance mechanism and circumvention in lung cancer. Biomed Pharmacother. 2017;96:659-66.

102. Frommann K, Appl B, Hundsdoerfer P, Reinshagen K, Eschenburg G. Vincristine resistance in relapsed neuroblastoma can be efficiently overcome by Smac mimetic LCL161 treatment. J Pediatr Surg. 2018;53(10):2059-64.

103. Waksman SA, Woodruff HB. Bacteriostatic and Bactericidal Substances Produced by a Soil Actinomyces. Proceedings of the Society for Experimental Biology and Medicine. 1940;45(2):609-14.

104. Singh SB, Genilloud O, Pelaéz F. Comprehensive Natural Products II: Elsevier BV; 2010.

105. Hackmann C. [Experimental investigations on the effects of actinomycin C (HBF 386) in malignancies]. Z Krebsforsch. 1952;58(4-5):607-13.

106. Farber S, D'Angio G, Evans A, Mitus A. Clinical studies on actinomycin D with special reference to Wilms' tumor in children. Ann N Y Acad Sci. 1960;89:421-5.

107. D'Angio GJ, Evans A, Breslow N, Beckwith B, Bishop H, Farewell V, Goodwin W, Leape L, Palmer N, Sinks L, Sutow W, Tefft M, Wolff J. The treatment of Wilms' tumor: results of the Second National Wilms' Tumor Study. Cancer. 1981;47(9):2302-11.

108. Jaffe N, Paed D, Traggis D, Salian S, Cassady JR. Improved outlook for Ewing's sarcoma with combination chemotherapy (vincristine, actinomycin D and cyclophosphamide) and radiation therapy. Cancer. 1976;38(5):1925-30.

109. Turan T, Karacay O, Tulunay G, Boran N, Koc S, Bozok S, Kose MF. Results with EMA/CO (etoposide, methotrexate, actinomycin D, cyclophosphamide, vincristine) chemotherapy in gestational trophoblastic neoplasia. Int J Gynecol Cancer. 2006;16(3):1432-8.

110. Bensaude O. Inhibiting eukaryotic transcription: Which compound to choose? How to evaluate its activity? Transcription. 2011;2(3):103-8.

111. Sobell HM. Actinomycin and DNA transcription. Proc Natl Acad Sci U S A. 1985;82(16):5328-31.

112. Kamitori S, Takusagawa F. Crystal structure of the 2:1 complex between d(GAAGCTTC) and the anticancer drug actinomycin D. J Mol Biol. 1992;225(2):445-56.

113. Liu C, Chen FM. Actinomycin D binds strongly and dissociates slowly at the dGpdC site with flanking T/T mismatches. Biochemistry. 1996;35(50):16346-53.

114. Robinson H, Gao YG, Yang X, Sanishvili R, Joachimiak A, Wang AH. Crystallographic analysis of a novel complex of actinomycin D bound to the DNA decamer CGATCGATCG. Biochemistry. 2001;40(19):5587-92.

115. Snyder JG, Hartman NG, D'Estantoit BL, Kennard O, Remeta DP, Breslauer KJ. Binding of actinomycin D to DNA: evidence for a nonclassical high-affinity binding mode that does not require GpC sites. Proc Natl Acad Sci U S A. 1989;86(11):3968-72.

116. Yoo H, Rill RL. Actinomycin D binding to unstructured, single-stranded DNA. J Mol Recognit. 2001;14(3):145-50.

117. Trask DK, Muller MT. Stabilization of type I topoisomerase-DNA covalent complexes by actinomycin D. Proc Natl Acad Sci U S A. 1988;85(5):1417-21.

118. Wassermann K, Markovits J, Jaxel C, Capranico G, Kohn KW, Pommier Y. Effects of morpholinyl doxorubicins, doxorubicin, and actinomycin D on mammalian DNA topoisomerases I and II. Mol Pharmacol. 1990;38(1):38-45.

119. Perry RP, Kelley DE. Inhibition of RNA synthesis by actinomycin D: characteristic dose-response of different RNA species. J Cell Physiol. 1970;76(2):127-39.

120. Schluederberg A, Hendel RC, Chavanich S. Actinomycin D; renewed RNA synthesis after removal from mammalian cells. Science. 1971;172(3983):577-9.

121. Miller MJ. Sensitivity of RNA synthesis to actinomycin D inhibition is dependent on the frequency of transcription: a mathematical model. J Theor Biol. 1987;129(3):289-99.

122. Mischo HE, Hemmerich P, Grosse F, Zhang S. Actinomycin D induces histone gamma-H2AX foci and complex formation of gamma-H2AX with Ku70 and nuclear DNA helicase II. J Biol Chem. 2005;280(10):9586-94.

123. Guy AL, Taylor JH. Actinomycin D inhibits initiation of DNA replication in mammalian cells. Proc Natl Acad Sci U S A. 1978;75(12):6088-92.

124. Merkel O, Wacht N, Sifft E, Melchardt T, Hamacher F, Kocher T, Denk U, Hofbauer JP, Egle A, Scheideler M, Schlederer M, Steurer M, Kenner L, Greil R. Actinomycin D induces p53-independent cell death and prolongs survival in high-risk chronic lymphocytic leukemia. Leukemia. 2012;26(12):2508-16.

125. Choong ML, Yang H, Lee MA, Lane DP. Specific activation of the p53 pathway by low dose actinomycin D: a new route to p53 based cyclotherapy. Cell Cycle. 2009;8(17):2810-8.

126. Shafi MA, Bresalier RS. The gastrointestinal complications of oncologic therapy. Gastroenterol Clin North Am. 2010;39(3):629-47.

127. Jones DP, Chesney RW. Renal toxicity of cancer chemotherapeutic agents in children: ifosfamide and cisplatin. Curr Opin Pediatr. 1995;7(2):208-13.

128. Galligan AJ. Childhood Cancer Survivorship and Long-Term Outcomes. Adv Pediatr. 2017;64(1):133-69.

129. Huang IC, Brinkman TM, Kenzik K, Gurney JG, Ness KK, Lanctot J, Shenkman E, Robison LL, Hudson MM, Krull KR. Association between the prevalence of symptoms and health-related quality of life in adult survivors of childhood cancer: a report from the St Jude Lifetime Cohort study. J Clin Oncol. 2013;31(33):4242-51.

130. Neglia JP, Friedman DL, Yasui Y, Mertens AC, Hammond S, Stovall M, Donaldson SS, Meadows AT, Robison LL. Second malignant neoplasms in five-year survivors of childhood cancer: childhood cancer survivor study. J Natl Cancer Inst. 2001;93(8):618-29.

131. Meadows AT, Friedman DL, Neglia JP, Mertens AC, Donaldson SS, Stovall M, Hammond S, Yasui Y, Inskip PD. Second neoplasms in survivors of childhood cancer: findings from the Childhood Cancer Survivor Study cohort. J Clin Oncol. 2009;27(14):2356-62.

132. Friedman DL, Whitton J, Leisenring W, Mertens AC, Hammond S, Stovall M, Donaldson SS, Meadows AT, Robison LL, Neglia JP. Subsequent neoplasms in 5-year survivors of childhood cancer: the Childhood Cancer Survivor Study. J Natl Cancer Inst. 2010;102(14):1083-95.

133. Hofsli E, Nissen-Meyer J. Reversal of drug resistance by erythromycin: erythromycin increases the accumulation of actinomycin D and doxorubicin in multidrug-resistant cells. Int J Cancer. 1989;44(1):149-54.

134. Hill CR, Jamieson D, Thomas HD, Brown CD, Boddy AV, Veal GJ. Characterisation of the roles of ABCB1, ABCC1, ABCC2 and ABCG2 in the transport and pharmacokinetics of actinomycin D in vitro and in vivo. Biochem Pharmacol. 2013;85(1):29-37.

135. Renes J, de Vries EG, Nienhuis EF, Jansen PL, Muller M. ATP- and glutathione-dependent transport of chemotherapeutic drugs by the multidrug resistance protein MRP1. Br J Pharmacol. 1999;126(3):681-8.

136. Prados J, Melguizo C, Marchal JA, Velez C, Alvarez L, Aranega A. Multidrug resistance phenotype in the RMS-GR human rhabdomyosarcoma cell line obtained after polychemotherapy. Jpn J Cancer Res. 1999;90(7):788-93.

137. Jiang B, Yan LJ, Wu Q. ABCB1 (C1236T) Polymorphism Affects P-Glycoprotein-Mediated Transport of Methotrexate, Doxorubicin, Actinomycin D, and Etoposide. DNA Cell Biol. 2019;38(5):485-90.

138. Hill CR, Cole M, Errington J, Malik G, Boddy AV, Veal GJ. Characterisation of the clinical pharmacokinetics of actinomycin D and the influence of ABCB1 pharmacogenetic variation on actinomycin D disposition in children with cancer. Clin Pharmacokinet. 2014;53(8):741-51.

139. Luqmani YA. Mechanisms of drug resistance in cancer chemotherapy. Med Princ Pract. 2005;14 Suppl 1:35-48.

140. DeMichele A, Yee D, Esserman L. Mechanisms of Resistance to Neoadjuvant Chemotherapy in Breast Cancer. N Engl J Med. 2017;377(23):2287-9.

141. Chen KY, Srinivasan T, Lin C, Tung KL, Gao Z, Hsu DS, Lipkin SM, Shen X. Single-Cell Transcriptomics Reveals Heterogeneity and Drug Response of Human Colorectal Cancer Organoids. Annu Int Conf IEEE Eng Med Biol Soc. 2018;2018:2378-81.

142. Boutros M, Kiger AA, Armknecht S, Kerr K, Hild M, Koch B, Haas SA, Paro R, Perrimon N, Heidelberg Fly Array C. Genome-wide RNAi analysis of growth and viability in Drosophila cells. Science. 2004;303(5659):832-5.

143. Berns K, Hijmans EM, Mullenders J, Brummelkamp TR, Velds A, Heimerikx M, Kerkhoven RM, Madiredjo M, Nijkamp W, Weigelt B, Agami R, Ge W, Cavet G, Linsley PS, Beijersbergen RL, Bernards R. A large-scale RNAi screen in human cells identifies new components of the p53 pathway. Nature. 2004;428(6981):431-7.

144. Konermann S, Brigham MD, Trevino AE, Joung J, Abudayyeh OO, Barcena C, Hsu PD, Habib N, Gootenberg JS, Nishimasu H, Nureki O, Zhang F. Genome-scale transcriptional activation by an engineered CRISPR-Cas9 complex. Nature. 2015;517(7536):583-8.

145. Shalem O, Sanjana NE, Hartenian E, Shi X, Scott DA, Mikkelson T, Heckl D, Ebert BL, Root DE, Doench JG, Zhang F. Genome-scale CRISPR-Cas9 knockout screening in human cells. Science. 2014;343(6166):84-7.

146. Maeder ML, Linder SJ, Cascio VM, Fu Y, Ho QH, Joung JK. CRISPR RNA-guided activation of endogenous human genes. Nat Methods. 2013;10(10):977-9.

147. Chavez A, Scheiman J, Vora S, Pruitt BW, Tuttle M, E PRI, Lin S, Kiani S, Guzman CD, Wiegand DJ, Ter-Ovanesyan D, Braff JL, Davidsohn N, Housden BE, Perrimon N, Weiss R, Aach J, Collins JJ, Church GM. Highly efficient Cas9-mediated transcriptional programming. Nat Methods. 2015;12(4):326-8.

148. Joung J, Konermann S, Gootenberg JS, Abudayyeh OO, Platt RJ, Brigham MD, Sanjana NE, Zhang F. Genome-scale CRISPR-Cas9 knockout and transcriptional activation screening. Nat Protoc. 2017;12(4):828-63.

149. Henssen AG, Jiang E, Zhuang J, Pinello L, Socci ND, Koche R, Gonen M, Villasante CM, Armstrong SA, Bauer DE, Weng Z, Kentsis A. Forward genetic screen of human transposase genomic rearrangements. BMC Genomics. 2016;17:548.

150. Riss T, Niles A, Moravec R, Karassina N, Vidugiriene J. Cytotoxicity Assays: In Vitro Methods to Measure Dead Cells. In: Markossian S, Grossman A, Brimacombe K, Arkin M, Auld D, Austin CP, et al., editors. Assay Guidance Manual. Bethesda (MD)2004.

151. Ye J, Coulouris G, Zaretskaya I, Cutcutache I, Rozen S, Madden TL. Primer-BLAST: a tool to design target-specific primers for polymerase chain reaction. BMC Bioinformatics. 2012;13:134.

152. Zipper H, Brunner H, Bernhagen J, Vitzthum F. Investigations on DNA intercalation and surface binding by SYBR Green I, its structure determination and methodological implications. Nucleic Acids Res. 2004;32(12):e103.

153. Janik ME, Szwed S, Grzmil P, Kaczmarek R, Czerwinski M, Hoja-Lukowicz D. RT-qPCR analysis of human melanoma progression-related genes - A novel workflow for selection and validation of candidate reference genes. Int J Biochem Cell Biol. 2018;101:12-8.

154. Livak KJ, Schmittgen TD. Analysis of relative gene expression data using real-time quantitative PCR and the 2(-Delta Delta C(T)) Method. Methods. 2001;25(4):402-8.

155. Engler C, Marillonnet S. Golden Gate cloning. Methods Mol Biol. 2014;1116:119-31.

156. Ewing B, Green P. Base-calling of automated sequencer traces using phred. II. Error probabilities. Genome Res. 1998;8(3):186-94.

157. Li W, Xu H, Xiao T, Cong L, Love MI, Zhang F, Irizarry RA, Liu JS, Brown M, Liu XS. MAGeCK enables robust identification of essential genes from genome-scale CRISPR/Cas9 knockout screens. Genome Biol. 2014;15(12):554.

158. Kolde R, Laur S, Adler P, Vilo J. Robust rank aggregation for gene list integration and meta-analysis. Bioinformatics. 2012;28(4):573-80.

159. Lazic SE, Clarke-Williams CJ, Munafo MR. What exactly is 'N' in cell culture and animal experiments? PLoS Biol. 2018;16(4):e2005282.

160. Hinson AR, Jones R, Crose LE, Belyea BC, Barr FG, Linardic CM. Human rhabdomyosarcoma cell lines for rhabdomyosarcoma research: utility and pitfalls. Front Oncol. 2013;3:183.

161. Felix CA, Kappel CC, Mitsudomi T, Nau MM, Tsokos M, Crouch GD, Nisen PD, Winick NJ, Helman LJ. Frequency and diversity of p53 mutations in childhood rhabdomyosarcoma. Cancer Res. 1992;52(8):2243-7.

162. Sleeth KM, Sorensen CS, Issaeva N, Dziegielewski J, Bartek J, Helleday T. RPA mediates recombination repair during replication stress and is displaced from DNA by checkpoint signalling in human cells. J Mol Biol. 2007;373(1):38-47.

163. Ashley AK, Shrivastav M, Nie J, Amerin C, Troksa K, Glanzer JG, Liu S, Opiyo SO, Dimitrova DD, Le P, Sishc B, Bailey SM, Oakley GG, Nickoloff JA. DNA-PK phosphorylation of RPA32 Ser4/Ser8 regulates replication stress checkpoint activation, fork restart, homologous recombination and mitotic catastrophe. DNA Repair (Amst). 2014;21:131-9.

164. Ranjan A, Iwakuma T. Non-Canonical Cell Death Induced by p53. Int J Mol Sci. 2016;17(12).

165. Wharam MD, Meza J, Anderson J, Breneman JC, Donaldson SS, Fitzgerald TJ, Michalski J, Teot LA, Wiener ES, Meyer WH. Failure pattern and factors predictive of local

failure in rhabdomyosarcoma: a report of group III patients on the third Intergroup Rhabdomyosarcoma Study. J Clin Oncol. 2004;22(10):1902-8.

166. Frisch SM, Farris JC, Pifer PM. Roles of Grainyhead-like transcription factors in cancer. Oncogene. 2017;36(44):6067-73.

167. Bai X, Wang J, Huo L, Xie Y, Xie W, Xu G, Wang M. Serine/Threonine Kinase CHEK1-Dependent Transcriptional Regulation of RAD54L Promotes Proliferation and Radio Resistance in Glioblastoma. Transl Oncol. 2018;11(1):140-6.

168. Prados J, Melguizo C, Fernandez A, Aranega AE, Alvarez L, Aranega A. Inverse expression of mdr 1 and c-myc genes in a rhabdomyosarcoma cell line resistant to actinomycin d. J Pathol. 1996;180(1):85-9.

169. Robey RW, Pluchino KM, Hall MD, Fojo AT, Bates SE, Gottesman MM. Revisiting the role of ABC transporters in multidrug-resistant cancer. Nat Rev Cancer. 2018;18(7):452-64.

170. Wang G, Lemos JR. Tetrandrine: a new ligand to block voltage-dependent Ca2+ and Ca(+)-activated K+ channels. Life Sci. 1995;56(5):295-306.

171. Wang TH, Wan JY, Gong X, Li HZ, Cheng Y. Tetrandrine enhances cytotoxicity of cisplatin in human drug-resistant esophageal squamous carcinoma cells by inhibition of multidrug resistance-associated protein 1. Oncol Rep. 2012;28(5):1681-6.

172. Fu L, Liang Y, Deng L, Ding Y, Chen L, Ye Y, Yang X, Pan Q. Characterization of tetrandrine, a potent inhibitor of P-glycoprotein-mediated multidrug resistance. Cancer Chemother Pharmacol. 2004;53(4):349-56.

173. Liu W, Zhang J, Ying C, Wang Q, Yan C, Jingyue Y, Zhaocai Y, Yan X, Heng-Jun S, Lin J. Tetrandrine combined with gemcitabine and Cisplatin for patients with advanced non-small cell lung cancer improve efficacy. Int J Biomed Sci. 2012;8(1):28-35.

174. Kumar A, Jaitak V. Natural products as multidrug resistance modulators in cancer. Eur J Med Chem. 2019;176:268-91.

175. Jiang M, Zhang R, Wang Y, Jing W, Liu Y, Ma Y, Sun B, Wang M, Chen P, Liu H, He Z. Reduction-sensitive Paclitaxel Prodrug Self-assembled Nanoparticles with Tetrandrine Effectively Promote Synergistic Therapy Against Drug-sensitive and Multidrug-resistant Breast Cancer. Mol Pharm. 2017;14(11):3628-35.

176. BLISS CI. THE TOXICITY OF POISONS APPLIED JOINTLY1. Annals of Applied Biology. 1939;26(3):585-615.

177. Demidenko E, Miller TW. Statistical determination of synergy based on Bliss definition of drugs independence. PLOS ONE. 2019;14(11):e0224137.

178. D'Angio GJ. Hepatotoxicity with actinomycin D. Lancet. 1987;2(8550):104.

179. Maesta I, Nitecki R, Desmarais CCF, Horowitz NS, Goldstein DP, Elias KM, Berkowitz RS. Effectiveness and toxicity of second-line actinomycin D in patients with methotrexate-resistant postmolar low-risk gestational trophoblastic neoplasia. Gynecol Oncol. 2020;157(2):372-8.

180. Limpongsanurak S. Prophylactic actinomycin D for high-risk complete hydatidiform mole. J Reprod Med. 2001;46(2):110-6.

181. Bochkareva E, Frappier L, Edwards AM, Bochkarev A. The RPA32 subunit of human replication protein A contains a single-stranded DNA-binding domain. J Biol Chem. 1998;273(7):3932-6.

182. Bochkareva E, Korolev S, Lees-Miller SP, Bochkarev A. Structure of the RPA trimerization core and its role in the multistep DNA-binding mechanism of RPA. EMBO J. 2002;21(7):1855-63.

183. Liu S, Opiyo SO, Manthey K, Glanzer JG, Ashley AK, Amerin C, Troksa K, Shrivastav M, Nickoloff JA, Oakley GG. Distinct roles for DNA-PK, ATM and ATR in RPA phosphorylation and checkpoint activation in response to replication stress. Nucleic Acids Res. 2012;40(21):10780-94.

184. Niu H, Erdjument-Bromage H, Pan ZQ, Lee SH, Tempst P, Hurwitz J. Mapping of amino acid residues in the p34 subunit of human single-stranded DNA-binding protein phosphorylated by DNA-dependent protein kinase and Cdc2 kinase in vitro. J Biol Chem. 1997;272(19):12634-41.

185. Block WD, Yu Y, Lees-Miller SP. Phosphatidyl inositol 3-kinase-like serine/threonine protein kinases (PIKKs) are required for DNA damage-induced phosphorylation of the 32 kDa subunit of replication protein A at threonine 21. Nucleic Acids Res. 2004;32(3):997-1005.

186. Chang D, Chen F, Zhang F, McKay BC, Ljungman M. Dose-dependent effects of DNA-damaging agents on p53-mediated cell cycle arrest. Cell Growth Differ. 1999;10(3):155-62.

187. el-Deiry WS, Kern SE, Pietenpol JA, Kinzler KW, Vogelstein B. Definition of a consensus binding site for p53. Nat Genet. 1992;1(1):45-9.

188. Shaw P, Bovey R, Tardy S, Sahli R, Sordat B, Costa J. Induction of apoptosis by wild-type p53 in a human colon tumor-derived cell line. Proc Natl Acad Sci U S A. 1992;89(10):4495-9.

189. Porter AG, Janicke RU. Emerging roles of caspase-3 in apoptosis. Cell Death Differ. 1999;6(2):99-104.

190. Schober P, Boer C, Schwarte LA. Correlation Coefficients: Appropriate Use and Interpretation. Anesth Analg. 2018;126(5):1763-8.

191. Fruci D, Cho WC, Nobili V, Locatelli F, Alisi A. Drug Transporters and Multiple Drug Resistance in Pediatric Solid Tumors. Curr Drug Metab. 2016;17(4):308-16.

192. Kuttesch JF, Parham DM, Luo X, Meyer WH, Bowman L, Shapiro DN, Pappo AS, Crist WM, Beck WT, Houghton PJ. P-glycoprotein expression at diagnosis may not be a primary mechanism of therapeutic failure in childhood rhabdomyosarcoma. J Clin Oncol. 1996;14(3):886-900.

193. Citti A, Boldrini R, Inserra A, Alisi A, Pessolano R, Mastronuzzi A, Zin A, De Sio L, Rosolen A, Locatelli F, Fruci D. Expression of multidrug resistance-associated proteins in paediatric soft tissue sarcomas before and after chemotherapy. Int J Oncol. 2012;41(1):117-24.

194. Seitz G, Warmann SW, Vokuhl CO, Heitmann H, Treuner C, Leuschner I, Fuchs J. Effects of standard chemotherapy on tumor growth and regulation of multidrug resistance genes and proteins in childhood rhabdomyosarcoma. Pediatr Surg Int. 2007;23(5):431-9.

195. Tivnan A, Zakaria Z, O'Leary C, Kogel D, Pokorny JL, Sarkaria JN, Prehn JH. Inhibition of multidrug resistance protein 1 (MRP1) improves chemotherapy drug response in primary and recurrent glioblastoma multiforme. Front Neurosci. 2015;9:218.

196. Alonso CAI, Lottero-Leconte R, Luque GM, Vernaz ZJ, Di Siervi N, Gervasi MG, Buffone MG, Davio C, Perez-Martinez S. MRP4-mediated cAMP efflux is essential for mouse spermatozoa capacitation. J Cell Sci. 2019;132(14).

197. Saleeb RM, Farag M, Lichner Z, Brimo F, Bartlett J, Bjarnason G, Finelli A, Rontondo F, Downes MR, Yousef GM. Modulating ATP binding cassette transporters in papillary renal cell carcinoma type 2 enhances its response to targeted molecular therapy. Mol Oncol. 2018;12(10):1673-88.

198. Sharma SV, Haber DA, Settleman J. Cell line-based platforms to evaluate the therapeutic efficacy of candidate anticancer agents. Nat Rev Cancer. 2010;10(4):241-53.

199. Gillet JP, Varma S, Gottesman MM. The clinical relevance of cancer cell lines. J Natl Cancer Inst. 2013;105(7):452-8.

200. Barretina J, Caponigro G, Stransky N, Venkatesan K, Margolin AA, Kim S, Wilson CJ, Lehar J, Kryukov GV, Sonkin D, Reddy A, Liu M, Murray L, Berger MF, Monahan JE, Morais P, Meltzer J, Korejwa A, Jane-Valbuena J, Mapa FA, Thibault J, Bric-Furlong E, Raman P, Shipway A, Engels IH, Cheng J, Yu GK, Yu J, Aspesi P, Jr., de Silva M, Jagtap K, Jones MD, Wang L, Hatton C, Palescandolo E, Gupta S, Mahan S, Sougnez C, Onofrio RC, Liefeld T, MacConaill L, Winckler W, Reich M, Li N, Mesirov JP, Gabriel SB, Getz G, Ardlie K, Chan V, Myer VE, Weber BL, Porter J, Warmuth M, Finan P, Harris JL, Meyerson M, Golub TR, Morrissey MP, Sellers WR, Schlegel R, Garraway LA. The Cancer Cell Line Encyclopedia enables predictive modelling of anticancer drug sensitivity. Nature. 2012;483(7391):603-7.

201. Ghandi M, Huang FW, Jane-Valbuena J, Kryukov GV, Lo CC, McDonald ER, 3rd, Barretina J, Gelfand ET, Bielski CM, Li H, Hu K, Andreev-Drakhlin AY, Kim J, Hess JM, Haas BJ, Aguet F, Weir BA, Rothberg MV, Paolella BR, Lawrence MS, Akbani R, Lu Y, Tiv HL, Gokhale PC, de Weck A, Mansour AA, Oh C, Shih J, Hadi K, Rosen Y, Bistline J, Venkatesan K, Reddy A, Sonkin D, Liu M, Lehar J, Korn JM, Porter DA, Jones MD, Golji J, Caponigro G, Taylor JE, Dunning CM, Creech AL, Warren AC, McFarland JM, Zamanighomi M, Kauffmann A, Stransky N, Imielinski M, Maruvka YE, Cherniack AD, Tsherniak A, Vazquez F, Jaffe JD, Lane AA, Weinstock DM, Johannessen CM, Morrissey MP, Stegmeier F, Schlegel R, Hahn WC, Getz G, Mills GB, Boehm JS, Golub TR, Garraway LA, Sellers WR. Next-generation characterization of the Cancer Cell Line Encyclopedia. Nature. 2019;569(7757):503-8.

202. Yang W, Soares J, Greninger P, Edelman EJ, Lightfoot H, Forbes S, Bindal N, Beare D, Smith JA, Thompson IR, Ramaswamy S, Futreal PA, Haber DA, Stratton MR, Benes C, McDermott U, Garnett MJ. Genomics of Drug Sensitivity in Cancer (GDSC): a resource for therapeutic biomarker discovery in cancer cells. Nucleic Acids Res. 2013;41(Database issue):D955-61.

203. Sondka Z, Bamford S, Cole CG, Ward SA, Dunham I, Forbes SA. The COSMIC Cancer Gene Census: describing genetic dysfunction across all human cancers. Nat Rev Cancer. 2018;18(11):696-705.

204. Tate JG, Bamford S, Jubb HC, Sondka Z, Beare DM, Bindal N, Boutselakis H, Cole CG, Creatore C, Dawson E, Fish P, Harsha B, Hathaway C, Jupe SC, Kok CY, Noble K, Ponting L, Ramshaw CC, Rye CE, Speedy HE, Stefancsik R, Thompson SL, Wang S, Ward S, Campbell PJ, Forbes SA. COSMIC: the Catalogue Of Somatic Mutations In Cancer. Nucleic Acids Res. 2019;47(D1):D941-D7.

205. Butler D. Translational research: crossing the valley of death. Nature. 2008;453(7197):840-2.

206. Morton CL, Houghton PJ. Establishment of human tumor xenografts in immunodeficient mice. Nat Protoc. 2007;2(2):247-50.

207. Murayama T, Gotoh N. Patient-Derived Xenograft Models of Breast Cancer and Their Application. Cells. 2019;8(6).

208. Hidalgo M, Amant F, Biankin AV, Budinska E, Byrne AT, Caldas C, Clarke RB, de Jong S, Jonkers J, Maelandsmo GM, Roman-Roman S, Seoane J, Trusolino L, Villanueva A. Patient-derived xenograft models: an emerging platform for translational cancer research. Cancer Discov. 2014;4(9):998-1013.

209. Teicher BA. Tumor models for efficacy determination. Mol Cancer Ther. 2006;5(10):2435-43.

210. Rusert JM, Juarez EF, Brabetz S, Jensen J, Garancher A, Chau LQ, Tacheva-Grigorova SK, Wahab S, Udaka YT, Finlay D, Seker-Cin H, Reardon B, Grobner S, Serrano J, Ecker J, Qi L, Kogiso M, Du Y, Baxter PA, Henderson JJ, Berens ME, Vuori K, Milde T, Cho YJ, Li XN, Olson JM, Reyes I, Snuderl M, Wong TC, Dimmock DP, Nahas SA, Malicki D, Crawford JR, Levy ML, Van Allen EM, Pfister SM, Tamayo P, Kool M, Mesirov JP, Wechsler-Reya RJ. Functional Precision Medicine Identifies New Therapeutic Candidates for Medulloblastoma. Cancer Res. 2020;80(23):5393-407.

211. Mohelnikova-Duchonova B, Brynychova V, Oliverius M, Honsova E, Kala Z, Muckova K, Soucek P. Differences in transcript levels of ABC transporters between pancreatic adenocarcinoma and nonneoplastic tissues. Pancreas. 2013;42(4):707-16.

212. Pajic M, Murray J, Marshall GM, Cole SP, Norris MD, Haber M. ABCC1 G2012T single nucleotide polymorphism is associated with patient outcome in primary neuroblastoma and altered stability of the ABCC1 gene transcript. Pharmacogenet Genomics. 2011;21(5):270-9.

213. Yin J, Zhang J. Multidrug resistance-associated protein 1 (MRP1/ABCC1) polymorphism: from discovery to clinical application. Zhong Nan Da Xue Xue Bao Yi Xue Ban. 2011;36(10):927-38.

214. Saito S, Iida A, Sekine A, Miura Y, Ogawa C, Kawauchi S, Higuchi S, Nakamura Y. Identification of 779 genetic variations in eight genes encoding members of the ATP-binding cassette, subfamily C (ABCC/MRP/CFTR. J Hum Genet. 2002;47(4):147-71.

215. Leschziner G, Zabaneh D, Pirmohamed M, Owen A, Rogers J, Coffey AJ, Balding DJ, Bentley DB, Johnson MR. Exon sequencing and high resolution haplotype analysis of ABC transporter genes implicated in drug resistance. Pharmacogenet Genomics. 2006;16(6):439-50.

216. Kadioglu O, Saeed M, Munder M, Spuller A, Greten HJ, Efferth T. Identification of Novel Rare ABCC1 Transporter Mutations in Tumor Biopsies of Cancer Patients. Cells. 2020;9(2).

10 Eidesstattliche Erklärung

10.1 Eidesstattliche Versicherung

„Ich, Jennifer von Stebut, versichere an Eides statt durch meine eigenhändige Unterschrift, dass ich die vorgelegte Dissertation mit dem Thema: „A CRISPR activation screen identifies *ABCC1* as a potential therapeutic target in actinomycin D-resistant high-risk pediatric rhabdomyosarcoma“; „Identifikation von *ABCC1* als potentiellen Angriffspunkt in Actinomycin D-resistenten, pädiatrischen Hochrisiko-Rhabdomyosarkomen: ein CRISPR-Aktivationsscreen“ selbstständig und ohne nicht offengelegte Hilfe Dritter verfasst und keine anderen als die angegebenen Quellen und Hilfsmittel genutzt habe.
Alle Stellen, die wörtlich oder dem Sinne nach auf Publikationen oder Vorträgen anderer Autoren/innen beruhen, sind als solche in korrekter Zitierung kenntlich gemacht. Die Abschnitte zu Methodik (insbesondere praktische Arbeiten, Laborbestimmungen, statistische Aufarbeitung) und Resultaten (insbesondere Abbildungen, Graphiken und Tabellen) werden von mir verantwortet.

Ich versichere ferner, dass ich die in Zusammenarbeit mit anderen Personen generierten Daten, Datenauswertungen und Schlussfolgerungen korrekt gekennzeichnet und meinen eigenen Beitrag sowie die Beiträge anderer Personen korrekt kenntlich gemacht habe (siehe Anteilserklärung). Texte oder Textteile, die gemeinsam mit anderen erstellt oder verwendet wurden, habe ich korrekt kenntlich gemacht.

Meine Anteile an etwaigen Publikationen zu dieser Dissertation entsprechen denen, die in der untenstehenden gemeinsamen Erklärung mit dem/der Erstbetreuer/in, angegeben sind. Für sämtliche im Rahmen der Dissertation entstandenen Publikationen wurden die Richtlinien des ICMJE (International Committee of Medical Journal Editors; www.icmje.og) zur Autorenschaft eingehalten. Ich erkläre ferner, dass ich mich zur Einhaltung der Satzung der Charité – Universitätsmedizin Berlin zur Sicherung Guter Wissenschaftlicher Praxis verpflichte.

Weiterhin versichere ich, dass ich diese Dissertation weder in gleicher noch in ähnlicher Form bereits an einer anderen Fakultät eingereicht habe.

Die Bedeutung dieser eidesstattlichen Versicherung und die strafrechtlichen Folgen einer unwahren eidesstattlichen Versicherung (§§156, 161 des Strafgesetzbuches) sind mir bekannt und bewusst.“

Datum Unterschrift

11 Lebenslauf

Mein Lebenslauf wird aus datenschutzrechtlichen Gründen in der elektronischen Version meiner Arbeit nicht veröffentlicht.

Mein Lebenslauf wird aus datenschutzrechtlichen Gründen in der elektronischen Version meiner Arbeit nicht veröffentlicht.

12 Komplette Publikationsliste

Im Rahmen meiner Tätigkeit als Doktorandin in der Arbeitsgruppe von Herrn Prof. Dr. med. Anton G. Henssen an der Klinik für pädiatrischen Hämatologie und Onkologie sind unter meiner Mitwirkung folgende Publikationen entstanden:

1. Henssen, A. G., C. Reed, E. Jiang, H. D. Garcia, **J. von Stebut**, I. C. MacArthur, P. Hundsdoerfer, J. H. Kim, E. de Stanchina, Y. Kuwahara, H. Hosoi, N. J. Ganem, F. Dela Cruz, A. L. Kung, J. H. Schulte, J. H. Petrini and A. Kentsis (2017). "Therapeutic targeting of PGBD5-induced DNA repair dependency in pediatric solid tumors." Sci Transl Med **9**(414).

2. Timme, N., Y. Han, S. Liu, H. O. Yosief, H. D. Garcia, Y. Bei, F. Klironomos, I. C. MacArthur, A. Szymansky, **J. von Stebut**, V. Bardinet, C. Dohna, A. Kunkele, J. Rolff, P. Hundsdorfer, A. Lissat, G. Seifert, A. Eggert, J. H. Schulte, W. Zhang and A. G. Henssen (2020). "Small-Molecule Dual PLK1 and BRD4 Inhibitors are Active Against Preclinical Models of Pediatric Solid Tumors." Transl Oncol **13**(2): 221-232.

3. Dorado Garcia, H., F. Pusch, Y. Bei, **J. von Stebut**, G. Ibanez, K. Guillan, K. Imami, D. Gurgen, J. Rolff, K. Helmsauer, S. Meyer-Liesener, N. Timme, V. Bardinet, R. Chamorro Gonzalez, I. C. MacArthur, C. Y. Chen, J. Schulz, A. M. Wengner, C. Furth, B. Lala, A. Eggert, G. Seifert, P. Hundsoerfer, M. Kirchner, P. Mertins, M. Selbach, A. Lissat, F. Dubois, D. Horst, J. H. Schulte, S. Spuler, D. You, F. Dela Cruz, A. L. Kung, K. Haase, M. DiVirgilio, M. Scheer, M. V. Ortiz and A. G. Henssen (2022). "Therapeutic targeting of ATR in alveolar rhabdomyosarcoma." Nat Commun **13**(1): 4297

13 Danksagung

An dieser Stelle möchte ich allen meinen großen Dank aussprechen, die mich während meiner Zeit im Labor und bei der Anfertigung meiner Dissertation unterstützt haben:

Mein besonderer Dank gilt meinem Erstbetreuer Prof. Dr. med. Anton G. Henssen für die hervorragenden Bedingungen zur Durchführung dieser Arbeit und seine stete Betreuung.

Nicht minder beteiligt war M. Sc. Heathcliff Dorado Garcia. Als geduldiger Mentor hat er durch seinen Rat, aufmunternde Worte und seine zuverlässige Unterstützung diese Arbeit erst ermöglicht.

Zusätzlich möchte ich mich Dipl.-Bioinf. Dr. rer. nat. Kerstin Haase, Yi Bei und Konstantin Helmsauer bedanken, die mir tatkräftig bei der bioinformatischen Analyse meiner CRISPRa Daten halfen.

Vielen Dank an die ganze AG Henssen, die mich für mehrere Jahre bei sich willkommen geheißen haben.

Nicht zuletzt möchte ich mich für die finanzielle Unterstützung durch das Berlin Institute of Health bedanken, die mich durch das BIH-MD Promotionsstipendium während meiner zwei Freisemester für den experimentellen Teil meiner Arbeit unterstützten.

Meinen Eltern und meinem Partner Jannik Marx danke ich für ihre Geduld und ihre ermutigenden Zusprüche während der Arbeit an dieser Dissertation.

14 Bescheinigung des akkreditierten Statistikers

CHARITÉ

CharitéCentrum für Human- und Gesundheitswissenschaften

Charité | Campus Charité Mitte | 10117 Berlin

Institut für Biometrie und klinische Epidemiologie (iBikE)

Direktor: Prof. Dr. Frank Konietschke

Postanschrift:
Charitéplatz 1 | 10117 Berlin
Besucheranschrift:
Reinhardtstr. 58 | 10117 Berlin

Tel. +49 (0)30 450 562171
frank.konietschke@charite.de
https://biometrie.charite.de/

Name, Vorname: von Stebut, Jennifer

Emailadresse: jennifer.von-stebut@charite.de
Matrikelnummer: 220550
PromotionsbetreuerIn: Prof. Dr. Anton G. Henssen

Promotionsinstitution: Klinik für Pädiatrie mit Schwerpunkt Hämatologie und Onkologie

Bescheinigung

Hiermit bescheinige ich, dass *Jennifer von Stebut* innerhalb der Service Unit Biometrie des Instituts für Biometrie und klinische Epidemiologie (iBikE) bei mir eine statistische Beratung zu einem Promotionsvorhaben wahrgenommen hat. Folgende Beratungstermine wurden wahrgenommen:

- Termin 1: 18.10.2022

Folgende wesentliche Ratschläge hinsichtlich einer sinnvollen Auswertung und Interpretation der Daten wurden während der Beratung erteilt:

- Annahmen des t-Tests
- Darstellung der Ergebnisse

Diese Bescheinigung garantiert nicht die richtige Umsetzung der in der Beratung gemachten Vorschläge, die korrekte Durchführung der empfohlenen statistischen Verfahren und die richtige Darstellung und Interpretation der Ergebnisse. Die Verantwortung hierfür obliegt allein dem Promovierenden. Das Institut für Biometrie und klinische Epidemiologie übernimmt hierfür keine Haftung.

Datum: 21.10.2022

[redacted]

Campus Charité Mitte
Charitéplatz 1 | D-10117 Berlin
Sitz: Reinhardtstr. 58